Structure development in polyketone and polyalcohol fibers

Lommerts, Bert Jan

STRUCTURE DEVELOPMENT IN POLYKETONE AND POLYALCOHOL FIBERS

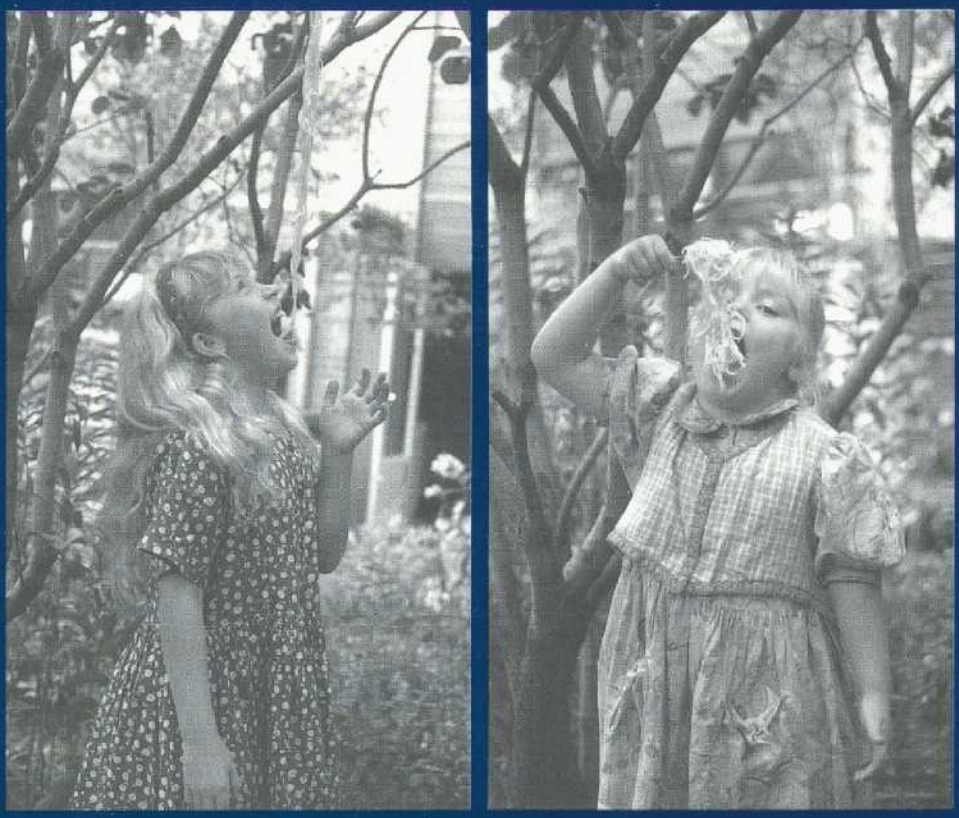

B.J. LOMMERTS

STRUCTURE DEVELOPMENT IN POLYKETONE AND POLYALCOHOL FIBERS

Druk: Krips Repro B.V. - Meppel

ISBN 90-9007596-8

Cover photograph : Spaghetti model demonstrating the polarity effect on the drawability of flexible chain polymers (with special thanks to Berdien and Annelies)

RIJKSUNIVERSITEIT GRONINGEN

STRUCTURE DEVELOPMENT IN POLYKETONE AND POLYALCOHOL FIBERS

PROEFSCHRIFT

ter verkrijging van het doctoraat in de
Wiskunde en Natuurwetenschappen
aan de Rijksuniversiteit Groningen
op gezag van de
Rector Magnificus Dr. F. van der Woude
in het openbaar te verdedigen op
vrijdag 21 oktober 1994
des namiddags te 2.45 uur precies

door

Bert Jan Lommerts

geboren op 24 augustus 1960
te Winschoten

Promotores: Prof. Dr. A.J. Pennings
Prof. Dr. Ir. P. Smith

Referent: Dr. Ir. J.J. van Aartsen

aan Frieda

Promotiecommissie: Prof. Dr. Ir. A.A.C.M. Beenackers
Prof. Dr. G. Hadziioannou
Prof. Dr. Ir. H.E.H. Meijer

Paranimfen W.L. de Hek
Dr. R. Huisman

DANKWOORD

Communicatie is een belangrijke bron van wetenschappelijke inspiratie. In de eerste plaats wil ik daarom de twee promotores prof. dr. Albert J. Pennings en prof. dr. ir. Paul Smith van harte bedanken voor de vele stimulerende discussies over de meest uiteenlopende onderwerpen. In de loop der jaren is een sterke band ontstaan, zowel op wetenschappelijk als op persoonlijk gebied, waaraan ik veel waarde hecht. Tevens hebben dr. ir. John J. van Aartsen, dr. Roelof Huisman, dr. ir. Maurits G. Northolt, dr. Doetze J. Sikkema en dr. ir. Jan Smook op een coöperatieve wijze bijgedragen aan mijn wetenschappelijke vorming tot polymeerchemicus, c.q. polymeertechnoloog. De leden van de promotiecommissie prof. dr. ir. Han Meijer, prof. dr. ir. Ton Beenackers en prof. dr. George Hadziioannou ben ik erkentelijk voor de snelle en kritische beoordeling van het proefschrift.

Vele handen maken licht werk en dit geldt zeker voor de "gePOKten" binnen Akzo Nobel Central Research. Hoewel velen, met name van de analytische afdelingen, een sterke betrokkenheid hebben getoond bij het reilen en zeilen van het projekt wil ik toch een aantal personen in het bijzonder vermelden. First of all I would like to acknowledge dr. Johst Burk, dr. Paul Hanna and dr. Andrew Piotrowski (ACR-Dobbs Ferry (NY)) for their many contributions to the project. During the last couple of years we have established a fruitful cooperation between the two ACR-institutes. Combining cultures is certainly not an easy task, but I am convinced that the differences in approach turned out to be advantageous for the various developments. Ing. Steven Leijenaar en Rob Bakker wil ik bedanken voor de vele polymeersyntheses en Gerrit Hoentjen en ir. Adri Witteveen voor de produktevaluaties. Hoewel de groep van spinners sterk aan veranderingen onderhevig geweest is wil ik toch de bijdragen van ing. Peter Cloos, Jeanette van Dijk, dr. Gert-Jan Jongerden, ing. Bas Krins, ing. Bert Leibbrand en dr. Harm van der Werff niet vergeten te vermelden. Ing. Henk Ter Maat ben ik in het bijzonder dankbaar voor het vele werk dat hij gedaan heeft aan de ontwikkeling van de diverse processen. Henk, jouw enthousiasme en technisch vernuft gecombineerd met je nuchtere kijk op de gang van zaken maken jou tot een zeer waardevolle collega. De structuuranalyses uitgevoerd door dr. Jos Aerts, dr. Enno Klop en ing. Jan Veurink zijn essentiële onderdelen geworden van dit proefschrift. Het

spreekt voor zich dat ik uiterst dankbaar ben om met deze kanjers te mogen samenwerken. Tevens wil ik dr. Hans Jansen, dr. Ad de Vries en drs. Joop Baltussen bedanken voor hun bijdragen aan het onderzoek naar de mechanische eigenschappen van polyketon vezels. Ook de samenwerking met ir. Caroline Boerma was zeer waardevol en is uitgemond in een aantal octrooischriften. Verder wil ik vele collegae van de afdeling CDS bedanken voor de belangstelling tijdens het voltooien van het proefschrift. In het bijzonder wil ik ir. Hanneke Boerstoel hier danken voor het onder de aandacht brengen van de externe polyketon ontwikkelingen en Frans van Swaaij voor het verzorgen van veel van het grafisch werk. Tevens ben ik ir. Noor van Andel, ir. Henk Brakel, ir. Frans Pluijm en dr. Gerrit Ruitenberg erkentelijk voor de mogelijkheid dit onderzoek binnen Akzo Nobel verband te voltooien.

Het thuisfront heeft mij gedurende de afgelopen periode altijd tot het uiterste ondersteund. Frieda, zonder jouw hulp had ik dit in de huidige situatie en in deze vorm niet kunnen volbrengen. Je was van onschatbare waarde vooral in de moeilijke periodes. Berdien en Annelies, ook jullie zaten betrekkelijk weinig te mopperen als ik 's avonds laat thuis kwam van het werk en weinig tijd over had om leuke dingen te doen. Gelukkig komt daar spoedig verandering in.

CONTENTS

Chapter 1.

INTRODUCTION

In the second half of this century the use of polymers in our daily life has rapidly grown in volume as well as in the number of applications. However, the European chemical industry faces an ongoing maturization of the polymer business and the concurrent developments has sometimes led to the belief that the rise and decline of polymer science is already behind us.[1]

During the last recession a number of companies have indeed reshuffled their product mix and have withdrawn themselves to core-activities.[2] Obviously the market entry-barriers for new products have increased in time, however, this should not imply that there is no room left for further improvement of the present product portfolio. In view of the high entry-barriers for mature markets, the economical feasibility of new developments is of primary concern in order to gain insight into the viability of new polymer products.

1.1 Scope of the Thesis

New or modified polymerization catalysts have provided the opportunity to produce new polymer materials. Some of these developments either have been commercialized or have potential to enter the highly competitive engineering or commodity plastics markets.

The development of new metallocene based catalyst systems allowed synthesis of several new resins with some exciting properties. In 1985 chemists from Idemitsu Kosan synthesized syndiotactic polystyrene (sPS) for the first time.[3,4] This process was later expanded by Dow Chemicals Company, which developed catalysts allowing

commercial production of sPS.[5,6] sPS is a semi-crystalline polymer with a relatively high glass transition temperature and a high melting point (270 °C).[7] In addition to these good thermal properties, sPS is both chemical and water/steam resistant, and the polymer can easily be formed and moulded.

Another important development was the use of metallocene catalysts to produce syndiotactic and isotactic polypropylene (sPP and iPP). Metallocene based iPP is being commercialized by Exxon Chemical Company under the trade name EXXPOL PP.[8] This polymer has a narrow molecular weight distribution (MWD) and a narrow tacticity distribution. The formation of atactic chains is completely surpressed. During melt processing metallocene based EXXPOL PP is more easily extensible in fiber spinning than its broader MWD counterparts. The narrow tacticity distribution increases stiffness, which is useful in durable goods applications. sPP is being commercialized by the Fina Oil Company.[9]

The most significant improvement in the area of polyolefins was the development of *constraint geometry catalysts* by the Dow Chemical Company.[10] Single site metallocene based catalyst technology is known to produce homogeneous random olefin copolymers with very narrow molecular weight distribution and comonomer distribution, which together improve the physical properties. *INSITE*-Technology is unique among single-site catalyst technologies as it utilizes a constraint geometry catalyst, which creates long branches on narrow MWD polymers.[11] It is found that this type of structure combines excellent processing and high performance, unusual given the conventional sacrifice of one for the other. Through *INSITE*-Technology, scientists at Dow Chemical have also been able to control the desired levels of long chain branches to meet customer performance and processing needs.

A recent approach to new polymer materials is the development of the group of *cis*-fixed palladium bidentate catalysts, which can be used for the production of alternating polyolefin ketones.[12-15] In view of the chemical structure of this class of polymers, it was anticipated that these materials can be used for engineering plastic and fiber applications.[16,17]

The present thesis is devoted to the structure development in oriented perfectly alternating ethylene-carbon monoxide copolymers (polyketone; POK-C_2). Furthermore, a new polyalcohol (PAl) has been produced by reduction of this polyketone.

POK-C_2 $\quad (CH_2CH_2C(O))_n$

PAl $\quad (CH_2CH_2CH(OH))_n$

The aim of this thesis is to evaluate the potential of these materials for advanced industrial fiber applications.

1.2 Industrial or Technical Fibers

High modulus industrial or technical fibers find their application mainly in tyres[18] and other mechanical rubber goods (e.g., V-belts, conveyer belts, hoses, ...).[19] In view of the high demands of such end-uses the mechanical performance of industrial fibers at elevated temperatures is of paramount importance. Especially the dimensional stability (i.e., the retention of the tensile modulus and the fiber length at elevated temperatures) is an important parameter. Presently, poly(ethylene terephthalate) (PET), cellulose, poly(vinyl alcohol) (PVAl) and nylon-6,6 fibers dominate these market segments. An important feature of cellulose (viscose) fibers is an excellent retention of the tensile modulus at elevated temperatures, but the tensile strength [at room temperature] is lower than for PET or nylon-6,6 fibers. Nylon-6,6 fibers show a relatively low initial tensile modulus, whereas low-speed-spun PET fibers show a moderate high-temperature performance. The shrinkage in hot air of high-speed-spun PET fibers is strongly reduced relative to low-speed-spun material.[20,21] This was an important break-through in the field of fiber science and these so-called high modulus/low shrinkage PET fibers are sufficiently dimensionally stable for many industrial fiber applications.

Traditionally PVAl fibers are spun from aqueous solutions into an alkaline or sodium sulfate coagulation bath.[22] Often a certain amount of boric acid is added to the spinning dope in order to reduce skin-core effects.[23] These high-modulus PVAl fibers, spun from aqueous solution, are commercialized mainly by Japanese companies. More recent developments involve the application of high-molecular-weight polymer and the use of organic solvents.[24-26] The aim of these investigations was to improve both the tensile properties and the hot-water-resistance of PVAl fibers. The latter approach was derived from the gelspinning concept developed for the production of high-strength polyethylene fibers.[27-29] Indeed high-strength PVAl fibers have been produced on bench-scale equipment, but the superior mechanical properties could not be reproduced at higher production speeds;[30] the obtained mechanical properties were only slightly higher than those of commercially available PVAl fibers spun from aqueous solutions. Also the fatigue behavior of these high-molecular-weight fibers is rather poor and a pronounced decline of the tensile modulus is observed at elevated temperatures,[31] which can be attributed to the atactic nature of PVAl.

1.3 Survey of this Thesis

To gain insight into the potential of the perfectly alternating ethylene-carbon monoxide copolymer (POK-C_2) as a starting material for industrial fibers, this polymer has been spun from phenolic solutions. In a subsequent drawing stage the required molecular orientation has been induced. It is well known that the mechanical properties of polymer fibers are strongly governed by the degree of molecular orientation in the direction of the fiber axis.[32,33] In Chapter 2 the structure of POK-C_2 copolymers is described and the crystal structure of oriented POK-C_2 fibers is presented. Based on the melting behavior of low-molecular-weight (symmetrical) POK-C_2 homologs a first estimate for the crystalline heat of fusion is derived. In Chapter 3 the preparation of high-strength POK-C_2 fibers is reported and the influence of the drawing conditions on the mechanical properties is discussed. The synthesis and structure of the polyalcohol prepared by reduction of POK-C_2 is described in Chapter 4. The two polymers of interest show a pronounced difference in deformation behavior

at elevated temperatures. The influence of the chemical structure, mainly polarity, and temperature on the topological constraints to the maximum attainable draw ratio of flexible polymer systems are discussed in Chapter 5. Oriented POK-C_2 fibers exhibit polymorphism and the study into a structural transition at elevated temperatures together with the effect of the fraction of chain defects (i.e., propylene-carbon monoxide defects) on the room temperature crystal structure of polyketone terpolymers is presented in Chapter 6. Finally, in Chapter 7 the dimensional stability, creep resistance, and high-temperature strength of polyketone fibers are reported.

References and Notes

1. The central theme of the 8th Rolduc Polymer Meeting (1993), May 1993, Rolduc Abbey, Kerkrade, the Netherlands, was "The Rise and Decline of High Performance Polymers in Europe".
2. See, for example, 1992-1994 editions of Chemical Week.
3. N. Ishihara, T. Seimiya, M. Kuramoto, and M. Uoi, *Macromolecules*, **19,** 2465 (1986).
4. Idemitsu Kosan Co., Japanese Patent 05,295,029 (Idemitsu), (1992).
5. R.E. Campbell and G.F. Schmidt, US-Patent 4,774,301 (Dow Chemicals), (1987).
6. D.R. Neithamer, J.C. Stevens, and D.R. Neithmer, European Patent 418,044 (Dow Chemicals), (1989).
7. Y.K. Wang, J.D. Savage, D. Yang, and S.L. Hsu, *Macromolecules*, **25,** 3659 (1992).
8. J.J. McAlpin, *MetCon '94 Proceedings*, 1994.
9. M.J. Elder, J.A. Ewen, and A. Razavi, European Patent 427,696 (Fina Technology Inc.), (1989).
10. G.M. Knight, Y. Lais, P.N. Nickias, R.K. Rosen, G.F. Schmidt, J.C. Stevens, F.J. Timmers, D.R. Wilson, G.W. Knight, S. Lai, L. Shih-Yaw, and S.Y. Lai, European Patent 416,815 (Dow Chemical), (1989).
11. K.W. Swogger, *MetCon '94 Proceedings*, 1994.
12. E. Drent, European Patent 121,965 (Shell), (1984).

13. E. Drent, J.A.M. van Broekhoven, and M.J. Doyle, *J. Organomet. Chem.*, **417,** 235 (1991).
14. A. Sen, *Acc. Chem. Res.*, **26,** 303 (1993).
15. M. Barsacchi, A. Batistini, G. Consiglio, and U.W. Suter, *Macromolecules*, **25,** 3604 (1992).
16. H. Boerstoel, (private communications).
17. J. Smook, G.J.H. Vos and H.L. Doppert, *J. Appl. Polym. Sci.*, **41,** 105 (1990).
18. W.R. Dorst, H.H.W. Feijen, W.G.N. Keizer, W. Weidenhaupt, W.H. Hupjé, and J.B.M. Nuyten, *Enka Tire Symposium 1987,* Product Group Industrial Fibers, Enka Information, Arnhem, The Netherlands, 1987.
19. F.W. Bridié, L. Daan, C.C.J. de Jong, G. Ruitenberg, and W.H. Hupjé, *Enka Industrial Fibers MRG Symposium 1985,* Product Group Industrial Fibers, Enka Information, Arnhem, The Netherlands, 1985.
20. A. Ziabicki and H. Kawai, *High-speed Fiber Spinning,* Wiley, New York, 1985.
21. R. Huisman and H.M Heuvel, *J. Appl. Polym. Sci.*, **37,** 595 (1989).
22. I. Sakurada, *Polyvinyl Alcohol Fibers,* Marcel Dekker, New York, (1985).
23. H. Fujiwara, M. Shibayama, J.H. Chem., and S. Nomura, *J. Appl. Polym. Sci.*, **37,** 1403 (1989).
24. H. Tanaka, M. Suzuki, and F. Ueda, European Patent 146,084 (Toray), (1984).
25. W-I Cha, S-H Hyon, and Y. Ikada, *J. Polym. Sci. Polym. Phys. Ed.*, **32,** 297 (1994).
26. C. Sawatari, Y. Yamamoto, N. Yanagida, and M. Matsuo, *Polymer,* **34,** 956 (1993).
27. B. Kalb and A.J. Pennings, *Poll. Bull.*, **1,** 871 (1979).
28. P. Smith, P.J. Lemstra, B. Kalb, and A.J. Pennings, *Poll. Bull.*, **1,** 733 (1979).
29. P. Smith and P.J. Lemstra, *J. Mater. Sci.*, **15,** 505 (1980).
30. B.J. Lommerts, Th. van Hees, and J. van Dijk, (unpublished results).
31. J. Smook, B.J. Lommerts, and H. Gorter, 5th Rolduc Polymer Meeting (1990), April 1990, Rolduc Abbey, Kerkrade, the Netherlands.
32. P.H. Hermans, *Physics and Chemistry of Cellulose Fibers,* Elsevier, Amsterdam, 1949.
33. I.M. Ward, *Mechanical Properties of Solid Polymers,* 2nd ed., Wiley, New York, 1983.

Chapter 2.

STRUCTURE AND MELTING OF PERFECTLY ALTERNATING ETHYLENE-CARBON MONOXIDE COPOLYMERS

Reproduced from:
B.J. Lommerts, E.A. Klop, and J. Aerts, *J. Polym. Sci. Polym. Phys. Ed.*, **31**, 1319 (1991).

2.1 Abstract

The perfectly alternating ethylene-carbon monoxide copolymer (polyketone; POK) has been studied by means of ^{1}H-nuclear magnetic resonance and thermal analysis, and the crystal structure, determined by wide angle x-ray scattering methods, is presented. The crystal structure of this polymer in well-oriented fibers (POK-α) is as follows: Space group Pbnm, a = 6.91(2) Å, b = 5.12(2) Å, c = 7.60(3) Å (fiber axis), ρ_c = 1383 kg/m^3. This differs from the structure reported earlier by Chatani et al. (POK-β). The very dense packing in the POK-α structure is a result of the arrangement of the dipoles in the crystal lattice, giving rise to strong lateral forces between the polymer chains. Owing to the all-trans conformation of the polymer chain in the crystal lattice, high moduli can be achieved for well-oriented fibers. A first approximation results in a value of 360 GPa for the theoretical modulus. From the melting data for a series of low-molecular-weight polyketone homologs, a first, estimate is derived for the heat of fusion (215-330 J/g) for crystals of infinite chain length. As a result of the strong lateral forces, this polymer shows a (very) high heat of fusion for perfectly crystalline material, and the creep resistance and compressive strength of oriented fibers are expected to be superior to those of high modulus polyethylene fibers.

2.2 Introduction

Since the development of the high-strength polyethylene fiber,[1-3] solution spinning of

linear high-molecular-weight flexible-chain polymers has received considerable interest. Compared with polyethylene, copolymers of carbon monoxide and ethylene (polyketones) with a high carbon monoxide content show significantly higher melting temperatures[4,5] as well as rather good adhesion properties.[6] Therefore, these polyketones may be interesting starting materials for fibers, provided that good mechanical properties can be obtained.

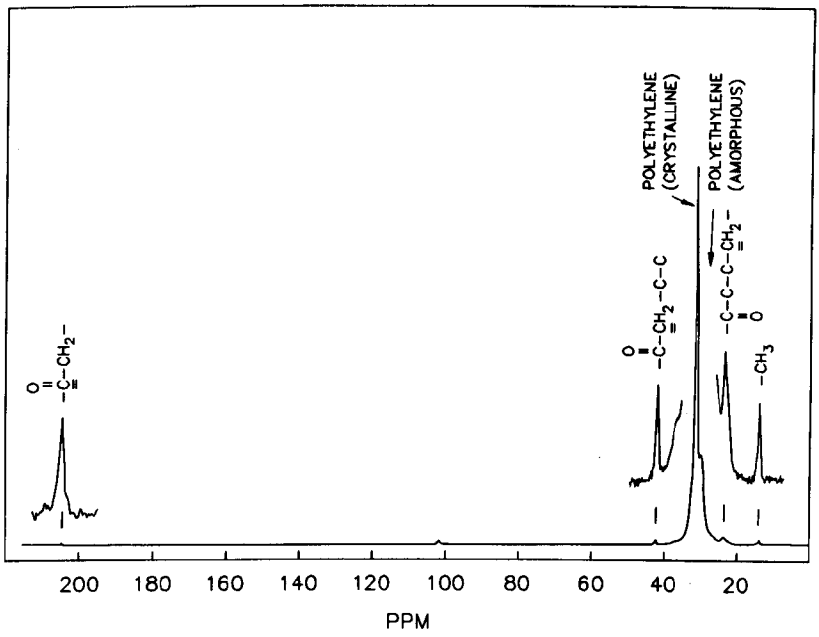

Figure 1. *Solid-state ^{13}C-NMR spectrum of photodegradable Budweiser "six-pack" yokes.*

A point of concern for fiber applications is the sensitivity of polyketones toward ultraviolet (UV) light, in particular when considering presently commercially available materials. Polyketones with a low carbon monoxide content are currently used as photodegradable plastics.[7,8] A solid-state ^{13}C nuclear magnetic resonance (NMR) trace of "six-pack" yokes[9] made of such a polymer is shown in Figure 1, revealing that some carbonyl groups (< 1 wt %) are incorporated into the polyethylene chain.

Ultraviolet radiation can induce Norrish-I and Norrish-II [the latter is predominant at room temperature] types of reactions (see Fig. 2), causing chain cleavage. The molecular weights of the fragments formed correspond to the molecular weights of the parts of the chain between carbonyl groups.[10-13]

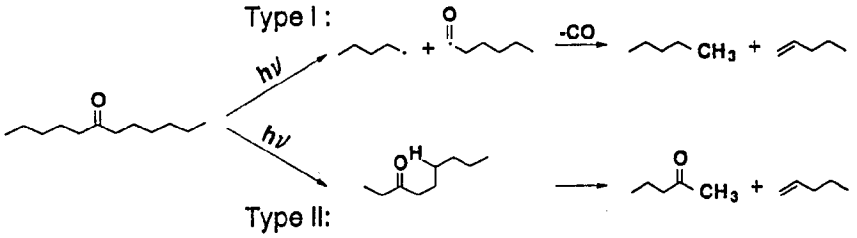

Figure 2. *Schemes of Norrish-I and Norrish-II types of chain cleavage reactions (ref. 10).*

In the past, several techniques have been developed for synthesizing polyolefin ketones, viz. radical copolymerization at high pressure[14-18] and transition-metal catalyzed copolymerization under moderate conditions.[19-23] A review of the different techniques is given by Sen.[24,25] Already in 1961 Chatani et al.[26] reported the crystal structure of an alternating polyketone copolymer from oriented film samples. The polymer was prepared by γ-radiation-initiated copolymerization and a melting point of 175-185 °C was reported. We designate this structure as polyolefin(C_2)-ketone β (POK-β).[27] The *ab* projection of the orthorhombic unit cell of this structure is very similar to that of polyethylene. The conformation of the extended polymer chain is planar (zig-zag) and owing to a small chain cross-section, high moduli can be achieved for well-oriented crystalline material.

More recently, a catalytic polymerization method has been developed by Drent et al.[28,29] of the Royal Dutch Shell laboratories, resulting in a perfectly alternating

copolymer with a melting point of 257 °C (Fig. 3). An interesting feature of this perfectly alternating copolymer is that Norrish-II reactions are inhibited owing to the absence of CH_2-groups at the γ-position of the carbonyl groups, resulting in an improved UV stability. It has also been shown by Gooden et al.[10] that for extended (crystalline) material the contribution of the Norrish-II type of chain scission to the total photodegradation is greatly decreased.

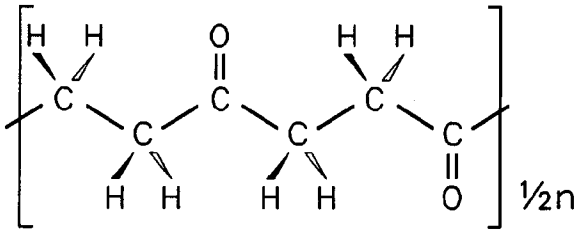

Figure 3. *Perfectly alternating ethylene carbon monoxide copolymer.*

Taking these features into account, alternating polyketones thus seem to fullfil all preconditions for attractive high-performance material applications. We were indeed able to spin this alternating copolymer from a solution[30] into a highly drawable fiber, resulting in well- oriented, highly crystalline material with good mechanical properties. The present Chapter describes the characterization of the copolymer by means of ^{1}H-NMR and thermal analysis. The crystal structure, as determined by wide-angle x-ray fiber diffraction, is presented. The differences between the latter structure, which will be designated as polyolefin(C_2)-ketone α (POK-α), and the POK-β structure are discussed. The melting points of a series of homologs and a series of copolymers are scrutinized. From these results, a first approximation for the theoretical modulus for the perfectly alternating polyketone is derived, and the crystallinity in oriented fibers has been estimated.

2.3 Experimental

-Materials

A low-molecular-weight copolymer of ethylene and carbon monoxide was prepared according to the description given in ref. 31, using a solution of 10.5 mg palladium acetate, 19.5 mg 1,3-*bis*(diphenylphosphino)propane, and 18.1 mg *p*-toluene sulfonic acid in 1 L of methanol as the catalyst system. The following bidentate complex compound, displayed in Figure 4, is the active species in the reaction.[28,29]

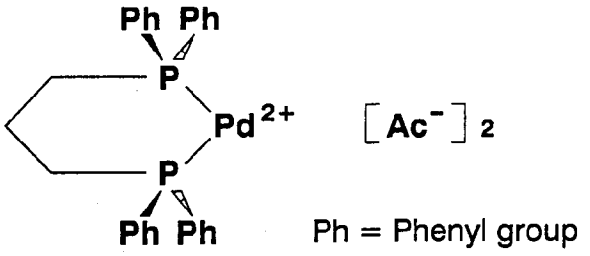

Figure 4. *Palladium 1,3-bis(diphenylphosphino)propane complex (the weakly coordinating p-toluenesulfonate anion(s) are not depicted).*

The solution was discharged into a 2 L stirred Hofer autoclave, which was subsequently pressurized at 60 bar at a temperature of 85 °C with a 1 : 1 mixture of carbon monoxide and ethylene. After pressurizing for 50 h, the resulting white powder was discharged and washed with methanol.

A high-molecular-weight sample was prepared by gas phase polymerization according to the description given in ref. 32. The catalyst system was prepared by adding a solution of 7.02 mg palladium acetate, 12.90 mg 1,3-*bis*(diphenylphosphino)propane and 12.04 mg *p*-toluene sulfonic acid in 20 mL of acetone to 10 g of the low-molecular-weight polymer. This mixture was thoroughly homogenized and discharged into the Hofer autoclave. After the acetone had evaporated, the autoclave was pressurized at 50 bar and kept at a temperature of 65 °C with a 1:1 gas mixture of

carbon monoxide and ethylene. After a reaction time of 100 h, 180 g of a high-molecular-weight polymer could be discharged from the autoclave. The limiting viscosity numbers of the two polymer samples, determined in *m*-cresol at 25 °C, are 0.52 and 6.1 dL/g.

As low-molecular-weight polyketone homologs 3,6,9-undecanetrione,[33-35] 2,5-hexanedione (Fluka) and 3-pentanone (Janssen) were used. The 2,5-hexanedione was first purified by distillation under vacuum. For comparison with literature data, two polyketone terpolymers (ethylene-CO/propylene-CO) were polymerized according to the description given in ref. 36, using the same catalyst recipe as for the copolymer.

-Yarn Sample

A 10 wt-% solution of the high-molecular-weight sample was prepared in a phenol/acetone mixture (9:1) at 110 °C. The solution was homogenized vigorously under a nitrogen atmosphere for 5 h, using a glass stirrer in order to avoid corrosion by the phenol. The solution was conditioned at 100 °C in a piston-cylinder apparatus for 90 min. The fiber was extruded at a speed of 2 m/min. through one capillary (500 μm, L/*d*=20) into a cold acetone bath (-5 °C). An air-gap of 2 mm was used in order to bridge the temperature difference. The yarn was collected almost tensionless on a bobbin at a speed close to 2 m/min, thereby allowing some shrinkage of the yarn during the evaporation of the residual acetone in the swollen fiber. The yarn was washed, dried and subsequently drawn in three steps using hot plates to a total draw ratio of 19 at temperatures of 217, 242 and 257 °C, respectively, resulting in a fiber with a maximum modulus of 45 GPa and a tensile strength of 1.9 GPa.

-X-Ray Diffraction Analysis

X-ray diffraction patterns of the yarn were made using several techniques: flat-plate fiber photographs, precession photographs and diffractometer scans (for intensity measurements) using CuKα- and MoKα-radiation. A precession photograph is shown in Figure 5. A model for the polymer chain assuming a planar zig-zag backbone was generated with the aid of a local computer program.

Table I. *Bond Lengths and Bond Angles Used for Constituting the Polymer Chain*

Bond Length		Bond Angle	
CH_2-CH_2	: 1.54 Å	CH_2-CH_2-CO	: 110°
CH_2-CO	: 1.51 Å	CH_2-CO-CH_2	: 120°
C=O	: 1.23 Å	CH_2-C=O	: 120°

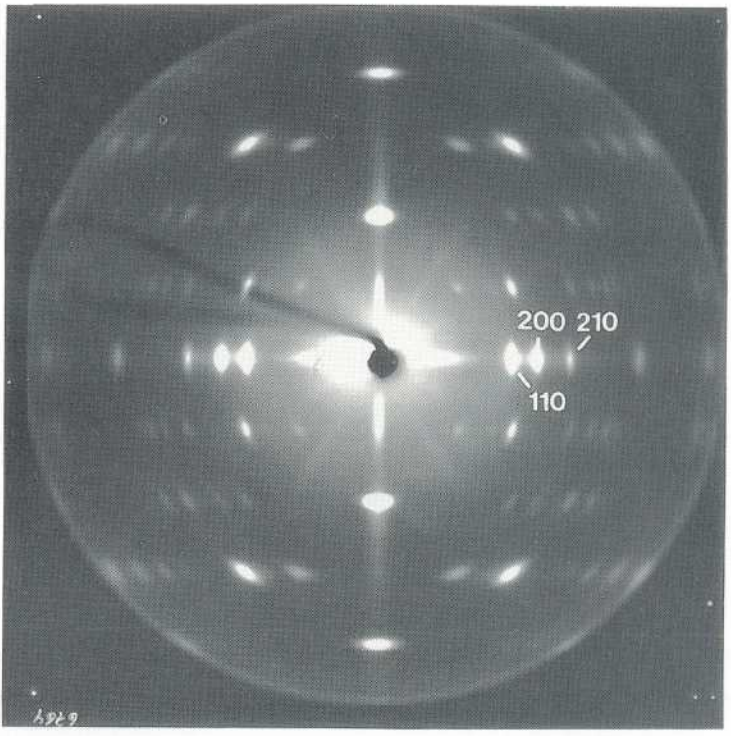

Figure 5. *Precession x-ray diffraction photograph of a perfectly alternating polyketone fiber, drawn in three stages to a total draw ratio of 19 at 217, 242 and 257 °C, respectively. The (110), (200), and (210) reflections are indicated.*

Table II. *Comparison Between Observed and Calculated Intensities of Different Reflections*

Reflection *hkl*	Intensity[a] Cal.	Obs.	Reflection *hkl*	Intensity[a] Cal.	Obs.
110	273	vs	002	1000	vs
200	132	vs	112	<1	w
210	40	s	202	1	w
020	<1	-	212	9	w-m
310	15	m	022	3	w
220	3	-			
400	<1	vw	103	14	m-s
320	<1	vw	113	40	s
130	<1	w			
101	28	w-m	004	95	vs
111	33	s			
211	<1	w			

[a] The observed reflections are indicated as very weak (vw), weak (w), medium (m), strong (s), or very strong (vs) reflections.

Standard bond lengths and bond angles were used (listed in Table 1). Twice the calculated monomer length agreed well with the observed fiber-axis unit-cell length. Intensities were calculated using a local computer program. No H atoms were included in the intensity calculations. The intensities of the (110) and (200) reflections were measured accurately by recording radial and azimuthal scans, using a transmission diffractometer. The measured intensity ratio of these reflections was found to be

2.08. The angle between the molecular plane and the *bc* plane was then adjusted until the calculated and the measured intensity ratios of the 110 and the 200 reflections were in agreement. The intensities of the other reflections, calculated by using the optimized angle between the molecular plane and the *bc* plane, are also in qualitative agreement with the observed intensities (see Table II).

-Analytical Methods

Thermograms of the materials were recorded using a Perkin Elmer DSC 7 thermal analyzer at a scanning speed of 20 °C/min. The melting temperatures were taken as peak melting temperatures and the heats of fusion were calculated from the area of the melting peaks. ^{1}H-NMR spectra of the as-synthesized polymers were recorded in d^6-phenol or in d^6-dimethyl sulfoxide (DMSO) on a Bruker AM 400 (400 MHz) spectrometer at a temperature of 100 °C.

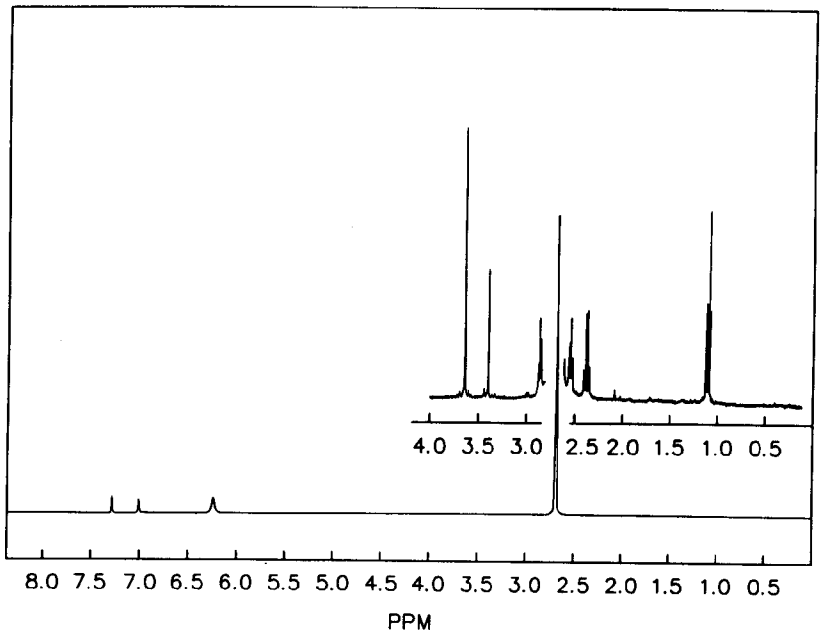

Figure 6. *^{1}H-NMR spectrum in d^6-phenol at 100 °C of the low-molecular-weight ethylene-carbon monoxide copolymer (LVN=0.52 dL/g).*

2.4 Results and Discussion

-1H-NMR Analysis

The ^{1}H-NMR spectrum of the low-molecular-weight ethylene- carbon monoxide copolymer in d^6-phenol is given in Figure 6. No significant enolization is detected. Solvents with a strong hydrogen-bonding capacity can stabilize the keto form; [37,38] and in order to rule out possible solvent effects, also d^6-dimethyl sulfoxide was used.

Table III. *^{1}H-NMR Spectral Data for the Low-Molecular-Weight Alternating Ethylene-Carbon Monoxide Copolymer*

	^{1}H-NMR[a](ppm)	Assignment	Integration[b]	
1	(t) 1.09	**CH_3**-CH_2	0.0047	(3)
2	(q) 2.36	CH_3-**CH_2**-C(O)	0.0050	(2)
3	(t) 2.53	O-C(O)-**CH_2**-CH_2-C(O)	0.0041	(2)
4	(s) 2.69	C(O)-(**CH_2**)$_2$-C(O)	1	(4)
5	(t) 2.85	O-C(O)-CH_2-**CH_2**-C(O)	0.0040	(2)
6	(s) 3.64	**CH_3**-O-C(O)	0.0032	(3)
MeOH	(s) 3.40	**CH_3**-OH	-	

[a] d^6-phenol (370 K) referenced to phenol (7.0 ppm) s=singlet, d=doublet, t=triplet, q=quartet. A small amount of methanol was added in order to ensure the methanol assignment.

[b] Integrated value per proton, numbers in parentheses indicate the number of protons.

Only a limited amount of polymer was soluble (10 wt% at 100 °C, quantified using dimethyl terephthalate as a standard), but again no enolization was observed in this aprotic solvent. Furthermore, end-groups of the low-molecular-weight polymer were investigated. The observed chemical shifts are listed in Table III. The end-groups observed are in agreement with the polymerization mechanism consisting of two interdependent reaction cycles as proposed by Drent et al.[29] Initiation is probably accomplished by the formation of a palladium methoxy bond, and subsequently a carbon monoxide molecule is incorporated, forming ester end-groups. Chain growth occurs by incorporating alternately ethylene and carbon monoxide. Termination is accomplished by the insertion of methanol into the palladium alkyl bond, while forming a new active palladium methoxy catalyst species. The alcoholic solvent present during the reaction can therefore be regarded as a chain transfer agent. When the alcoholic solvent is incorporated into a palladium acyl bond, chain growth is terminated by the formation of a methyl ester end-group and an active palladium hydride catalyst species is formed. The latter can induce a new polymerization cycle, which is comparable to the reaction mechanism as proposed by Lai and Sen,[23] where initiation is accomplished by the formation of alkyl end-groups. It should be noted that no aldehyde or methyl ether end-groups are observed for our polymer samples.

The formation of ester end-groups is confirmed by other investigators.[23,24,39,40] Chepaikin et al.[40] used acetic acid as part of the solvent mixture for a palladium-based catalyst system and observed also ester end-groups. This result seems to support the proposed mechanism for initiation via the palladium methoxy (or palladium acetoxy) complex; otherwise, in the case of acetic acid as a solvent one would have expected anhydride (or acid) terminated end-groups to be present in the polymer. However, in strong acidic solvents protonolysis of palladium-alkyl bonds is more likely to occur. Owing to a stronger coordination ability of carbon monoxide, the net rate of insertion of carbon monoxide into the polymer backbone will be much faster than that of ethylene. Consequently the amount of palladium alkyl bonds is much lower than the amount of palladium acyl bonds. Because the formation of 1,2-diketone structures seems to be impossible under these conditions, the rate-determining step for the polymerization will be the coordination and/or the

incorporation of ethylene. Therefore, the observed end-groups do not present conclusive evidence for distinguishing between the two possible mechanisms of initiation.

-Crystal Structure

From the observed x-ray reflections, an orthorhombic unit cell was deduced with a=6.91(2) Å, b=5.12(2) Å, and c(fiber axis)=7.60(3) Å. The calculated density with four monomer units in the unit cell is 1383 kg/m^3. From systematic extinctions, the space group Pbnm (a variant of space group Pnma-Nr. 62 in the International Tables[41]) was determined. The symmetry of this space group fixes the position of the chain in the unit cell so that the chain must have its backbone at x=0, y=0 (corner chain) and x=0.5, y=0.5 (center chain), and the z-axis coordinates of the carbonyl groups must be 0.25 and 0.75, where x, y and z are fractional coordinates. As a result, the polymer chain is highly symmetric. This results in only one degree of freedom for the chain in the cell (i.e., the angle between the plane of the zig-zag chain and the *bc* plane of the unit cell). For a series of angles between the molecular plane and the *bc* plane, the intensities were calculated and compared with the observed ones. The best agreement was found for an angle of 26°. The estimated standard deviation is 2°. The atomic coordinates of this structure, designated as POK-α, are given in Table IV and the equivalent positions of the space group are listed in Table V.

Table IV. *Crystal (Fractional) Coordinates for the POK-α Structure*

	x	y	z
C	-0.032	0.087	0.077
C(O)	0.016	-0.045	0.25
O	0.095	-0.261	0.25

Table V. *Equivalent Positions of the Space Group Pbnm*[a]

x,	*y*,	*z*,	-*x*,	-*y*,	-*z*
½+*x*,	½-*y*,	½+*z*,	½-*x*,	½+*y*,	½-*z*
x,	*y*,	½-*z*,	-*x*,	-*y*,	½+*z*
½+*x*,	½-*y*,	-*z*,	-*x*,	½+*y*,	*z*

[a] All other atoms in the unit cell can be generated by applying the symmetry operations of this space group.

Plots of the POK-α structure are given in Figures 7 and 8. Also a plot of the structure of Chatani et al.[42] (POK-β) is displayed (Fig. 9). Comparison of the structures reveals some interesting points. The calculated crystalline density of the POK-β structure is 1.297 g/cm^3, whereas the density of the POK-α structure is 1.383 g/cm^3. The conformation of the polymer backbone is identical for the two structures; however, the packing is rather different. This difference can be attributed to the different orientation of the carbonyl groups of the centre chain relative to the corner chains. The angle between the molecular plane and the *bc* plane is 26° for the POK-α structure and 40° for the POK-β structure. In POK-α the symmetry operation relating corner and centre chain is ½-*x*, ½+*y*, *z*, whereas for the POK-β structure this operation is ½+*x*, ½-*y*, *z*. Hence, the difference between the two structures can be described by a rotation of the centre chain through an angle of approximately 180° about the chain axis or equivalently by a translation of the centre chain over half the fiber-axis unit cell length. For the POK-α structure all carbonyl dipoles point in about the same direction at equal height *z*, whereas in the POK-β structure the dipole of the carbonyl group of the corner and the centre chain point in different directions. Therefore, the packing in the POK-α structure is very effective. The cross-sectional area of the unit cell perpendicular to the fiber axis amounts to 35.2 Å^2, which is even smaller than for the polyethylene unit cell[43,44] (36.2 Å^2).

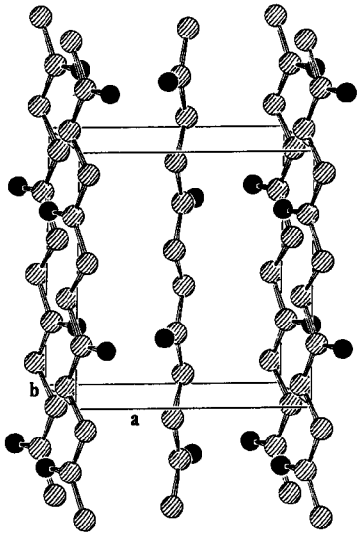

Figure 7. *View of crystal structure (POK-α) of perfectly alternating ethylene-carbon monoxide copolymer (fiber, c-axis is vertical).*

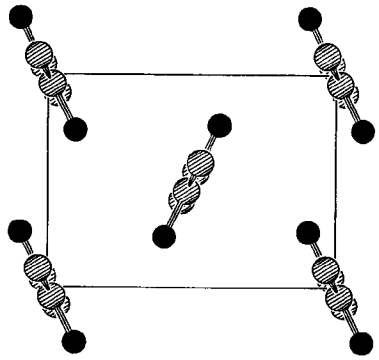

Figure 8. *ab Projection of POK-α unit cell.*

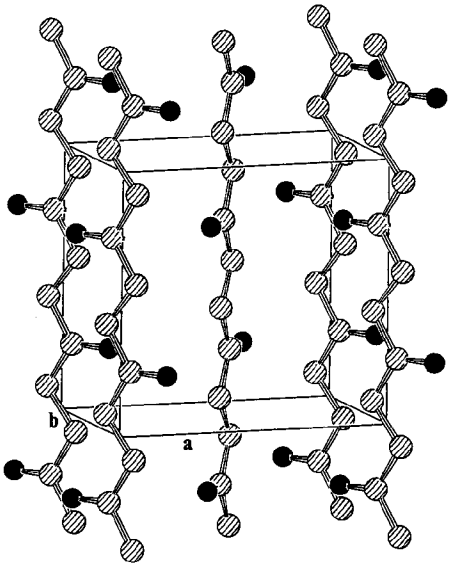

Figure 9. *View of POK-β crystal structure of polyketone, as determined by Chatani et al.*[26] *(fiber, c-axis vertical).*

Table VI. *Contact Distances (Å) Between Neighbouring Carbonyl Groups*

Contact	POK-α	POK-β
C—C	4.12	4.42
O—O	3.34	3.99
C—O	3.05	3.38

The occurrence of the POK-β structure, observed by Chatani et al.,[26] may have been the result of molecular defects in the polymer chain. The POK-β packing is less dense than the POK-α packing, as is obvious from an increased cross-section of 37.9 Å². The intermolecular distances (see Table VI) in the POK-α structure are smaller than in the POK-β structure.

-Melting

The melting point of ethylene-carbon monoxide copolymers has been a subject of discussion among three groups.[4,5,26,45] Chatani et al.[26] stated that the slight difference in the melting point of the copolymer they studied with respect to polyethylene can be attributed partly to a decrease in rotational freedom, due to the presence of the carbonyl group. Starkweather[5] determined a heat of fusion of 134 J/g. (2.5 kJ/mol chain atoms) from a series of non-alternating ethylene-carbon monoxide copolymers by applying the Flory-Huggins copolymer melting point relation[46]. On the basis of this result, he stated that the high melting point of the perfectly alternating copolymer (244 °C) is due to the low entropy of fusion, which was reported to be about 60 % of the value found for polyethylene per mol of chain atoms. Starkweather's results do not coincide with those of Wittwer et al.[45] The latter authors have developed a rotational isomeric state scheme and concluded that on the basis of the results of their calculations, the unperturbed chain dimensions are of the same order of magnitude as those of a polyethylene chain. Hence, to a first approximation the entropy change upon melting can be taken equal to that for polyethylene and the high melting point must, accordingly, be attributed to a high packing energy in the crystal. According to their results, this high packing energy is also reflected in the low solubility of the perfectly alternating polyketone copolymer.

In order to gain a clear insight into the melting behaviour of the perfectly alternating copolymer we have scrutinized melting data for a series of low-molecular-weight polyketone homologs as given in Table VII. A rough approximation for the heat of fusion for crystals of infinite chain lenght can be obtained by following a procedure similar to that described by Garner et al.[48] for polyethylene. The heats of fusion for the low-molecular-weight (symmetrical) homologs are extrapolated towards zero

defects, where the fraction of defects is given by

$$x_{defect} = \frac{2}{N_{C\text{-}atoms}} \quad (1)$$

where $N_{C\text{-}atoms}$ is the number of carbon atoms in the chain.

Table VII. *Enthalpy and Entropy of Fusion of Low-Molecular-Weight Polyethylene and (Symmetrical) Polyketone Homologs*

	ΔH_f kJ/mole Chain Atoms		ΔS_f J/mole Chain Atoms · K	
	Olefins	Olefin Ketones	Olefins	Olefin Ketones
C_3	1.2	1.9	12.8	10.6
C_5	1.7	2.0	11.7	8.8
C_6	2.2	2.9	12.2	10.8
C_{10}	2.9	-	11.8	-
C_{11}	2.0	3.1	8.2	8.6
C_{12}	3.0	-	11.5	-
C_∞	4.1	4-6	9.9	7.3

Heats of fusion of the olefin ketones C_5-C_{11} (3-pentanone, 2,5-hexanedione and 3,6,9-undecanetrione) are determined by thermal analysis (scanning speed 20 °C/min) and the melting point of 3,6,9-undecanetrione is taken from ref. 33. Other data are taken from ref. 47.

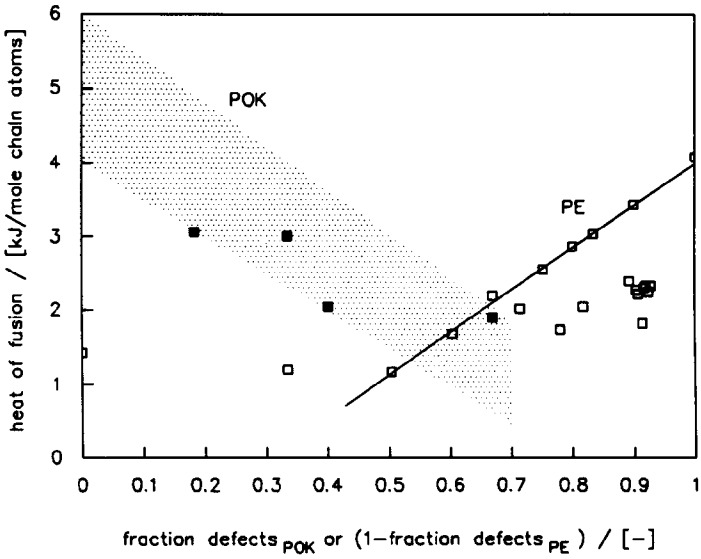

Figure 10. *Heats of fusion for low-molecular-weight polyketone and low-molecular-weight polyethylene homologs. (The shaded area indicates the range expected for higher molecular-weight polyketone homologs, solid line represents the heats of fusion for polyethylene homologs mainly with even number of chain atoms; (■) : Polyketone homologs (Table VII); (□) : Polyethylene homologs (ref. 47 and 50)).*

Though less pronounced, the effect observed for the heats of fusion is similar to the well-known odd-even effects for the heats of fusion of low-molecular-weight polyethylene homologs, as is shown in Figure 10. Although this effect can be attributed partly to the type of end-groups, viz. methyl or ethyl end-groups, crystal structure differences should also be considered.[49]. Therefore, the estimated value based on this rather small data set (i.e. 4 kJ/mol chain atoms) can be regarded as an underestimation. Because the end-group effect will diminish for higher molecular-weight compounds, the heat of fusion will converge to a higher and probably more

reliable value for crystals of infinite chain length (see Table VII).

In order to understand the significant discrepancy between the derived underestimated value and the value reported by Starkweather, an analysis based on the melting points of non-(perfectly) alternating polyolefin ketones (data set ref. 5) and terpolymers containing propylene-carbon monoxide and ethylene-carbon monoxide units (data set ref. 51) has also been carried out. The latter data set is verified by means of ^{1}H-NMR-analysis in d^6-phenol for two terpolymer samples and the data of both sets are plotted in Figure 11, where the fraction of defects in the terpolymers is calculated from the number of ethylene and propylene units,

$$x_{defect}=\frac{N_{propene}}{N_{ethene}+N_{propene}} \tag{2}$$

whereas the fraction of defects in imperfectly alternating copolymers is given by

$$x_{defect}=\frac{N_{ethene}-N_{CO}}{N_{ethene}} \tag{3}$$

A regression analysis has been conducted using both data sets by applying the Flory-Huggins copolymer melting point relation,[46]

$$\frac{1}{T_m}-\frac{1}{T_m^0}=-\frac{R}{\Delta H_f}\ln(1-x_{defect}) \tag{4}$$

and this regression resulted again in too low a value (2.23 kJ/mol chain atoms for $x_{defect}<0.4$, $r^2=0.992$) for the crystalline heat of fusion. This result gives rise to the conclusion that, notwithstanding the good correlation, Flory's lattice theory is not applicable for describing the melting point depression caused by the incorporation of molecular defects for polyketone polymers, at least for the examples evaluated.

According to Bunn and Peiser[52] the carbonyl group can be incorporated in low concentrations into the crystal lattice of polyethylene without inducing structural changes and evidence for this is presented by Chatani et al.[42] More elaborated models have been reported to describe the thermodynamics of the partial exclusion of molecular defects from the crystalline phase; [53-56] but these models require extensive data on the crystallization kinetics of the copolymers and terpolymers in order to derive a value for the excess free energy for the different type of defects.

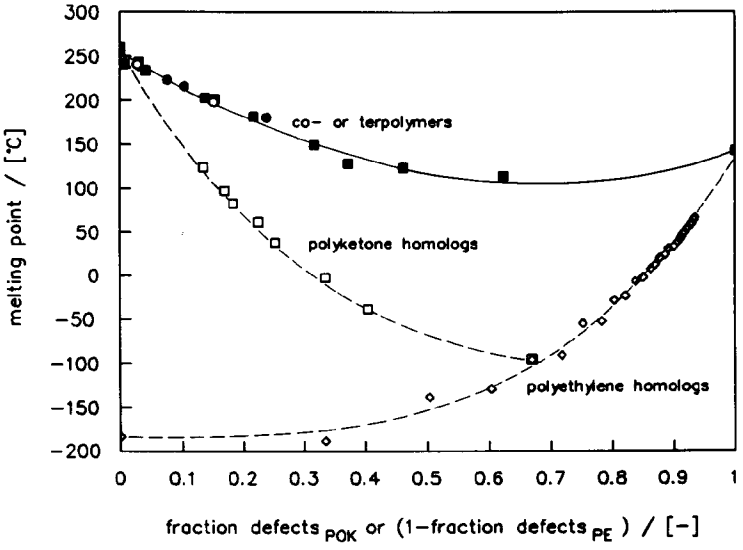

Figure 11. *Melting points of imperfectly alternating ethylene-carbon monoxide copolymers (solid line), ethylene-carbon monoxide/propylene-carbon monoxide terpolymers, low-molecular-weight (symmetrical) polyketone ($<C_{16}$) and polyethylene homologs ($<C_{30}$). ((■) : Imperfectly alternating ethylene-carbon monoxide copolymers (refs. 5 and 50); (●) : Ethylene-carbon monoxide/propylene-carbon monoxide terpolymers (ref. 51); (○) : thermal and ^{1}H-NMR analysis; (□) : Polyketone low-molecular-weight homologs (refs. 28, 33 and 47); (◇) : Polyethylene low-molecular-weight homologs (refs. 47 and 50)).*

Wu and Ovenall[57] have shown that chain branching can occur in non-alternating polyketones. However, branching does not seem to be an important aspect for the imperfectly alternating polyketones prepared by radical induced copolymerization, because the melting point depression is comparable with that of the unbranched ethylene-CO/propylene-CO terpolymers (see Figure 11).

Melting points of the low-molecular-weight polyketone homologs are depicted in Figure 11. Again a slight, though consistent, end-group effect on the melting point is observed. Flory and Vrij[58] derived a thermodynamic expression, which relates the melting point to the number of atoms in the polymer chain. We will use the simplified expression [eq.(5)], introduced by Hay,[59] to establish a heat of fusion for crystals of infinite chain length (ΔH_f):

$$T_m = T_m^0\left(1 - \frac{2RT_m^0}{\Delta H_f}\frac{\ln(N)}{N}\right) \qquad (5)$$

The heat of fusion calculated by this method is sensitive to the value for the equilibrium melting temperature (T_m^0). For polyethylene it is known that the melting temperature for well-oriented crystalline material is a good approximation for the actual equilibrium melting temperature.[60,61] Therefore, the maximum measured melting temperature for the highly drawn fiber, i.e 278 °C, is substituted in eq. (5). It should be remarked that for most polymers a linear correlation is only obtained for $\ln(N)/N < 0.2$. For low- molecular-weight homologs of polyethylene and polyketone, the relation between $T_m/2R(T_m^0)^2$ and $\ln(N)/N$ can be well described with the help of a third-order polynome (r_{PE}^2= 0.993 and r_{POK}^2=1.000). In the case of polyethylene, higher molecular-weight homologs (up to C_{29}) were included in the regression analysis in order to diminish the discontinuities caused by strong odd-even effects (see Figure 12). From the initial slope at $\ln(N)/N=0$ the heat of fusion is calculated, resulting in $\Delta H_{f(POK)}$=6.2 and $\Delta H_{f(PE)}$=4.7 kJ/mol chain atoms (330 and 340 J/g, respectively). Despite the broad extrapolation range, the latter value is in good agreement with the well-accepted value for the heat of fusion of polyethylene[50] (i.e., 4.1 kJ/mol chain

atoms (293 J/g)). Therefore, this procedure results in slightly overestimated values and taking the extrapolation based on the measured heats of fusion for the low-molecular-weight polyketone homologs into account, the true value for $\Delta H_{f(POK)}$ is expected to be between 4 and 6.2 kJ/mol chain atoms (215-330 J/g).

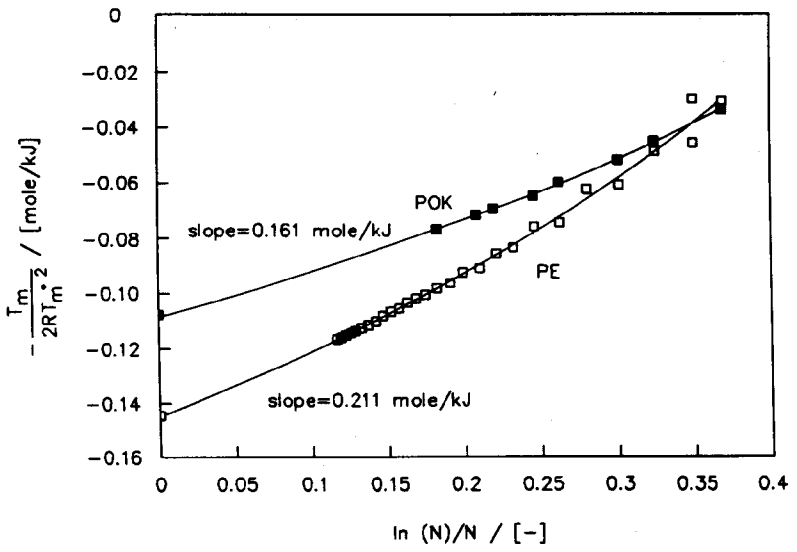

Figure 12. *Melting point analysis for low-molecular-weight (symmetrical) polyketone and polyethylene homologs (T_m°(POK)=278 °C and T_m°(PE)=141.4 °C for N→∞; (■) : Polyketone homologs (refs. 28,33 and 47); (□) : Polyethylene homologs (refs. 47 and 50).*

Both crystal structures POK-α and POK-β show a high packing fraction (i.e., the fraction of volume in the unit cell occupied by the atoms). The packing fraction for the POK-α structure (78 %, calculated using the method described by Wunderlich[62]) is to our knowledge the highest ever observed for organic polymers. This remarkably high

packing fraction is a result of the arrangement of the dipoles of the carbonyl groups in the crystal lattice (see Figure 7). Because of the strong electrostatic interactions the packing energy for both structures will be high. However, not all dipole interactions will disappear upon melting, but to what extend this will affect enthalpy of fusion and the entropy of fusion is unclear.

Table VIII. *Melting Data for Some Flexible Chain Polymers*

	ΔH_f [kJ/mole.Chain Atoms]	T_m [K]	ΔS_f [J/mole . K]	Packing Fraction [-]
POK-low	4	551	7.3	0.78 (α)
				0.73 (β)
PEO	2.9	342	8.4	0.65
PE	4.1	415	9.9	0.60
PG	3.7	506	11.0	0.72
POK-high	6.2	551	11.3	0.78 (α)
				0.73 (β)

Source: ref. 50. (PEO,Polyethylene oxide; PG,Polyglycolic acid).

Therefore, a compilation is made in Table VIII of the results of the extrapolations for the low-molecular-weight polyketone homolog series and melting data for several other polymers. The estimated range for the entropy of fusion covers the range expected for flexible chain polymers. All-carbon backbone macromolecules with all-*trans* conformations in the crystalline state show a significant volume change upon melting, which can be understood in terms of the difference in packing fraction in the

crystalline state and the amorphous state at room temperature. Both the POK-α and the POK-β crystal structure show an all-*trans* conformation of the polymer backbone and therefore the change in packing fraction upon melting is expected to be similar to the value for polyethylene and polyglycolic acid[50] for which these changes amount to 14 and 11 %, respectively.

The change in packing fraction upon melting will be reflected in a high entropy of fusion, and the true value for the heat of fusion will likely be at the upper end of the 4-6.2 kJ/(mol chain atoms) range. Therefore, the high melting point of the perfectly alternating copolymer is not due to a low entropy of fusion but to a (very) high enthalpy of fusion.

-Polyketone as a Starting Material for Fibers

From the presented crystal structure, a first approximation to the theoretical chain modulus can be derived simply by substituting an all-*trans* polyethylene chain in the POK-α unit cell. Values for the theoretical modulus of polyethylene are reported in the literature, but show a considerable variation (186-380 GPa[63-67]). Maximum Young's moduli up to 264 GPa can be achieved nowadays after hot drawing a gelspun polyethylene fiber.[68,69] Therefore, a value for the theoretical modulus amounting to 350 GPa, which is based on experimental results obtained by Fanconi and Rabolt,[67] seems to predict the theoretical modulus of polyethylene most realistically. Correction of this value for the slightly lower cross-section of the POK-α unit cell compared with the cross-section of the polyethylene unit cell leads to a prediction of a theoretical modulus of 360 GPa for the perfectly alternating copolymer. In this approach the elastic constants for the two bond types are taken equal, as in the case of polyethylene.

The crystallinity of the oriented fibers can be calculated from the enthalpy of fusion. For the highly drawn fiber (185 J/g) the crystallinity will be between 55 and 85 %. On the basis of our experience with other gelspun flexible chain polymers (e.g., polyamide 6 and polyvinyl alcohol), this value is reasonable. For an estimate of the crystallinity on the basis of the measured density of the drawn fiber (i.e., 1.32 g/cm^3) the

amorphous density is required. Based on the estimated crystallinity of oriented POK-C_2 fibers an amorphous density (ρ_a) of 1.2 g/cm^3 is obtained after substitution of ρ_c=1.38 g/cm^3, ρ=1.32 g/cm^3 and X_c = 0.7 in expression (6).

$$X_c = \frac{\rho - \rho_a}{\rho_c - \rho_a} \qquad (6)$$

As in the case of polyethylene, the amorphous density at room temperature is approximately 15 % less than the crystalline density. The estimate for the amorphous density of polyketone is consistent with the expected difference between the crystalline density and the amorphous density at room temperature.

Another interesting feature of polyketone fibers is the presence of strong lateral forces due to the dipole interactions of the carbonyl groups. It was concluded that the high melting point is a result of the strong lateral forces in the crystal. Moreover, increased lateral forces will improve properties governed by the interactions in transversal direction of the fibers (e.g., compressive strength and creep resistance).

2.5 Conclusions

The perfectly alternating polyketone copolymer is an interesting starting material for fiber applications. The crystal structure of this polymer was determined and turns out to have a very dense packing. Owing to the all-*trans* conformation of the polymer chain in the crystal lattice and the small chain cross-section, high moduli can be achieved in well-oriented crystalline material. The crystallinity in oriented fibers will exceed 50 %. Rather strong interactions between the polymer chains result in a high melting point of the material, whereas the mechanical properties governed by transverse interactions (e.g., creep resistance and compressive strength) will be superior to those of polyethylene fibers.

2.6 References and Notes

1. B. Kalb and A.J. Pennings, *Polym. Bull.*, **1,** 871 (1979).
2. P. Smith, P.J. Lemstra, B. Kalb and A.J. Pennings, *Polym. Bull.*, **1,** 733 (1979).
3. P. Smith and P.J. Lemstra, *J. Mater. Sci.*, **15,** 505 (1980).
4. H. Starkweather, in *Encyclopedia of Polymer Science and Engineering,* 2th ed., Vol. 10, *Olefin-Carbon Monoxide Copolymers,* John Wiley, New York, (1987).
5. H.W. Starkweather, *J. Polym. Sci. Polym. Phys. Ed.*, **15,** 247 (1977).
6. R.M. Ward and D.C. Kelley, *Tappi J.*, **71**(6), 140 (1988).
7. W.P. Bremer, *Polym. Plat. Technol. Eng.*, **18**(2), 137 (1982).
8. R. Leaversuch, *Mod. Plast. Int.*, **17**(10), 94 (1987).
9. The Budweiser "six-pack" yokes analysed were bought during the Gordon Research Conference "Fiber Science":, New London (NH), U.S.A., July 1-5, (1991).
10. R. Gooden, D.D. Davis, M.Y. Hellman, A.J. Lovinger and F.H. Winslow, *Macromolecules,* **21,** 1212 (1988).
11. G.H. Hartley and J.E. Guillet, *Macromolecules,* **1,** 165 (1968).
12. G.H. Hartley and J.E. Guillet, *Macromolecules,* **1,** 413 (1968).
13. M. Heskins and J.E. Guillet, *Macromolecules,* **3,** 224 (1970).
14. F. Ballauf, O. Bayer and L. Teichmann, German Patent 863,711 (Bayer), (1941).
15. British Patent 583,172 (Imperial Chemical Industries), (1946).
16. M.M. Brubaker, U.S. Patent 2,495,286 (Du Pont), (1950).
17. M.M. Brubaker, D.D. Coffman and H.H. Hoehn, *J. Am. Chem. Soc.*, **74,** 1509 (1952).
18. P. Colombo, L.E. Kukacka, J. Fontana, R.N. Chapman and M. Steinberg, *J. Polym. Sci. Part A-1,* **4,** 29 (1966).
19. K. Nozaki and E. Cerrito, U.S. Patent 3,689,460 (Shell), (1972).
20. K. Nozaki, U.S. Patent 3,835,123 (Shell), (1974).
21. J.S. Brumbaugh, R.R. Whittle, M. Parvez and A. Sen, *Organometallics,* **9,** 1735 (1990).
22. A. Sen and T-W. Lai, *J. Am. Chem. Soc.*, **104,** 3520 (1982).
23. T-W. Lai and A. Sen, *Organometallics,* **3,** 866 (1984).

24. A. Sen, in *Advances in Polymer Science,* Vol. 73/74, *The Copolymerization of Carbon Monoxide with Olefins,* Springer-Verlag, Berlin, (1986).
25. A. Sen, *Chemtech* **1986,** 48.
26. Y. Chatani, T. Takizawa, S. Murahashi, Y. Sakata and Y. Nishmura, *J. Polym. Sci.,* **55,** 811 (1961).
27. In order to avoid confusion with polyaryl ketones like PEEK and PEK we have abbreviated this polymer as polyolefin ketone; POK.
28. E. Drent, European Patent 121,965 (Shell), (1984).
29. E. Drent, J.A.M. v. Broekhoven and M.J: Doyle, *J. Organomet. Chem.,* **417,** 235 (1991).
30. B.J. Lommerts, J. Smook, B. Krins, A. Piotrowski and E. Band, European Patent 456,306 (Akzo), (1989).
31. J.A.M. Broekhoven and R.L. Wife, European Patent 257,663 (Shell), (1987).
32. M.J. Doyle, J.C. Van Ravenswaay-Claasen, G.G. Rosenbrand and R.L. Wife, European Patent 248,483 (Shell), (1987).
33. H. Stetter, W. Basse, H. Kuhlman, A. Landscheidt and W. Schenkler, *Chem. Ber.,* **110,** 1007 (1977).
34. G. Hoentjen and A.J. Witteveen, Internal report Akzo, 3,6,9-undecanetrione was prepared according to a similar synthesis route as described in ref. 35.
35. R. Ballini, M. Petrini, E. Marcantoni and G. Rosini, *Synthesis,* **1988,** 231.
36. J.A.M. van Broekhoven, E. Drent and E. Klei, European Patent 213,671 (Shell), (1986).
37. M.H. Abraham, P.L. Grellier, J-L.M. Abboud, R.M. Doherty and R.W. Taft, *Can. J. Chem.,* **66,** 2673 (1988).
38. U. Hauer, W. Freiberg and C-F Kröger, *Z. Chem.,* **24**(4), 147 (1983).
39. A.X. Zhao and J.C.W. Chien, *Macromolecules* (submitted).
40. E.G. Chepaikin, A.P. Bezruchenko, G.P. Belov, G.N. Boiko, B.B. Tarasov and S.Y. Tkachenko, *Vysokomol. Soedin., Ser. B,* **32**(8), 593 (1990).
41. *International Tables for X-ray Crystallography,* Kynoch Press, Birmingham, England, (1965).
42. Y. Chatani, T. Takizawa and S. Murahashi, *J. Polym. Sci.,* **62,** S27 (1962).
43. C.W. Bunn, *Trans. Faraday Soc.,* **35,** 492 (1939).

44. E.R. Walter and F.P. Reding, *J. Polym. Sci.*, **21,** 561 (1956).
45. H. Wittwer, P. Pino and U.W. Suter, *Macromolecules,* **21,** 1262 (1988).
46. P.J. Flory, *Principles of Polymer Chemistry,* Cornell University Press, Ithaca, New York, (1953).
47. *Handbook of Chemistry and Physics,* 63th ed., CRC Press, Boca Raton, FL, (1982).
48. W.E. Garner, F.C. Madden and J.E. Rushbrooke, *J. Chem. Soc. London,* **2491,** (1926).
49. M.G. Broadhurst, *J. Chem. Phys.*, **36,** 2578 (1962).
50. B. Wunderlich, *Macromolecular Physics,* Volume III, *Crystal Melting,* Academic Press, New York, 1980.
51. J.A.M. van Broekhoven, E. Drent and E. Klei, European Patent 213,671 (Shell), (1986).
52. C.W. Bunn and H.S. Peiser, *Nature,* **159,** 161 (1947).
53. I.C. Sanchez and R.K. Eby, *J. Res. Natl. Bur. Stand., Sect. A,* **77,** 353 (1973).
54. I.C. Sanchez and R.K. Eby, *Macromolecules,* **8,** 638 (1975).
55. G. Goldbeck-Wood and D.M. Sadler, *Polym. Commun.*, **31,** 143 (1990).
56. G. Goldbeck-Wood, *Polymer,* **31,** 586 (1990).
57. T.K. Wu and D.W. Ovenall, *ACS Polym. Prepr.*, **17,** 693 (1976).
58. P.J. Flory and A. Vrij, *J. Am. Chem. Soc.*, **85,** 3548 (1963).
59. J.N. Hay, *J. Polym. Sci. Polym. Chem. Ed.*, **14,** 2845 (1976).
60. J. Smook, Ph.D. thesis, University of Groningen, The Netherlands (1984).
61. J. Smook and A.J. Pennings, *Coll. Pol. Sci.*, **262,** 712 (1984).
62. B. Wunderlich, *Macromolecular Physics,* Vol.1, *Crystal Structure, Morphology, Defects,* Academic Press, New York, (1973).
63. L.R.G. Treloar, *Polymer,* **1,** 95 (1960).
64. R.P. Wool, R.S. Bretzlaff, B.Y. Li, C.H. Wang and R.H. Boyd, *J. Polym. Sci. Polym. Phys. Ed.*, **24,** 1039 (1986).
65. R.L. McCullough, A.J. Eisenstein and D.F. Weikart, *J. Polym. Sci. Polym. Phys. Ed.*, **15,** 1837 (1977).
66. P.A. Irvine and P. Smith, *Macromolecules,* **19,** 240 (1986).
67. B. Fanconi and J.F. Rabolt, *J. Polym. Sci. Polym. Phys. Ed.*, **23,** 1201 (1985).

68. H. v.d. Werff, Ph.D. thesis, University of Groningen, The Netherlands (1991).

69. H. v.d. Werff and A.J. Pennings, *Coll. Pol. Sci.*, **269,** 747 (1991).

Chapter 3.

PREPARATION OF HIGH-STRENGTH POLYKETONE FIBERS

Reproduced from:
B.J. Lommerts, H. ter Maat, and R. Huisman, *Polymer (submitted for publication).*

3.1 Summary

High-strength fibers are prepared by spinning high-molecular-weight perfectly-alternating ethylene-carbon monoxide copolymer from phenolic solutions followed by solid-state drawing at elevated temperatures. The maximum tensile strength attained for highly oriented fibers is 3.8-3.9 GPa. The initial tensile modulus is strongly dependent on the drawing temperature, which can be explained by the semi-crystalline nature of the polyketone. Fibers with a high elongation at break are prepared by allowing some orientation relaxation within non-crystalline domains. Unrelaxed fully oriented high-strength fibers show an elongation at break of 4-5 % and an initial tensile modulus of 50-55 GPa. As a result of relaxation the elongation at break can be increased to 7-8 %, at the expense of a lower modulus (40-45 GPa). The maximum attainable draw ratio is limited to a value of 26, and above a draw ratio of 17 the formation of cracks in the material was encountered. The temperature has a pronounced positive effect on the drawability, but the maximum temperature for efficient draw is limited by the onset of melting. When crystals start to melt a deterioration in lateral stress transfer between the chains sets in, and as a result less effective orientation is observed due to slippage of chain ends through entanglements.

3.2 Introduction

Solid-state drawing is a common technique to induce molecular orientation in flexible polymer systems. It is well-known that the tensile modulus of polymer fibers is governed by the degree of molecular orientation in the direction of deformation.[1-3] For

non-polar polymers (e.g., polyethylene) the orientability is strongly influenced by the amount of remnant topological defects in the material, which can be altered by rearrangement of macromolecules in solution.[4] The latter is controlled by the initial polymer concentration, since by a dilution of these topological interactions the contour length between network nodes (e.g., entanglements) is increased. During fiber spinning a low entanglement density present in semi-dilute solutions can effectively be preserved in the solid-state by means of gelation crystallization.

In addition to the influence of the dissolution conditions, the maximum attainable draw ratio is also dependent on the nature of the lateral (polar) interactions between the chains.[5] The deformation of polymers requires a certain mobility within the network to accomodate large strains. Because of the complexity of the molecular rearrangement upon large-scale deformation, we proposed recently that the polarity dominates the effectiveness of entanglement transport through and along the formed oriented fibrillar structures.[6] A reduction in the effective number of topological interchain couplings will increase the contour length between network nodes, resulting in appreciably higher draw ratios. This process requires the dissociation of lateral bonds between the chains, which is more likely to occur in a less polar environment and/or at elevated temperatures. Hence, in this respect non-polar polymers are favored for achieving high degrees of orientation at the obvious expense of high-temperature performance, creep properties and compressive strength.

Polymers with intermediate polarity, like poly(vinyl alcohol), can also be drawn to satisfactory ratios (λ_{max}>30) and good tensile properties have been reported.[7] An additional advantage of these materials is the relatively high melting temperature, which makes them more suited for advanced industrial applications.

In the present thesis, we have focussed our efforts on a new, moderately polar polymer (i.e., the perfectly alternating ethylene-carbon monoxide copolymer (polyketone-C_2; POK-C_2)).[8] A first approximation for the theoretical chain modulus of this material gave a high value (360 GPa) compared to other moderately polar flexible polymers.[9] Due to the strong electrostatic interactions between the carbonyl

groups, the packing of the chains in the crystal lattice is very dense, and the cross section of the polyketone (POK-α) crystal unit cell (35.2 Å^2) is even smaller than that of the polyethylene unit cell (36.2 Å^2). In addition to its high melting temperature (260 °C), this polymer exhibits some other favorable characteristics for fiber applications, viz. good adhesion properties and a satisfactory creep resistance. Due to the limited thermal stability of the 1,4-arrangement of carbonyls, high-melting polyketones seem to suffer from degradation during meltprocessing. Therefore, at present we restricted ourselves to solution spun fibers (i.e., high-molecular-weight fibers in which the entanglement density has been reduced). Oriented fibers were prepared from phenolic solutions followed by solid-state drawing at elevated temperatures. The aim of the present investigations is to gain insight into the mechanism of chain alignment in order to produce high strength polyketone fibers.

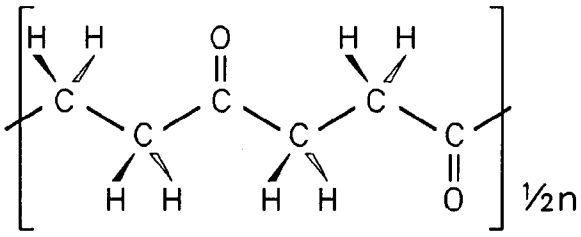

Figure 1. *Perfectly alternating ethylene-carbon monoxide copolymer (polyketone).*

3.3 Experimental

-Spinning

Perfectly alternating copolymers can be synthesized from ethylene and carbon monoxide using a *cis*-fixed palladium bidentate catalyst system.[8] Polyketones are not commercially available and the polymer was, therefore, produced according to the procedure given in ref. 10. Some variation in molecular weight occurred between different batches. The intrinsic viscosity (*m*-cresol, 25 °C) of the samples used ranges

from 4.6 to 6.1 dL/g, corresponding to a molecular weight of 300,000 to 420,000 kg/kmol.[11] In the present work, we observed that this limited variation in molecular weight had no significant effect on the properties studied.

A representative description of the solution spinning method applied follows. Polyketone fibers were prepared from thoroughly homogenized semi-dilute (9-15 wt-%) solutions in phenol.[12] A small amount of acetone was added in order to avoid the interference of solvent crystallization with the fiber formation process. These solutions were dry-jet-wet spun at 70 °C through capillaries of 250 μm into an acetone cooling/coagulation bath (-5 °C), and fibers were collected on a bobbin at a winding speed of 1 m/min. Relaxation in both the air-gap as well as in the swollen state was allowed to avoid preferential molecular orientation in the as-spun material.

-Drawing

Thoroughly washed and dried fibers were subjected to tensile drawing at elevated temperatures. The elongation at break of unoriented material (ϵ_b) was determined at various temperatures and at an initial draw rate of 100 %/min (0.017 s^{-1}) and 1000 %/min (0.17 s^{-1}), using a horizontal tensile tester equipped with an oven. The maximum draw ratio ($\lambda_{max}=\epsilon_b+1$) was derived from the average value for the elongation at break of at least 20 single filaments. The same tensile tester was applied to prepare short fiber samples at a draw rate of 100 %/min. In this batchwise drawing process the stretching was stopped at the required draw ratio, and the sample was cooled to room temperature under tension. In some cases, the tension upon cooling was lowered, whereby some orientation relaxation was allowed.

Yarn samples were also continuously drawn to various ratios at a yarn feeding speed of 1 and 10 mm/s using hot plates, and the temperature of the plates was measured using a contact thermocouple. The drawing stress was measured on-line using a Schmidt™ Yarn Tension Meter (0-5 N). The maximum attainable draw ratio in our single stage continuous drawing procedure was limited to a value of 13. Therefore, a second stage was applied to achieve higher draw ratios ($\lambda=\lambda_1 \cdot \lambda_2$ with $\lambda_1=9.5$). The deformation in the first drawing stage occurred in a high temperature trajectory of

about 4 cm. In this case the draw rate was derived from the residence time of the yarn in the deformation zone assuming a linear velocity profile. Experiments were also carried out at a suffiently high temperature that partial melting occurred (i.e., T_{draw}=247 °C). In order to avoid premature sample failure due to melting, somewhat higher draw rates were applied (i.e., a feeding speed of 20 mm/s).

-Analysis

Prior to testing, the oriented yarns were conditioned for at least 24 hours at 21 °C and 65 % relative humidity. The tensile tests were performed on single filament samples using an Instron Tensile Tester, equipped with pneumatic clamps (type 3A) covered with Arnitel™ faces. The gauge length was 500 mm and the cross-head speed 50 mm/min (10 %/min). All tensile measurements were repeated five times.

Differential scanning calorimetry was carried out in a nitrogen atmosphere at a scanning speed of 20 °C/min on about 1.5 mg of short pieces (5 mm) of fiber sample, using a Perkin Elmer™ DSC-7, equipped with a sample changer. The DSC was calibrated with indium (onset temperature 156.6°C) and zinc (onset temperature 417.5°C) test samples. Perkin Elmer™ software was used to derive the peak melting temperature and melting enthalpy from the recorded DSC trace.

A Kiessig camera and an x-ray tube with copper anode were employed to record the small angle x-ray diffraction pattern of highly oriented fibers. Long periods were calculated from the peak positions of the meridional reflection, using Bragg's formula.[13] Also, confocal laser scanning microscopic images were taken from the center section of the fiber using a Leica™ CLSM.

3.4 Results and Discussion

-Spinning and High Temperature Drawing

Semi-dilute solutions of polyketones (< 10 wt-%) in phenolic solvents do not crystallize at a rate sufficient for thermo-reversible gelation to occur on a time scale

corresponding to the residence time in the cooling trajectory of the spinning process. The diffusion of an appropriate non-solvent (e.g., a small polar organic molecule) enhances the crystallization rate and we succeeded in collecting fibers at practical winding speeds using acetone as the coagulation medium.

The maximum draw ratio (λ_{max}) of these solution spun polyketone fibers is dependent on the temperature, as is shown in Figure 2. The perfectly alternating ethylene-carbon monoxide copolymer exhibits a solid-solid phase transition from the POK-α (orthorhombic) to the POK-β (orthorhombic) crystal structure at 110-130 °C (see Fig. 3).[14,15] As is indicated in Figure 2, the change in packing of the chains affects the drawing behavior above the transition temperature (T^{-1}=0.0026 K^{-1}).

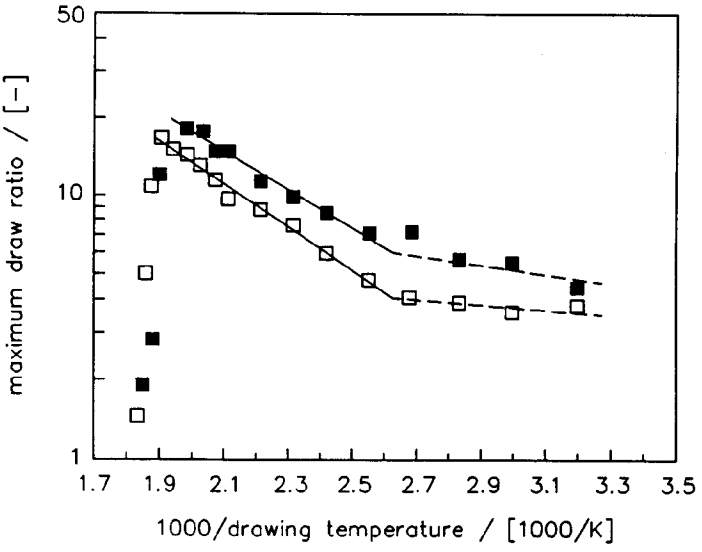

Figure 2. *The maximum attainable draw ratio for polyketone fibers vs temperature (M_w = 300,000 kg/kmol; fibers drawn batchwise, initial draw rate: 0.017 s^{-1} (■) and 0.17 s^{-1} (□)).*

At an initial deformation rate of 0.017 s^{-1}, a strong decline in drawability is observed above 225 °C (T^{-1}=0.002 K^{-1}). This temperature is 20-25 °C lower than the peak

melting temperature of as-spun fiber and coincides with the onset temperature of melting. Hence, the decline in drawability is associated with first melting phenomena of poorly formed (POK-β) crystals in unoriented material. To demonstrate the effect of (partial) melting on the drawing behavior, DSC traces of oriented polyketone yarns were recorded. The yarns were produced by orienting as-spun fiber via a continuous drawing operation using a hot plate and two roller sets.

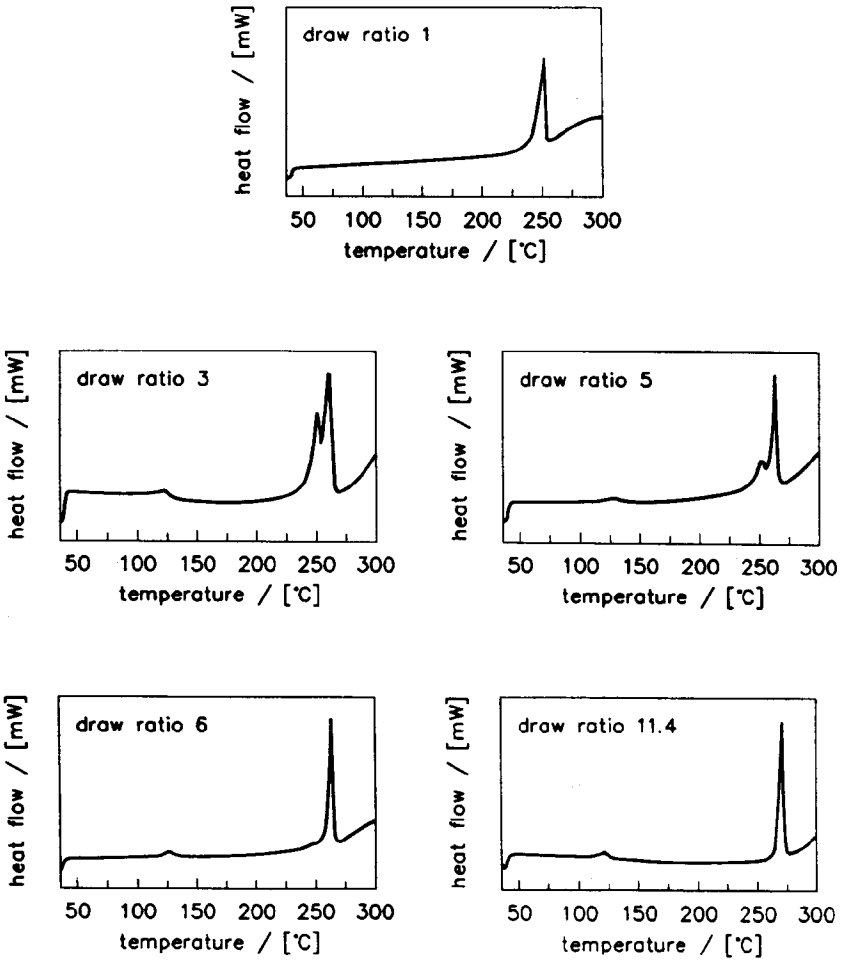

Figure 3. *Thermograms of polyketone fibers continuously drawn to various ratios at 247 °C (M_w = 340,000 kg/kmol: feeding speed was kept constant and in this series the draw rate increases from approximately 2 s^{-1} to 20 s^{-1}).*

The drawing temperature in this particular case was 247 °C (i.e., significantly above the onset of the melting endotherm) and in this series the rate of deformation was increased from approximately 2 s^{-1} to 20 s^{-1}. These deformation speeds allow the unoriented fibers to be processed under these conditions, as the onset of the decline in drawability is shifted toward higher temperatures at increasing draw rates (see Fig. 2). This shift can be attributed to a time-temperature superposition generally observed for macromolecular relaxation processes.[16] At low draw ratios two melting endotherms are observed; the first one at about the same temperature as for the undrawn material; the second one at slightly higher temperatures. The latter peak can be ascribed to melting of oriented (fibrillar) material, which shifts toward higher temperatures with increasing draw ratio. The endotherm at lower temperatures is due to melting of less extended lamellar-like crystals. In this series the fraction of low-melting material steadily decreases implying that during the deformation process an increasing amount of chains become elongated in the direction of orientation.

As is demonstrated in Figure 4, fibers drawn at somewhat lower temperatures (i.e., below 230 °C) show a continuous increase in melting temperature, viz. from about 250 °C for unoriented material (λ=1) to 273 °C for drawn fibers (λ=11).[17] For these oriented fibers no low-melting crystal population was observed in the thermograms. Generally, the increase in melting temperature upon stretching (i.e., orientation) can be explained by a reduction in surface free energy of the oblong-shaped crystals formed.[18] The presence of two populations of crystals in fibers prepared under partially molten conditions implies that under these circumstances the polymer network breaks up into different morphological entities. In melts or solutions of flexible polymers this phenomenon has been described using Taylor's meniscus instabilities.[19] When crystalline interactions diminish, stress transfer along the chains prevails. As a result, intermolecular stress transfer by means of topological interchain coupling (i.e., entanglements) becomes increasingly important.

High-strength polyethylene fibers are prepared from very high-molecular-weight polymer (M_w = $4 \cdot 10^6$ kg/kmol; m = 28 kg/kmol).[4] In comparison, the number of chain ends in the polyketone sample used (M_w = $3.4 \cdot 10^5$ kg/kmol; m = 56 kg/kmol) is high.

Network imperfections in the unoriented polyketone fiber cause that slippage of chain ends through entanglements occurs under the applied temperature conditions. Disentangled (unloaded) chain segments will recoil to gain conformational entropy leading to less extended lamellar-like (low-melting) crystals upon cooling. The lower fraction of low-melting material in the more oriented fibers suggests that the time scale on which these flow-related events take place is dominated by the complexity of the required reptation process.

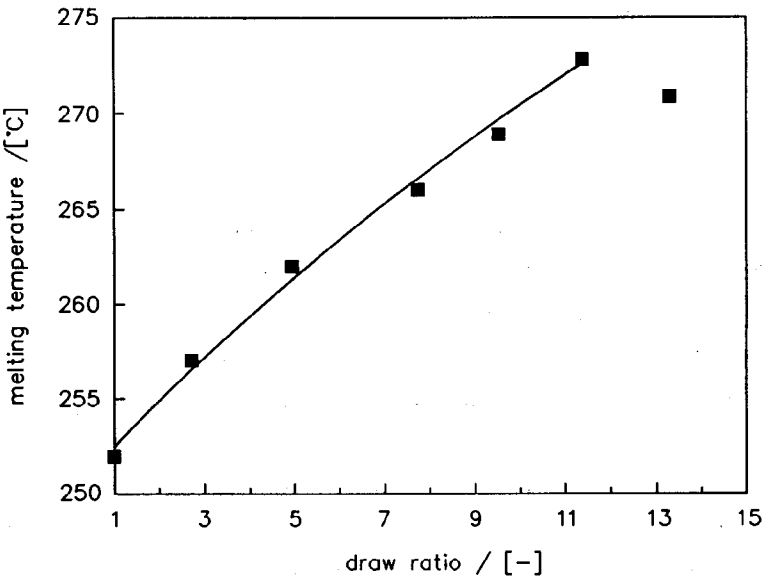

Figure 4. *Melting temperature of polyketone fibers (M_w = 420,000 kg/kmol) continuously drawn to various ratios slightly below the critical drawing temperature (230 °C). In a one stage drawing process fibers show "overdrawing" characteristics at λ>11.*

The elongational "solid-state" flow field is regarded to nucleate the formation of fibrils between entanglements,[20] which are still effective at the rate of deformation applied

to the *transient* network. The more extended chains between these entanglements will aggregate into the oblong-shaped fibrillar crystals, and, supposedly, the lamellar-like crystals will grow at somewhat lower temperatures epitaxially on the surface of these fibrils.[21] As a consequence, the fibrillar crystals will predominantly provide the stress transfer in this composite material.

These so-called "shish-kebab" composite structures[22,23] generally show a low tensile strength, due to the limited capacity for axial stress transfer. Also, a large amount of topological defects are incorporated into the polymer matrix surrounding the extended material, which contribute to local stress concentrations to occur upon loading.

-Tenacity Development

To improve the tensile strength of polyketone fibers the influence of the drawing temperature on the mechanical properties was investigated. As expected, the tenacity development is less for fibers oriented in a partially molten stage than for fibers drawn below the onset of first melting phenomena (see Fig. 5). Furthermore, these fibers do not show a pronounced "shish-kebab" composite structure as is evidenced by a single melting endotherm observed during thermal analysis (see Fig. 4). These findings clearly indicate that to prepare high-strength fibers from relatively low-molecular-weight polymers the drawing temperature should be lower than the onset temperature of the decline in the lateral stress transfer mechanism.

Due to the limited drawability at lower temperatures, however, premature damage (e.g., cracks) can be caused. This process, here referred to as "overdrawing", results in a shiny white, non-transparent appearance of the oriented fiber. The onset of the formation of cracks, as indicated by the arrows in Figure 5, is shifted toward higher temperatures according to a similar relation (see Fig. 2). These phenomena are not uniquely related to polyketone fibers and have been observed for a number of other flexible polymers as well.[24,25] Overdrawing is accompanied by a decreased tenacity development upon streching, whereas the increase in initial tensile modulus remains in line with the improved molecular orientation. In some cases, a drop in melting

temperature can also be observed, as is shown in Figure 4.

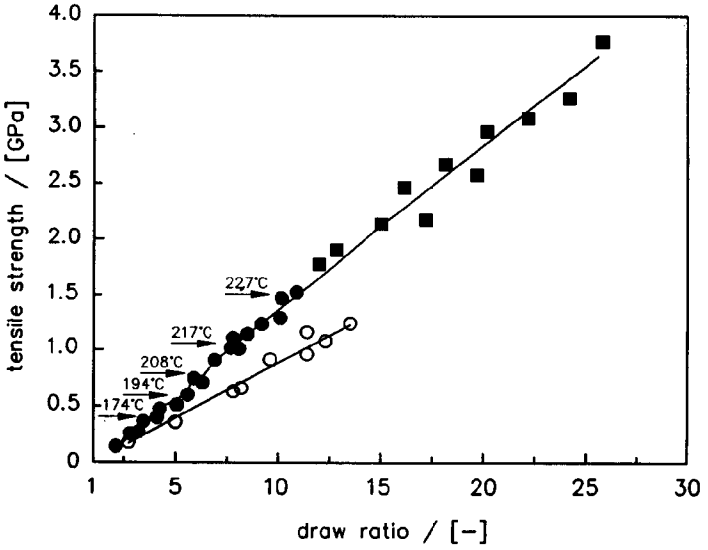

Figure 5. *Tensile strength of polyketone fibers drawn under different conditions at a feeding speed of 1 mm/s, the arrows indicate the onset of crack formation and for λ>17 only the maximum values are presented ((●) : fibers continuously drawn at T < 230 °C (M_w = 340,000 kg/kmol, fibers drawn according to a multi-stage procedure are not included); (○) : fibers continuously drawn at T = 234 °C (M_w = 340,000 kg/kmol); (■) : fibers drawn batchwise in two stages (M_w = 420,000 kg/kmol, initial draw rate 0.017 s^{-1}, T_1 = 225 °C (λ_1<10) and T_2 = 250 °C)).*

The introduction of morphological defects is reflected in a lower density of the material, due to the formation of voids. A confocal laser scanning microscopic image of an overdrawn polyketone sample is displayed in Figure 6. At low magnifications the cracks are visible as an irregular banded structure, where the bands are oriented perpendicular to the fiber axis. At higher magnifications, it becomes clear that the cracks have a similar appearance as crazes in glassy polymers.[26] The first stage is the lateral isolation of fibrils, which is associated with the formation of relatively large oblong-shaped voids. The formation of these voids is related to a premature fracture

mechanism initiating catastrophic failure of the sample. At higher strains, a larger number of fibrils propagating through the growing craze-like regions start to fail and cracks are formed. Ultimately, the few intact fibrils can not sustain the fiber load and the sample breaks. Obviously, these irreversible flaws in the fiber should be avoided, as they give rise to local stress concentrations in the material, which result in a deterioration of its mechanical performance, especially under dynamic conditions.

The tensile strength of "crack-free" fibers oriented at different temperatures between 170 and 230 °C is uniquely related to the draw ratio, pointing to a single deformation mechanism in this temperature regime. After the first drawing stage, the melting temperature of the material increases significantly (see Fig. 4), allowing the fibers to be processed at higher temperatures in subsequent stages. Accordingly, in a multi-stage drawing procedure the onset of crack formation is shifted toward higher draw ratios as is indicated in Figures 2 and 5.

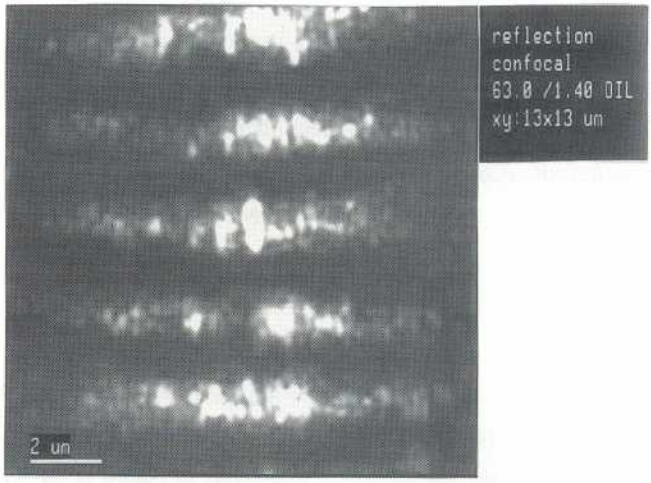

Figure 6. *Confocal microscopic image of an "overdrawn" polyketone fiber (fiber direction vertical, filament diameter is about 10 μm).*

In spite of the extensive work done to produce very high degrees of molecular alignment, like four-stage drawing or applying very low feeding speeds, we have not

been able to prepare crack-free fibers at draw ratios exceeding the value of 17 in a continuous fashion. Accordingly, the tensile strength of multi-filament yarns was limited to a value of 2.5-3 GPa. In order to investigate the development in mechanical properties at higher draw ratios, fibers were also prepared batchwise according to a two-stage procedure, and the results are included in Figure 5. In case of regularly drawn fibers (λ<17), the average values for the tensile strength of at least 5 independent single filament tests are presented. It should be noted, that we observed a broad distribution in tensile strength for fibers prepared at higher draw ratios (λ > 17), due to the statistical nature of the fracture process. In order to rule out the effects of local stress concentrations due to formation of voids, only the maximum values for the tensile strength of selected single filaments are presented in this draw ratio regime. The maximum attainable draw ratio of solution spun polyketone fibers seemed to be limited to a value of 26. At higher draw ratios the probability of fracture has became so high that it was impossible to produce single filaments with a length of more than 500 mm at an initial draw rate of 0.017 s^{-1}. The near to linear correlation between the tensile strength and the draw ratio indicates the effectiveness of the drawing procedure to induce molecular alignment at different temperatures below 230 °C. In the high draw ratio range the amount of load bearing molecules still gradually increases with the macroscopic degree of stretching; the large scatter in tensile strength data can be attributed to overdrawing.

The maximum attained tensile strength of 3.8 GPa for oriented polyketone is rather high, especially considering its low draw ratio (λ = 26). For example, for poly(vinyl alcohol) with comparable molecular weight (DP = 5,000), a tensile strength of 2.8 GPa has been reported for a highly drawn fiber (λ_{max} > 30).[7] The superior tensile strength of polyketone is attributed to a higher capacity for stress transfer (i.e., covalent linkages per unit of cross sectional area).

-Modulus Development

In contrast to the tensile strength of continuously drawn polyketone fibers, the initial tensile modulus [at room temperature] steadily decreases with the applied drawing temperature, as is shown in Figure 7.

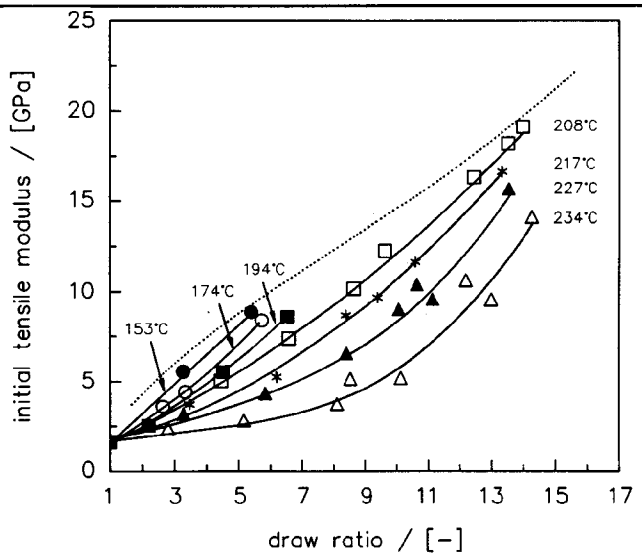

Figure 7. *The initial tensile modulus of polyketone fibers (M_w = 340,000 kg/kmol) continuously drawn at a feeding speed of 1 mm/s (drawing temperatures are indicated, the dashed line represents the modulus development under optimized conditions (see Figure 10)).*

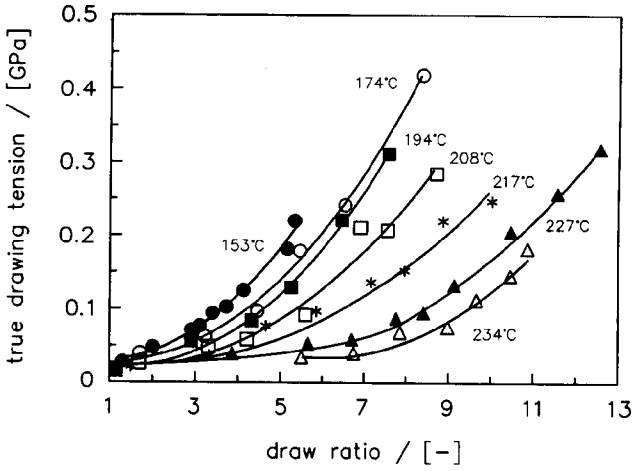

Figure 8. *True drawing tension vs the draw ratio; drawing temperatures are indicated. (As-spun fibers (M_w = 340,000 kg/kmol) continuously drawn at a feeding speed of 1 mm/s).*

This effect is related to the reduction in the drawing stress at higher temperatures (see Figure 8).

In Figure 9 a small angle x-ray (SAXS) pattern of an oriented polyketone fiber is displayed. The pronounced streaking on the equator can be attributed to longitudinal void scattering typical for highly drawn material. After prolonged exposure, the SAXS pattern also reveals a long period of about 190 Å, which is caused by density fluctuations within the material. The presence of a long period reflex implies that the material consists of a sequence of crystalline and less perfect or even non-crystalline (amorphous) domains in the axial direction of the fiber. This result demonstrates the semi-crystalline nature of the material and from a first approximation to the heat of fusion of perfectly crystalline material we estimate a crystallinity of 70-80 % for well-oriented polyketone fiber.[9]

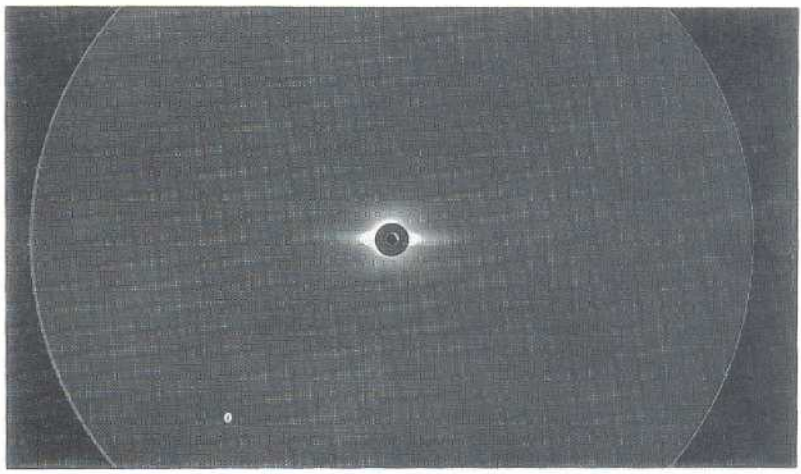

Figure 9. *Small angle x-ray pattern of an "overdrawn" polyketone fiber (λ = 19.5) showing longitudinal void scattering and a long period of about 190 Å. (Note the low intensity of the reflex on the meridian even after an exposure time of 1 day).*

The modulus of amorphous material at elevated temperatures and accordingly the macroscopic shrinkage forces are proportional to the thermal energy at a given temperature,[27] viz. RT. At high temperatures, the low tension acting on the fiber allows some orientation relaxation of chain segments in the amorphous rubber-like state resulting in a decrease in tensile modulus.

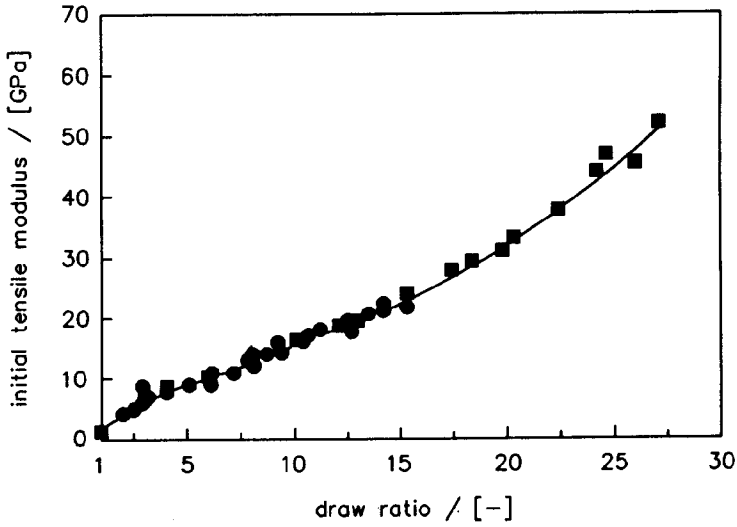

Figure 10. *The initial tensile modulus of polyketone fibers prepared under optimized drawing conditions ((●) : feeding speed of 10 mm/s (M_w = 340,000 kg/kmol, T_1 < 230 °C (λ_1<10) and T_2 = 245 °C); (■) : fibers drawn batchwise in two stages (M_w = 420,000 kg/kmol, initial draw rate 0.017 s^{-1}, T_1 = 225 °C (λ_1<10) and T_2 = 250 °C)).*

Loss of orientation of these chain segments can be avoided by cooling down to room temperature, whilst maintaining a high tension to the material. Room temperature is close to the glass transition temperature of unoriented polyketone (T_g = 5-10 °C), and the driving force to recoil is vanishingly small under these conditions. In the present work, the latter constraint cooling procedure is followed for the batchwise preparation of drawn fibers.

A more convenient and practical way to avoid molecular relaxation phenomena is to

carry out the drawing procedure at higher speeds. These conditions are accompanied by significantly higher drawing stresses. The tensile modulus of fibers produced according to the latter technique and those of batchwise drawn fibers are presented in Figure 10. Under these conditions, the modulus increases at a steeper slope with the applied draw ratio, implying that the molecular relaxation of chain segments in the non-crystalline state is noticeably surpressed. Fibers oriented to the maximum attainable draw ratio of 26 show an initial tensile modulus of 50-55 GPa. Another way to accomplish higher drawing stresses might be to increase the polymer concentration during fiber spinning. Although we have not investigated concentration effects extensively, the increase in the amount of topological defects (e.g., entanglements) will likely alter the drawing behavior, since these interchain interactions act as barriers for orienting dissipative flow.

-Orientation Development

The overall degree of molecular orientation or the Hermans' orientation factor relates to the molecular orientation distribution,[1]

$$\langle P_2 \rangle = \frac{3 \langle \cos^2 \phi \rangle - 1}{2} \qquad (1)$$

where Φ is the angle between the local director of a chain segment and the fiber axis and the parameter $\langle \cos^2 \Phi \rangle$ characterizes the orientation distribution. The orientation parameter $\langle P_2 \rangle$ increases with the degree of streching of an unoriented solid flexible polymer, viz. the ratio to which an as-spun fiber is drawn (λ). The overall molecular orientation parameter $\langle P_2 \rangle$ is proportional to the optical anisotropy, viz. the birefringence of the material (Δn),[1]

$$\langle P_2 \rangle = \frac{\Delta n}{\Delta n_{max}} \qquad (2)$$

where Δn_{max} is the birefringence of perfectly axially oriented fiber. In section we will derive a first approximation to this value.

In Figure 11 a comparison is made of the development of the birefringence of fibers prepared under different drawing conditions. As is obvious from the results described above, the development of the degree of molecular orientation in solution spun polyketone fibers is strongly improved under optimized drawing conditions.

In order to establish a first approximation to Δn_{max}, we assume that the orientation development under optimized conditions has been accomplished according to an affine type of deformation.

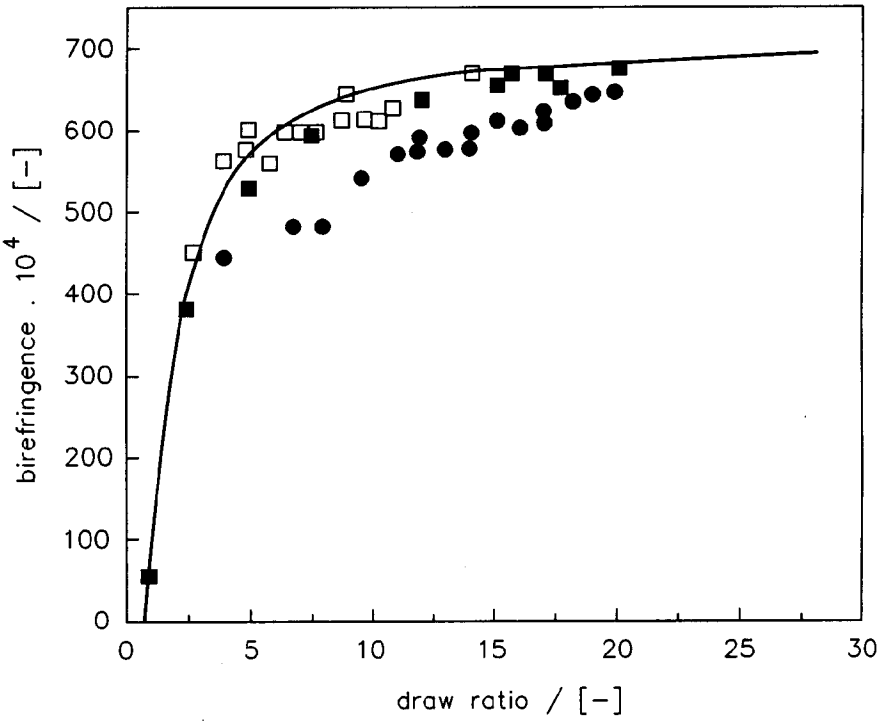

Figure 11. *The birefringence of polyketone fibers oriented under different circumstances ((●) : unoptimized continuous drawing; (□) : optimized continuous drawing; (■) : optimized batch-wise drawing; solid line : eq. 3 with $\Delta n_{max} = 710 \cdot 10^{-4}$).*

The affine deformation scheme of Kuhn and Grun[28] has been used to described the orientation development in flexible polymers [2,29] as well as the domain orientation order in more worm-like liquid crystalline polymers, like *para*-aramids.[30] According to the Kuhn and Grun theory $<P_2>$ relates to the macroscopic degree of extension (λ) via

$$<P_2> = \frac{2\lambda^3 + 1}{2(\lambda^3 - 1)} - \frac{3\lambda^3}{2(\lambda^3 - 1)^{3/2}} \tan^{-1}((\lambda^3 - 1)^{1/2}) \qquad (3)$$

Eq. (3) suggests a unique relation between the draw ratio and $<P_2>$, but in this approach molecular relaxation and non-orienting deformation are not taken into consideration. Clearly, this relation is not generally applicable as is evidenced in Figure 11. On the other hand an equal development of both the birefringence and the tensile modulus of the two types of fibers prepared under optimized conditions is observed (see Figures 10 and 11, symbols represent comparable experiments). The latter result suggests that orientation relaxation phenomena are entirely or at least largely surpressed. Accordingly, equation (3) is used to describe the overall orientation parameter in these fibers and a value of $710 \cdot 10^{-4}$ for Δn_{max} gave a good match between the predicted and the observed values for the birefringence.

Summarizing our results on the optimization of the drawing process, we conclude that variations in processing conditions result in polyketone fibers with largely different mechanical properties. The tensile modulus and molecular orientation of oriented fibers strongly depends on the drawing stress, which is controlled by the process temperature and drawing rate. At lower temperatures, the modulus development in polyketone fibers is improved. However, overdrawing should be avoided since this results in a deterioration of the tensile strength. In comparison to solution spun polyethylene fibers the modulus development with the draw ratio is less rapid.[29] In view of the expected higher theoretical modulus of POK-$_2$ fibers,[9] the latter remarkable observation might be attributed to a lower average (macroscopic) shear modulus. Preliminary investigations indeed corroborated this idea, but still more work has to be done to provide a better understanding of this intriguing phenomenon.

To demonstrate the effect of orientation relaxation on the overall stress-strain behavior of polyketone fibers, some fibers were prepared batchwise at less constraint cooling conditions. The high elongation at break, which can be achieved this way, is advantageous for various industrial applications. As is demonstrated in the stress-strain curves in Figure 12, the elongation at break of an unrelaxed highly oriented polyketone fiber is typically between 4-5 %.

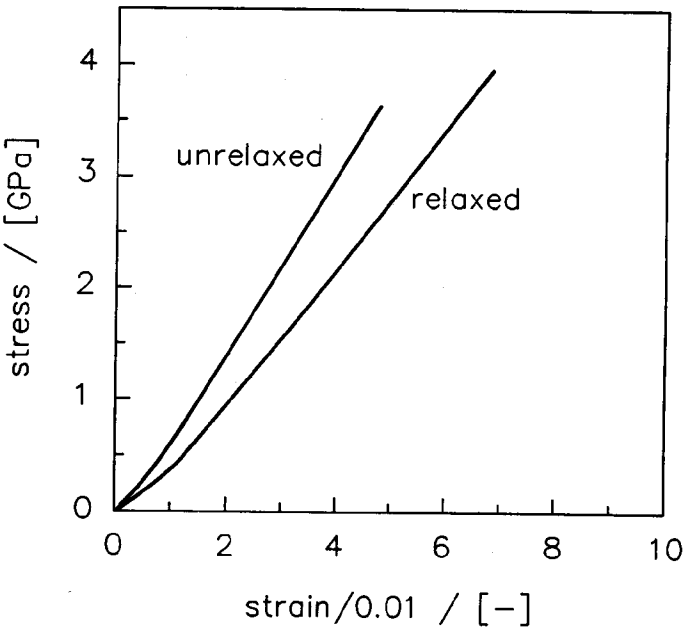

Figure 12. *The stress-strain curves of highly oriented relaxed and of unrelaxed polyketone fiber (M_w = 340,000 kg/kmol).*

In contrast, for a (partially) relaxed fiber with a comparable tensile strength (3.9 GPa), but a lower modulus (42 GPa), the elongation at break can be as high as 7-8 %. Obviously, the increase in the elongation at break occurs at the expense of a lower modulus. We attempted to produce similar high-elongation yarns by relaxing drawn fibers by means of a low tension aftertreatment at elevated temperatures. This route

was, however, not successful, due to low hot air shrinkage (at 160 °C below 2 %). The latter result may indicate that additional stiffening and reorganisation occurs within the non-crystalline domains upon cooling and after the drawing procedure has been completed.

3.5 Conclusions

The drawability of polyketone increases with temperature. However, the temperature for effective drawing is limited by the onset of slippage of chain ends through entanglements. This non-orienting flow occurs under conditions when lateral stress transfer by means of crystalline interactions starts to vanish (T > 230 °C). The semi-crystalline nature of the material becomes very noticeable when orientation relaxation within non-crystalline domains is allowed. A marked improvement in the development of both the tensile modulus and the degree of molecular orientation is observed at lower drawing temperatures. Under these drawing conditions the induced degree of molecular orientation can be described using the affine deformation concept in combination with a value for the maximum birefringence of perfectly oriented fiber (Δn_{max}) of $710 \cdot 10^{-4}$. The development of the tensile strength at T_{draw} < 230 °C is independent of the drawing temperature and is solely governed by the draw ratio, provided that the material has not been overdrawn. Beyond a draw ratio of 17 the formation of local stress concentrations (i.e., voids and cracks) in solution spun multi-filament yarns seems to be inevitable.

Although the drawability of solution spun fibers prepared from perfectly alternating ethylene-carbon monoxide copolymer (λ_{max} = 26) is significantly less than for the non-polar polyethylene, a high strength of about 4 GPa and a satisfactory modulus of about 50-55 GPa can be attained. The combination of a high strength, and a low initial tensile modulus/high elongation at break is an unique feature of relaxed polyketone fibers. This set of properties clearly demonstrates the possibility to prepare tough high-strength polyketone fibers with a relatively high energy absorption.

3.6 References and Notes

1. P.H. Hermans, *Physics and Chemistry of Cellulose Fibers*, Elsevier, Amsterdam, 1949.
2. I.M. Ward, *Mechanical Properties of Solid Polymers*, 2nd ed., Wiley, New York, 1983.
3. M.G. Northolt and R. v.d. Hout, *Polymer*, **26**, 240 (1986).
4. P. Smith and P.J. Lemstra, *J. Mater. Sci.*, **15**, 505 (1980).
5. J. Smook, G.J.H. Vos, and H.L. Doppert, *J. Appl. Pol. Sci.*, **41**, 105 (1990).
6. B.J. Lommerts and D.J. Sikkema, *Macromolecules*, (submitted, Chapter 5).
7. W-I Cha, S-H Hyon, and Y. Ikada, *J. Polym. Sci. Polym. Phys. Ed.*, **32**, 297 (1994).
8. E. Drent, J.A.M. v. Broekhoven, and M.J. Doyle, *J. Organomet. Chem.*, **417**, 235 (1991).
9. B.J. Lommerts, E.A. Klop, and J. Aerts, *J. Polym. Sci. Polym. Phys. Eds.*, **31**, 1319 (1993).
10. M.J. Doyle, J.C. Van Ravenswaay-Claasen, G.G. Rosenbrand, and R.L. Wife, European Patent 248,483 (Shell), (1987).
11. The molecular weights were derived from size exclusion chromatography (SEC/GPC) measurements carried out by A. Buijtenhuijs and coworkers (to be published).
12. B.J. Lommerts, J. Smook, B. Krins, A. Piotrowski, and E. Band, European Patent 456,306 (Akzo Nobel), (1989).
13. W.L. Bragg, *Proc. Cambridge Phil. Soc.*, **17**, 43 (1913).
14. Y. Chatani, T. Takizawa, S. Murahashi, Y. Sakata, and Y. Nishmura, *J. Polym. Sci.*, **55**, 811 (1961).
15. E.A. Klop, B.J. Lommerts, J. Veurink, J. Aerts, and R.R. v. Puijenbroek, *J. Polym. Sci. Polym. Phys. Ed.*, (accepted for publication).
16. Y. Termonia, S.R. Allen, and P. Smith, *Macromolecules*, **21**, 3485 (1988).
17. Highly oriented fibers (λ = 20), prepared via a multi stage drawing process, can show a melting temperature as high as 282 °C.
18. B. Wunderlich, *Macromolecular Physics*, Volume III, *Crystal Melting*, Academic Press, New York, 1980.

19. G.I. Taylor, *Proc. Roy. Soc. Lond.*, **A201,** 192 (1950).
20. J.D. Hoffman, *Polymer,* **20,** 1071 (1979).
21. J. Smook and A.J. Pennings, *J. Mater. Sci.,* **19,** 31 (1984).
22. A.J. Pennings, M. Roukema, and A. v.d. Veen, *Polym. Bull.,* **23,** 353 (1990).
23. P.F. v. Hutten, C.E. Koning, and A.J. Pennings, *J. Mater. Sci.,* **20,** 1556 (1985).
24. L. Jarecki and D.J. Meier, *J. Polym. Sci. Polym. Phys. Ed.,* **17,** 1611 (1979).
25. Similar overdrawing phenomena have been observed in meltspun poly(ethylene terephthalate), polyethylene and in solution spun poly(vinyl alcohol) fibers, J. Veurink, (private communications).
26. E.J. Kramer and L.L. Berger, *Adv. Polym. Sci.,* **91/92,** 1 (1990).
27. L.R.G. Treloar, *The Physics of Rubber Elasticity,* 2nd ed., Clarendon, Oxford, 1958.
28. W. Kuhn and F. Grun, *Kolloid-Z,* **101,** 248 (1942).
29. P.A. Irvine and P. Smith, *Macromolecules,* **26,** 240 (1986).
30. S.J. Picken, S. v.d. Zwaag, and M.G. Northolt, *Polymer,* **33,** 2998 (1992).

Chapter 4.

SYNTHESIS AND STRUCTURE OF A NEW POLYALCOHOL

Reproduced from:
B.J. Lommerts and D.J. Sikkema, *Macromolecules (submitted for publication).*

4.1 Summary

A new polyalcohol is prepared by reduction of the perfectly alternating ethylene-carbon monoxide copolymer. The low melting temperature of this atactic material (137 °C) is attributed to the 1,4-arrangement of the hydroxyl side-groups. The different orientations of these slightly bulky groups with respect to the molecular plane contribute to a less efficient packing of the chains in the crystal lattice. The reflections in the x-ray diffraction pattern are indexed on the basis of an orthorhombic lattice. The derived unit cell dimension are a=8.78 Å, b=5.47 Å and c=7.47 Å, and the crystalline density (1.08 g/cm^3) is significantly less than the crystalline density of poly(vinyl alcohol) (1.35 g/cm^3), which has a 1,3-arrangement of the hydroxyl substituents. Solution cast polyalcohol films could be drawn to a ratio of about 10; a tensile strength of 0.5-0.6 GPa and a (maximum) tensile modulus of 11 GPa are attained.

4.2 Introduction

Organometallic catalyst systems enable the production of perfectly alternating ethylene-carbon monoxide copolymers (polyketones),[1,2] and a regular 1,4-arrangement of the dipolar carbonyl functionallity is obtained. In comparison to polyethylene, the polyketone shows a much higher melting temperature (260 °C) due to the more polar nature of the polymer.[3]

In Table I the members of two groups of polymers are arranged in the order of the

degree of oxidation. Commercially available atactic poly(vinyl alcohol) grades are prepared by polymerization of vinyl acetate followed by hydrolysis.[4] Polyketene can be synthesized from ketene using a BF3/benzonitrile catalyst.[5] An amorphous low-molecular-weight material is obtained presumably due to mainly chemical defects and perhaps the steric hindrance and significant repulsion forces between the carbonyl groups. Polyglycolic acid is commonly prepared by ring-opening polymerisation of glycolide.[6]

Table I. *Melting Temperature (T_m) and Crystalline Density (ρ_c) of Various Flexible Chain Polymers Arranged in the Order of the Degree of Oxidation.*

	Formula	ρ_c [g/cm^3]	T_m [°C]		Formula	ρ_c [g/cm^3]	T_m [°C]
PE	$(\text{-}CH_2\text{-}CH_2\text{-})_n$	1.00	141				
PVAl	$(\text{-}CH_2\text{-}CH(OH)\text{-})_n$	1.35	267	PAl	$(\text{-}CH_2\text{-}CH_2\text{-}CH(OH)\text{-})_n$		
PK[a]	$(\text{-}CH_2\text{-}C(O)\text{-})_n$	-	-	POK-C_2	$(\text{-}CH_2\text{-}CH_2\text{-}C(O)\text{-})_n$	1.38[b]	278
PG	$(\text{-}CH_2\text{-}C(O)\text{-}O\text{-})_n$	1.70	233	PHA	$(\text{-}CH_2\text{-}CH_2\text{-}C(O)\text{-}O\text{-})_n$	1.44[c]	122

[a] amorphous polymer

[b] crystalline density of the POK-α structure

[c] crystalline density of the β-form

(PE : Polyethylene (ref. 7); PVAl : Poly(vinyl alcohol) (ref. 7); PK : Polyketene (ref. 5); PG : Polyglycolic acid (ref. 7); PAl : Polyalcohol (this work); POK-C_2 : Polyolefin ketone (ref. 5); PHA : Polyhydracrylic acid (ref. 7)).

From imperfectly alternating ethylene-carbon monoxide copolymers two new polymers have been synthesized, viz. a polyalcohol[8] and a polyester.[9] The latter polymer was produced via oxidation with hydrogen peroxide or organic peracids. A random terpolymer, containing ethylene glycol/succinic acid and hydracrylic acid units, is obtained, but this synthesis route is unlikely to yield complete conversion. A more convenient route to such a polyester is the synthesis of polyhydracrylic acid from β-propiolactone by ring-opening polymerization.[10] Two crystalline structures have been reported for this homopolymer, i.e. the α-form and the β-form.[11,12] The melting temperature is rather low and its thermal stability is poor, because the polymer easily decomposes forming acrylic acid.

In the present work, we have prepared a polyalcohol (PAl) from the perfectly alternating ethylene-carbon monoxide copolymer by reduction with sodium borohydride. Oriented solution cast film samples are characterized by means of thermal, IR and NMR analysis and x-ray diffraction techniques. The differences in melting temperature and crystal packing between this regular, though atactic, 1,4-polyalcohol and poly(vinyl alcohol) (i.e., a 1,3-polyalcohol) are studied.

4.3 Experimental

-Materials

Commercial laboratory grade starting materials were used as received. Alternating polyketones were prepared according to the description given in Chapter 2. The molecular weights of these polyketone samples were derived from the intrinsic viscosity in *m*-cresol (25 °C) using the following Mark-Houwink equation.[13]

$$[\eta]_{m\text{-cresol},\,25\,^{\circ}C} = 1.01 \cdot 10^{-4}\ \overline{M_w}^{\,0.65} \qquad (1)$$

-Polyalcohol Synthesis and Sample Preparation

Polyalcohol was synthesized by reduction of polyketone using sodium borohydride. Various polyketone samples were used with weight average molecular weights of 45,000, 175,000, 310,000 and 450,000 kg/kmol. The polyketone powder (4 grams) was dispersed in 160 ml of a 1:1 (v/v) mixture of ethanol and water. After heating to 78 °C, 4.7 g of $NaBH_4$ was slowly added. After 24 hours of stirring at that temperature, all solids had disappeared; upon cooling the lower layer of salt- and water-rich liquid was discarded; the upper layer was neutralized with 10 % HCL and concentrated in a rotary evaporator to about 20 % of its original volume inducing precipitation of the polyalcohol. After cooling, the product was filtered off, redissolved in 1:1 aqueous ethanol and reprecipitated three times by evaporative concentration. Transparant films were cast from viscous solutions in N-methyl pyrrolidinone; the solvent was subsequently removed under vacuum. The thin films (60-200 μm) were cut into small strands (2-3 mm width) and drawn batch-wise at 110 °C (initial rate of deformation 100 %/min).

-Analysis

IR spectra were recorded on a BioRad™ FTS40 FT-IR equipment. ^{1}H-NMR spectra in d^6-dimethyl sulfoxide (DMSO) were obtained using a Bruker™ AC 300 (300 MHz) apparatus. In order to shift the absorption of moisture, d^1-trifluoro acetic was added in some cases. Thermograms of the materials were recorded using a Perkin Elmer™ DSC 7 thermal analyzer at a scanning speed of 20 °C/min. The peak temperatures were taken as melting points and the heats of fusion were calculated from the area of the melting peaks. X-ray diffraction patterns were recorded using a Statton camera equipped with a graphite monochromator with a sample to film distance of 33.7 mm. Tensile testing of drawn films and fibers were performed at room temperature (21 °C) and 65 % relative humidity, using an Instron Tensile Tester, operating at a crosshead speed of 10 mm/min for a sample gauge length of 100 mm.

Infra-red spectrum (transmission, film on silicon wafer, from aqueous methanol solution): 3301 (strong), 2937, 2920, 2858, 1668 (very weak), 1572 (very weak), 1446, 1338, 1188 (weak), 1102, 1038, 761 (weak), 639 cm^{-1}.

^{1}H-Nuclear magnetic resonance (NMR) spectrum (d^6-DMSO): δ=1.25 ppm triplet-like broadened band assigned to the syndiotactic, δ=1.36 ppm, band assigned heterotactic, and δ=1.48 ppm doublet-like broadened resonance assigned to isotactic, about 1:2:1 intensities, CH_2; δ=3.34 ppm a broadened absorption attributed to CH, and δ=4.32 ppm a multiplet for OH. All absorptions were referenced to tetramethyl silane (TMS).

^{13}C-NMR spectrum (d^6-DMSO): δ=33.5, 33.7 ppm assigned to CH_2; δ=70.1, 70.5, 70.9 ppm attributed to CH with different tacticities. All absorptions were referenced to TMS and no carbonyl absorptions were visible in the 200-220 ppm region.

Thermal analysis (20 °C/min): For unoriented material thoroughly dried at 250 °C the observed glass transition temperature ranges from 53 °C for low-molecular-weight polymer to 56 °C for high-molecular-weight polymer. For unoriented low-molecular-weight samples a small melting endotherm is detected between 128 and 132 °C.

4.4 Results and Discussion

-Polyalcohol Synthesis

Exploratory reduction experiments with $NaBH_4$ using a perfectly alternating low-molecular-weight polyketone were run in *m*-cresol as an effective solvent for the starting material. The reduced product could be isolated by coagulation with water, acetone, methanol, or ethanol as anti-solvents. It was discovered serendipitously that a 1:1 (wt/wt) mixture of ethanol and water redissolved the polyalcohol, even though each of these solvents alone did not. Thus, reduction in aqueous ethanol as a dispersant for polyketone was investigated with a view to eliminate the need for *m*-cresol with its practical drawbacks, viz. toxicity and stench. The latter synthesis route resembles the reduction of an imperfectly alternating low-molecular-weight polyketone in methanol, as described by Morishima et al.[8] Even though polyketone shows a vanishingly small solubility in aqueous ethanol, the reaction could be carried out in this medium, albeit that high-molecular-weight polymer required fine grinding prior to

reaction. As a consequence of a heterogeneous reduction reaction, long reaction times were necessary in all cases. Product isolation could be performed by separating the clear polymer-containing solution from the heavier salt-rich lower layer, neutralizing the polymer solution with HCl, evaporating until the polymer precipitated upon removal of most of the ethanol/water mixture and washing or dissolution-concentration-precipitation. Progress of the reaction could be monitored easily by observing the disappearance of solids, followed by verification by IR in a sample isolate, that the 1700 cm^{-1} carbonyl absorption had disappeared.

Table II. *Solvents and Non-Solvents at Room Temperature for High-Molecular-Weight Polyalcohol (M_w=450,000 kg/kmol)*

non-solvents	swelling agents	solvents
2-propanol	acetic acid (25 %)	water/ethanol (1:1 wt/wt)
tetrahydrofuran	acetic acid (99 %)	water/methanol (1:1 wt/wt)
sec. butylalcohol	trifluoroacetic acid (50 %)[a]	acetic acid (50 %)
trifluoroacetic acid	dimethyl formate	N-methylpyrrolidinone
formic acid (50 %)	dimethyl sulfoxide	*m*-cresol
diethyl ether	water	
methyl ethyl ketone	methanol	
dichloromethane	ethanol	
dioxan		
nitrobenzene		
pyridine		
p-xylene		
toluene		

[a] a slight discoloration of the polymer occurred

-Oriented Polyalcohol Films

To process the resulting polyalcohol from solution, a number of solvents have been screened; the results are listed in Table II. Aqueous ethanol or aqueous methanol cannot be applied to cast a film from solution and to achieve subsequent concentration of the polymer. Water is only a swelling agent and due to the faster evaporation of the alcoholic solvent liquid-liquid demixing was observed prior to solidification and a non-transparant brittle film is formed. In order to avoid these concentration fluctuations during solidification, N-methyl pyrrolidinone was used and strong transparant films were cast. The solvent was removed at room temperature by evaporation under vacuum.

Thermograms of oriented films, drawn to a ratio of 9 at 100 °C, are given in Figure 1. Usually, a glass transition temperature is visible at 40-45 °C; for unoriented material thoroughly dried at 220 °C it is found at 53-56 °C.

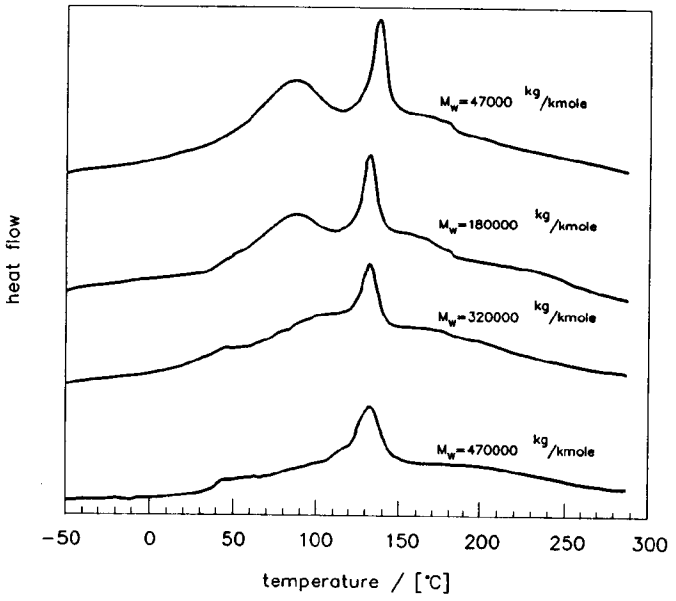

Figure 1. *Thermograms of oriented polyalcohol films drawn to a ratio of 9 at 100 °C (scanning speed 20 °C/min).*

During thermal analysis the weight loss was monitored and a pronounced reduction in weight occured at 100 °C for undried material. Thus, the reduction in glass transition temperature can be ascribed to moisture. Furthermore, in some cases a broad endotherm is observed in the thermograms between 60 and 110 °C, resulting from remnants of the reduction reaction. The strong endotherm, observed between 130 and 140 °C, can be attributed to the melting of crystalline polymer.

At increasing molecular weight a broadening of the melting endotherm is observed, which is accompanied by a slight reduction in the melting temperature (from 137 °C to 132 °C) and in the area of the melting peak (from 38 J/g to 29 J/g). This result implies that the crystallinity is less developed in the higher molecular weight materials.

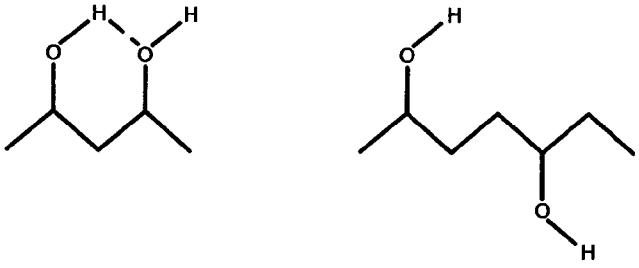

Figure 2. *The repeating units in poly(vinyl alcohol) (1,3-glycol units) and polyalcohol (1,4-glycol units), demonstrating the capability of poly(vinyl alcohol) to form intramolecular hydrogen bonds.*

We were expecting a melting temperature for the polyalcohol in the temperature region of 180-220 °C. Due to the increased intermolecular interactions (hydrogen bonds) the melting temperature was thought to be significantly higher than for polyethylene. Like poly(vinyl alcohol), the polyalcohol is basically an atactic material, but we anticipated that the non-stereo-regular defects can easily be incorporated into the crystal lattice.[14] Moreover, it has been argued that ethylene-vinyl alcohol

copolymers (EVAl) are co-crystallizable over the whole composition range.[15] For example, for a random (atactic) EVAl copolymer with about the same molar ratio of methylene (CH_2) to hydroxy methine (CH(OH)) units as the polyalcohol, a melting temperature of 182 °C is reported,[15,16] and the crystalline density is about $1.2 \cdot 10^3$ kg/m^3. The incorporation of ethylene units into the poly(vinyl alcohol) crystal lattice predominantly affects the packing of the chains in the direction of the intermolecular hydrogen bonds (i.e., along the *a*-axis in the crystal unit cell).

The polyalcohol produced via reduction of polyketone can be regarded as an atactic homopolymer and in NMR and IR analysis chain defects in the form of unreduced carbonyl groups were below the detection limit. These particular features are generally favorable for a high melting temperature. Notwithstanding the good purity of the polymer, the melting temperature is even 4-10 °C lower than that for polyethylene. This effect can be explained by the different orientations of neighbouring hydroxyl groups compared to those of poly(vinyl alcohol) or ethylene-vinyl alcohol copolymers. Polyalcohol consists of 1,4-glycol units, whereas poly(vinyl alcohol) consists of 1,3-glycol units (see Fig. 2). It can be expected that intramolecular hydrogen bonding in poly(vinyl alcohol) via a 6-membered ring facilitates the incorporation of the non-stereo-regular defects into the crystal lattice. The formation of an intramolecular hydrogen bond in polyalcohol is less favorable, because of the required 7-membered ring formation, which is less stable and additionally distorts the conformation characteristics of an extended chain.

In case of an all-*trans* conformation of the polyalcohol backbone, the different orientations of the slightly bulky hydroxyl side groups with respect to the molecular plane can contribute to a less efficient lateral packing of the chains in the crystal lattice than for poly(vinyl alcohol). To gain insight into the crystal packing density, drawn film samples were studied using x-ray diffraction techniques. Flat-plate and precession x-ray diffraction photographs were recorded; a flat plate photograph is displayed in Figure 3. From the discrete reflections on the equator it can be concluded that the polymer chains are periodically packed in the lateral direction with respect to the fiber axis. The low degree of arcing of the reflections implies that the molecular

chains are effectively oriented by the drawing process. Moreover, the clearly visible layer lines point to periodicity of the polymer chains along the fiber axis. However, in spite of the good molecular alignment, some streaking is observed especially on the second layer line. This observation points to a distortion of the side-by-side packing of the chains in the direction of the fiber axis. The distortion is probably caused by the different orientations of the hydroxyl groups with respect to the molecular plane. In other words, due to the different tacticities of the hydroxyl side-groups, the chains cannot pack in a perfectly regular fashion in the fiber axis direction.

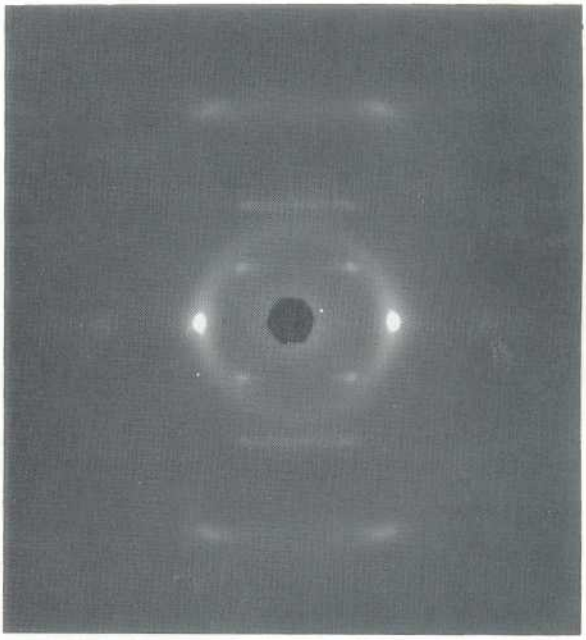

Figure 3. *Flate-plate x-ray diffraction photograph of an oriented polyalcohol film drawn to a ratio of 9 and 110 °C (fiber axis is vertical).*

The reflections were indexed on the basis of an orthorhombic lattice. From five reflections the dimensions of the crystal unit cell were derived using a least-squares procedure. Comparison of these unit cell dimensions, together with the dimensions of the unit cells of some other all-carbon backbone macromolecules, reveals some

interesting points. In contrast to the starting material polyketone, the dimension of the polyalcohol unit cell in the direction of the fiber axis is slightly less than three times the fiber axis unit cell length of polyethylene or poly(vinyl alcohol). Furthermore, the lateral dimensions of the polyalcohol unit cell are significantly larger than those of the poly(vinyl alcohol) unit cell, resulting in a rather low crystalline density (see Table III). By contrast, in the polyketone (POK-α) crystal structure the strong dipolar interactions between well-arranged adjacent carbonyl groups result in an even slightly denser packing of the chains than observed for polyethylene (see Table III).[3]

Table III. *Unit Cell Dimensions of Various Flexible Chain Polymers with an All-Carbon Backbone.*

	a [Å]	*b* [Å]	*c* [Å]	ρ_c [g/cm^3]	structure
PAI	8.78	5.47	7.47[a]	1.08	-
POK-α	6.91	5.12	7.60[a]	1.38	orthorhombic
POK-β	7.97	4.76	7.57[a]	1.30	orthorhombic
PVAI	7.81	2.52[a]	5.51	1.35	monoclinic (β = 91.7 °)
PE	7.40	4.93	2.54[a]	1.00	orthorhombic

[a] direction of the fiber axis

(PAI: this work; POK-α: ref. 3; POK-β: ref.'s 17 and 18; PVAI: ref. 14; PE: ref. 19 and 20)

Even though we have not looked into the detailed molecular arrangement in the polyalcohol crystal structure, it is obvious from the above-mentioned results that the increased intermolecular interactions between neighbouring hydroxyl groups cannot

compensate for the size plus stereo-irregularity of these groups relative to polyketone, in which the latter issue is absent.

To study the development of the tensile modulus with the molecular orientation, tensile tests were performed on a series of films of different molecular weights and drawn to different ratios, up to 9. In Figure 4 the maximum slope in the stress-strain curves (i.e., the maximum tensile modulus) is presented in relation to the tensile strength. Compared with poly(vinyl alcohol) and polyketone fibers, the tensile strength increases at about the same slope with the development of the modulus.

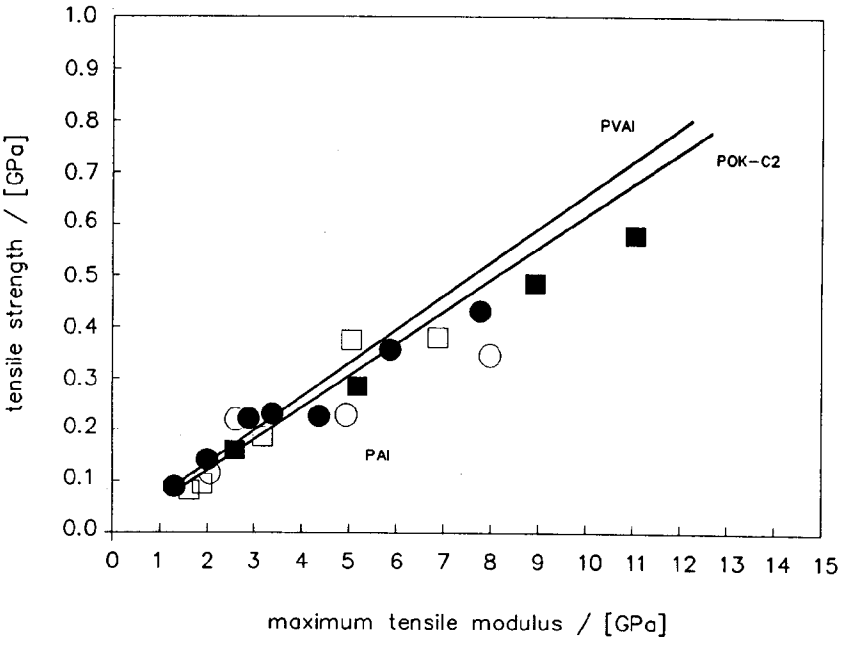

Figure 6. *The tensile strength of drawn polyalcohol films cast from solution in NMP vs the maximum tangential modulus. The solid lines represent the correlations found for polyketone (POK-C_2) and poly(vinyl alcohol) (PVAl) fibers (□) : M_w = 47,000 kg/kmol; (■) : M_w=180,000 g/mol; (●) : M_w = 320,000 kg/kmol; (○) : M_w=470,000 kg/kmol).*

It is also noteworthy that at these rather low degrees of orientation no effect is visible of the molecular weight on the tenacity, which is, amongst other polymers, also observed for polyethylene fibers. But the properties we obtained by drawing polyalcohol films are significantly below those of the other all-carbon backbone molecules of interest. In fact, we were able to achieve only 20-30% of the values found for both the tensile strength and tensile modulus of oriented gelspun polyketone fibers.[21] Clearly, these poor tensile properties combined with the low melting temperature demonstrate the limited potential of this polymer, and hence, no attention was paid to a further optimization of the fiber preparation conditions.

Notwithstanding these particular drawbacks, a comparison between the drawability of this polymer and polyketone and poly(vinyl alcohol) fibers is instructive, when looking at the related chain-polarities. In Chapter 5, we will describe the results obtained in our study of the influence of the drawing temperature on the drawability of these flexible polymers with intermediate polarity.

4.5 Conclusions

An atactic 1,3-polyalcohol is synthesized by reduction with sodium borohydride of the perfectly alternating ethylene-carbon monoxide copolymer. Oriented semi-crystalline samples are prepared by drawing solution cast films at 110 °C. These samples were studied by means of x-ray diffraction techniques. The low melting temperature (137 °C) is attributed to the low packing density of the chains in the crystal lattice. Some streaking is observed, especially on the second layer line, which indicates that the side-by-side packing of the chains is distorded due to the different orientations of the slightly bulky hydroxyl side-groups. The 1,4-arrangement of the hydroxyl substituents results in a significantly lower crystalline density than for poly(vinyl alcohol), which has a 1,3-arrangement of the hydroxyl substituents.

4.6 References and Notes

1. E. Drent, J.A.M. v. Broekhoven, and M.J. Doyle, *J. Organomet. Chem.*, **417,** 235 (1991).
2. A. Sen, *Acc. Chem. Res.*, **26,** 303 (1993).
3. B.J. Lommerts, E.A. Klop and J. Aerts, *J. Polym. Sci. Polym. Phys. Ed.*, **31,** 1319 (1993).
4. I. Sakurada, *Polyvinyl Alcohol Fibers,* Dekker, New York, 1985.
5. R. Oda, S. Munemiya and M. Okano, *Makromol. Chem.*, **43,** 149 (1961).
6. K. Chujo, H. Kobayashi, J. Suzuki, S. Tokuhara and M. Tanabe, *Makromol. Chem.*, **100,** 262 (1967).
7. R.L. Miller in: *Polymer Handbook,* 2nd ed., J. Brandrup and E.H. Immergut (ed.), Wiley, New York, 1975.
8. Y. Morishima, T. Takizawa and S. Murahashi, *Eur. Pol. J.*, **9,** 669 (1973).
9. B-H Chang, *U.S. Patent,* 5,140,080 (Quantum Chemical Corporation) (1992).
10. G. Wasai, T. Saegusa and J. Furukawa, *Kogyo Kaguku Zasshi,* **67,** 601 (1964).
11. K. Suehiro, Y. Chatani and H. Tadokoro, *Polymer J.*, **7,** 352 (1975).
12. H. Tadokoro, *Structure of Crystalline Polymers,* Wiley, New York, 1979.
13. The Mark-Houwink relation is derived from molecular weight measurements using size exclusion chromatography, light scattering and (quantitative) NMR analysis.
14. C.W. Bunn, *Nature,* **161,** 929 (1948).
15. T. Matsumato, K. Nakamae, N. Ogoshi, M. Kawazoe and H. Oka, *Kobunshi Kagaku,* **28,** 610 (1971).
16. R. Schellekens and H. Ketels, *Polym. Comm.*, **31,** 212 (1990).
17. Y. Chatani, T. Takizawa, S. Murahashi, Y. Sakata and Y. Nishnura, *J. Polym. Sci.*, **55,** 811 (1961).
18. E.A. Klop, J. Aerts, J. Veurink and B.J. Lommerts, *J. Polym. Sci. Polym. Phys. Ed.*, (accepted for publication).
19. C.W. Bunn, *Trans. Faraday Soc.*, **35,** 492 (1939).
20. E.R. Walter and F.P. Reding, *J. Polym. Sci.*, **21,** 562 (1956).
21. B.J. Lommerts, H. ter Maat and R. Huisman, (submitted, Chapter 3).

Chapter 5.

ORIENTABILITY OF A NEW POLYALCOHOL AND RELATED FLEXIBLE CHAIN POLYMERS OF INTERMEDIATE POLARITY

Reproduced in part from:
B.J. Lommerts and D.J. Sikkema, *Macromolecules (submitted for publication).*

5.1 Summary

The orientability of three moderately polar flexible polymers, viz. the perfectly alternating ethylene-carbon monoxide copolymer (polyketone), poly(vinyl alcohol) and a new polyalcohol, has been investigated. Both polyketone and poly(vinyl alcohol) are high melting polymers and can be drawn to ratios above 20. In spite of the lower crystalline density of the polyalcohol (1.08 g/cm^3), which is reflected in a low melting temperature (137 °C) and accordingly in a low crystal packing energy, the maximum attainable draw ratio is limited to a value of 10. A comparison of these results with those of a large number of materials, covering a broad polarity range, is presented. In addition to the molecular weight and entanglement density, the drawability of flexible chain polymers is largely governed by chemical structure, mainly polarity, and temperature. A good measure for the polarity is the cohesive energy (E_{coh}), which reflects the barrier to transport topological defects along and through the oriented structures formed. The ratio E_{coh}/RT_m can be used to predict the maximum attainable draw ratio of new fiber materials. The maximum temperature for effective drawing is at the melting temperature of the polymer. The correlation found between the melting temperature and the maximum attainable draw ratio of a number of poly-hydroxy-polymers (i.e., polymers with comparable polar interactions), corroborates the limitations in drawability due to a decline in the lateral stress transfer above the melting temperature.

5.2 Introduction

The mechanical properties of polymeric fibers depend strongly on the molecular orientation in the direction of the fiber axis.[1] Nowadays, well-oriented fibers can be prepared in various, fundamentally different, ways. Spinning techniques, where the alignment of the macromolecules is induced in a liquid state, are very effective for rod-like polymers. During the spinning process, the molecules are aligned in the direction of flow and the intrinsic rigidity of this type of polymer chain, combined with the limited lateral mobility, lowers the orientation relaxation.[2,3] Consequently, highly oriented fibers can be produced on an industrial scale, showing impressive mechanical properties (Twaron™ (Akzo Nobel), Kevlar™ (DuPont)).[4]

At relatively high flow rates, melts of flexible polymers can also be partially oriented. When the deformation in the melt is accompanied by a fast crystallization, the molecular orientation can be largely consolidated in the solid phase.[5] This spinning process is currently carried out for the production of high modulus/low shrinkage polyester fibers.[6] Pennings et al.[7] showed that this technique can also successfully be applied to the spinning of high modulus fibers from dilute solutions of high-molecular-weight polyethylene.

A more traditional way to induce molecular orientation in flexible polymers is to apply solid-state tensile drawing at elevated temperatures, where the temperature for maximum drawability is often close to the melting temperature of the polymer. During the last decade, this technique has regained considerable interest after the development of the gelspinning process for ultra-high molecular weight polyethylene.[8,9] After solidification the extruded unoriented fibers are subjected to tensile deformation either in the presence of solvent or in the fully extracted/dried state.

Tensile deformation of solid polymers is a complex issue and can occur in various modes (i.e., yielding, brittle fracture, strain hardening, etc.).[1,10,11] Especially the influences of the chemical structure, morphology, molecular weight and temperature on the extensibility of isotropic polymers are topics of paramount importance. In spite

of the extensive work, a complete understanding has not emerged in this field, and a number of these interrelated subjects still need to be investigated.

It is now generally accepted that the entanglement spacing largely governs the extensibility of glassy polymers.[12] The deformation can be located either in shear deformation zones or in regions in which crazing occurs. In the latter case the limiting (local) extension of fibrils propagating through the formed crazes was shown to depend on the molecular weight between network nodes (e.g., entanglements).[13]

In semi-crystalline polymers, the entanglement topology in the solid state can be controlled by the dissolution conditions, (i.e., concentration and solvent quality),[14] and by the conditions under which solidification (crystallization) has taken place.[15] A convenient way to obtain a low entanglement density in an as-spun material is by means of gelation crystallization.[16] Even though this technique can be used for a number of different polymers, the most striking differences between the drawing behavior of melt-crystallized and gel-crystallized polymer have been observed for polyolefins. Melt-crystallized ultra-high molecular weight polyethylene, for example, can be drawn to a ratio of 5-10, whereas for gel-crystallized fibers (effective) draw ratios up to 100-150 have been reported.[17,18] Hence, a very good molecular alignment can be induced and the maximum tensile modulus reported for ultra-high molecular weight material (i.e., 264 GPa) exceeds 70 % of the theoretical modulus predicted for polyethylene.[19] Due to the limited Van der Waals interactions between the chains, properties governed by interactions in the transverse direction of the fiber, such as creep and compressive strength,[20] are mediocre and the use of this fiber is limited mainly to short-term loading applications, like in ballistic protection, and low-temperatures uses. To improve the former properties, a number of research groups have focused their efforts on orientation of polymers with increased lateral chain interactions, such as polyamides[21] and poly(vinyl alcohol).[22-23] However, these more polar materials could not be oriented to a high degree and significantly lower tensile moduli were reported than for polyethylene.

Smook et al.[21] postulated that the drawability and consequently the orientability of

flexible polymers depends on the polarity of the chain. The authors reported an Arrhenius-type correlation between the maximum attainable draw ratio (λ_{max}) and the cohesive energy (E_{coh}) of the material, viz.

$$\lambda_{max} = 360 \exp -\sqrt{\left(\frac{E_{coh}}{RT_{draw}}\right)} \qquad (1)$$

The square root of the activation term in this expression has been introduced in conjunction with the solubility parameter concept,[24] commonly used to describe the solvent strength of low molecular weight liquids. The latter parameter accounts for the heat necessary to create a cavity[25] in a polymer matrix as it is closely linked to the enthalpy of evaporation (i.e., a complete isolation of a segment from its interacting matrix).

The aim of the present investigations is to further explore the relation between the maximum drawability and the chemical structure of flexible polymers, which is reflected in the value for the heat of cavity formation (cohesive energy) as well as in the limiting maximum temperature for effective tensile deformation. In order to demonstrate the predictive potential of the convenient and simple relation [eq. (1)], the investigations into the orientability of poly(vinyl alcohol) and two new polymers, viz. the perfectly alternating ethylene-carbon monoxide copolymer (polyketone, POK-C_2)[26] and a new polyalcohol (PAl), will be reported. The synthesis and structure of the polyalcohol has been described in the previous Chapter.

5.3 Experimental

-Sample Preparation

Commercial laboratory grade starting materials were used as received. Alternating polyketones were prepared according to the description given in Chapter 2. For comparison, also a commercially available poly(vinyl alcohol) grade was used with a weight average molecular weight of 220,000 kg/kmol (Mowiol™ 66-100

(Hoechst/Celanese)) and a degree of hydrolysis of more than 99.9%. The same polyalcohol samples were used as described in the previous Chapter. Transparent polyalcohol films were cast from viscous solutions in N-methyl pyrrolidinone. After the solvent had been removed under vacuum, the thin films (60-200 μm) were cut into small strands (2-3 mm width). Polyketone fibers were spun from phenolic solutions similar to the description given in Chapter 3. To compare the drawability of polyalcohol films with poly(vinyl alcohol), thoroughly homogenized solutions of PVAl in α-pyrrolidinone or in N-methyl pyrrolidinone were spun into a methanol coagulation bath. The fibers were subsequently washed with methanol and dried in air.

-Tensile Testing

The elongation at break (ϵ_b) of the as-spun fibers or cast films at elevated temperatures was determined using a horizontal tensile tester, equipped with an oven made in our laboratories. After placing the oven around the specimen, it took about 5 seconds till the sample had been heated through. The maximum draw ratio ($\lambda_{max} = \epsilon_b + 1$) at each temperature was determined at a cross-head speed of 30 mm/min for a sample gauge length of 30 mm (initial elongation rate: 100 %/min). The average value for λ_{max} was derived from at least 20 experiments.

5.4 Results and Discussion

-Deformation Behavior of Polyalcohol, Poly(vinyl alcohol) and Polyketone

Upon large-scale tensile deformation of flexible polymers at elevated temperatures, lamellar crystals are transformed into microfibrillar structures.[27,28] The most dominating parameter with respect to the properties of the oriented structures is the degree of stretching or draw ratio, to which an unoriented polymer is subjected. Furthermore, the temperature regime in which the deformation takes place strongly affects the final arrangement of molecular aggregates obtained in the oriented sample.[29] At the onset of melting lateral stress transfer in the form of crystalline interactions diminishes, which leads to slippage of chain ends through entanglements. As described in Chapter 3, the latter phenomenon causes a local break-up of the

network and a contribution of a non-orienting deformation becomes noticeable.

At present, we would like to restrict ourselves to the deformation of a polymer in the solid-state (i.e., below the melting temperature of crystals present in unoriented material). In this temperature regime it has been suggested that after the initial break-up of lamellae the orientation mechanism involves merely the slip of fibrils past each other.[30] For polyketone fibers, we recently demonstrated that the formation of cracks becomes visible beyond a certain critical extension limit.[31] This limit is thought to be reached when parts of the chains between entanglements have reached full extension. At this stage of drawing the formed fibrillar units act more or less as rod-like entities and uniaxial stress-transfer prevails. The amorphous fraction in these fibrillar units becomes highly stressed due to a limited capacity to dissipate elastic energy by means of transport of topological defects in the direction of deformation (i.e., along the fibrillar structures). Due to a stronger fixation of topological defects in polyketone as opposed to, for example, the non-polar polyethylene, the development of the tensile modulus with the degree of stretching is less rapid.[32] This effect may be contributed to a lower modulus for shear due to a lower degree of perfection of the fibrillar structures formed. The pronounced effect of the drawing temperature on the initial tensile modulus indicated that the non-crystalline phase in polyketone fibers provides the mechanical continuity in the fiber (see Chapter 3). At high temperatures a loss of orientation occurs in the amorphous rubber-like domains, resulting in a lower modulus as well as in an increase in the elongation at break.

Here, we propose that similar to craze nucleation in glassy polymers, the orienting plastic flow in polymer networks is facilitated by the formation of small cavities caused by breaking lateral bonds via a thermally activated process.[33] These cavities create the required mobility to transport network junction points along and through the oriented structures formed. The latter forced reptation might also lead to a noticeable reduction in the entanglement density, since the extension ratios achieved at elevated temperatures can exceed the limiting low temperature value,[34] which is largely governed by the initial contour length between entanglements. Penning et al.[35] also demonstrated that for chemically crosslinked poly(L-lactide) networks the amount of

effective network nodes was substantially reduced after large-scale tensile deformation at elevated temperatures.

In a computer simulation of the deformation of polyethylene networks, Termonia and Smith[33,36] used, among other concepts, the kinetic theory of fracture, for describing the probability of a lateral bond to break at a rate υ,

$$\nu = \tau \exp -\frac{(U - \beta\sigma)}{kT} \qquad (2)$$

where τ is the thermal vibration frequency, U and β are the activation energy and volume, respectively, and σ is the applied stress. They explicitly stated that crystalline interactions are neglected in the computer simulations and that certain differences between the calculated and true stress-strain curves were attributed to these effects. The activation term in equation (2) is regarded to reflect the enthalpy required to isolate a chain segment from its interacting surroundings, or equivalently to create a cavity in the cohesive matrix.[37] In conjunction with a number of other investigators, we take the cohesive energy to be a good measure for the latter process.[21,25,38]

The values for the maximum attainable draw ratio of polyalcohol films and poly(vinyl alcohol) and polyketone fibers were determined by performing tensile tests (initial rate of deformation: 100 %/min) at various temperatures. In view of the statistical nature of fracture,[39] the average value was derived from at least 20 experiments at each temperature. We found that for the three moderately polar polymers of interest, good linear correlations are obtained when displaying the experimental results in the form of Arrhenius plots (see Fig.'s 1,2 and 3). Obviously, the observed linear correlations demonstrate the thermally activated nature of the deformation process. As explained before, we take the maximum temperature for effective drawing as the melting temperature of the polymer. Extrapolation of the regression towards the melting temperature provides information on the ultimate drawability of the material.

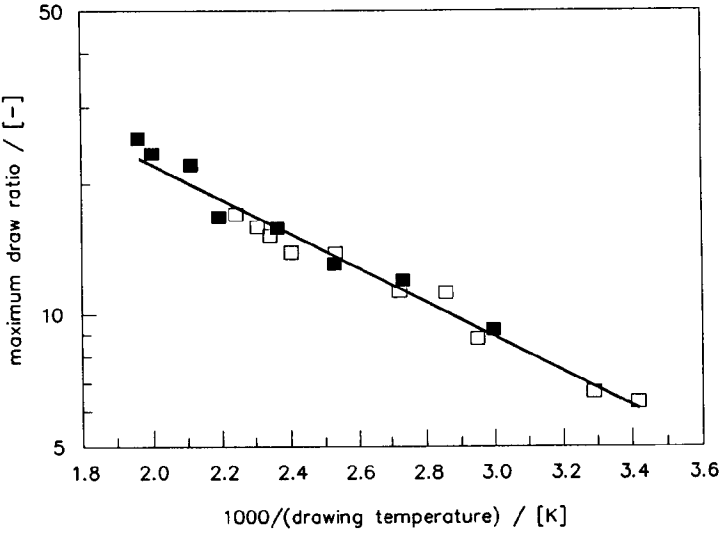

Figure 1. *The influence of the temperature on the drawability of poly(vinyl alcohol) fibers spun from two different solvents (T_m^{-1} = 1.88·10^{-3} K^{-1}) (□) : α-pyrrolidinone (20 wt.-%); (■) : N-methyl pyrrolidinone (24 wt.-%))*

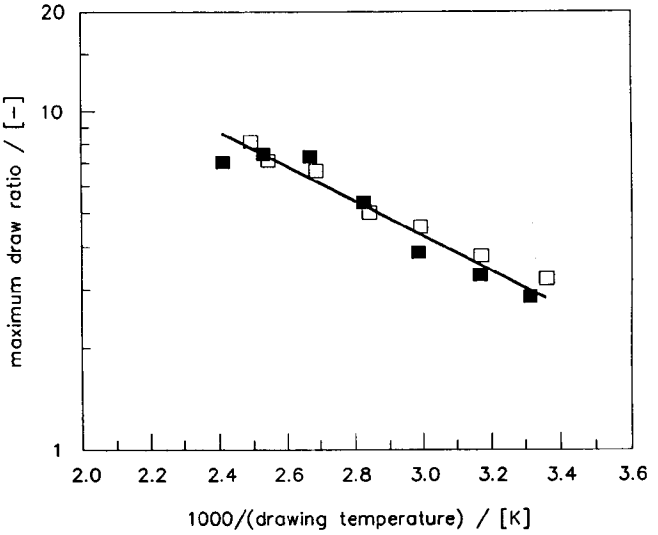

Figure 2. *The influence of the temperature on the drawability of polyalcohol films cast from solution in N-methyl pyrrolidinone (T_m^{-1} = 2.42·10^{-3} K^{-1}) (□) : M_w = 175,000 kg/kmol; (■) : M_w = 310,000 kg/kmol)*

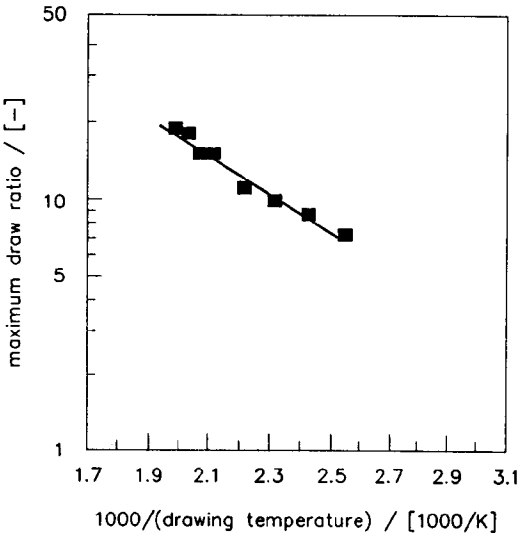

Figure 3. *The influence of the temperature on the drawability of solution spun polyketone fibers (M_w = 310,000 kg/kmol, T_m^{-1} = 1.82·10^{-3} K^{-1}).*

The value thus obtained for the maximum draw ratio of poly(vinyl alcohol) (i.e., 26 at 260 °C) is in good agreement with the value reported by Tanaka et al.[40] for ultra-high molecular weight polymer. It is also noteworthy that the two solvents used for spinning these poly(vinyl alcohol) fibers (i.e., an aprotic and a protic solvent), do not result in a different deformation behavior at elevated temperatures.

For the polyalcohol films, we determined a value for the maximum attainable draw ratio of about 10 at a maximum drawing temperature of 140 °C. In view of the similarities in chemical structure, we have also compared this result with those reported on the drawability of ethylene-vinyl alcohol copolymers with different compositions.[41,42] For the latter polymers it has been suggested that the maximum draw ratio is limited by the chain length. We were able to prepare polyalcohol samples with molecular weights in the same range as commercial high-molecular-weight poly(vinyl alcohol) grades, but no appreciable influence of the molecular weight was observed on the maximum attainable draw ratio of the solution cast films (see

Fig. 2). This finding implies that the chain length is not the dominating factor in these experiments.

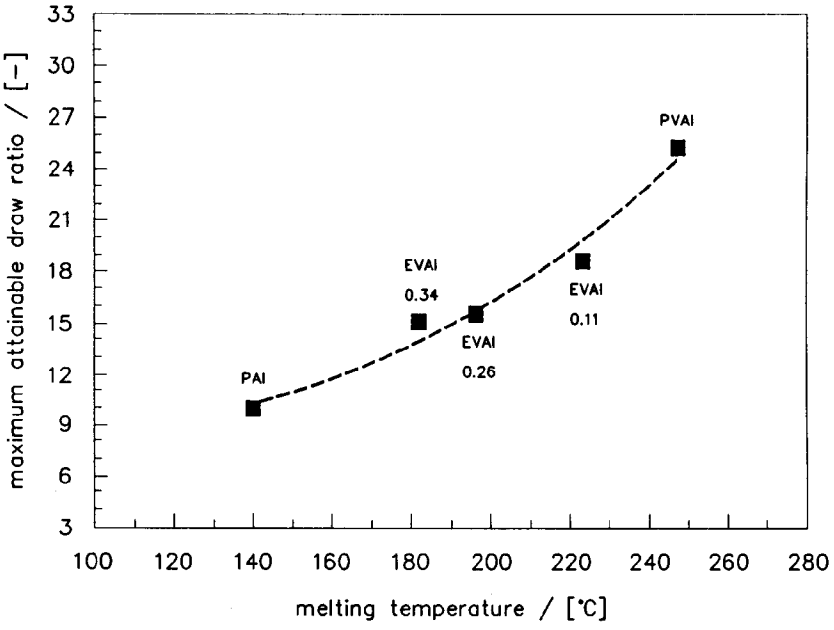

Figure 4. *The maximum attainable draw ratio of polyalcohol (PAI), ethylene-vinyl alcohol copolymers (EVAI) and poly(vinyl alcohol) (PVAI) vs the melting temperature. For the EVAI copolymers the mole fraction of ethylene units are indicated (The EVAI data are taken from ref. 41).*

In line with the thermally activated nature of the drawing process, the results presented in Figure 4 indicate that the drawability of these materials is predominantly limited by the melting temperature. We conclude from the whole range of poly-hydroxy-polymers discussed here that the activation process for allowing entanglement transport is dominated mainly by dissociation of hydrogen bonded pairs as opposed to the weak contribution of the Van der Waals forces. Thus, at higher temperatures the probability for cavitation increases [see eq. (2)] and higher draw ratio values are expected. Consequently, for the low melting polymers the dissociation of hydrogen

bonds slightly below the onset of melting is too low to allow the required transport of entanglements during tensile deformation to achieve high draw ratios. No evidence was found for any solid-solid phase transition in the temperature regime of interest. The low packing density of the chains in the polyalcohol crystal lattice results in a lower packing energy, and accordingly, in an increased pliability of the crystalline phase. If crystals were to act as the predominant barriers for large-scale deformation, we expect that the polyalcohol would be the most drawable polymer in this regard. This is not indicated by the experiments, which substantiates the importance of *non-crystalline* cohesive (topological) interactions at the limiting drawing temperature to the transport of topological defects through the network.

Polyketone has roughly the same cohesive energy density as poly(vinyl alcohol)[44] and according to eq. (1) a similar value for the ultimate draw ratio is predicted. Indeed, the value derived by extrapolating the regression line, given in Figure 3, towards a melting temperature of 277 °C yields a value of 22. Although the slope of the regression line is steeper than for the two alcoholic polymers (see Fig. 1 and 2), the predicted and the experimental value are in good agreement. In view of the different nature of the intermolecular interactions, viz. weak hydrogen bonds and dipolar interactions, the cohesive energy density is a good overall measure of the relevant interactions. Obviously, the value for the cohesive energy is dominated by polar interactions, if present, when compared with Van der Waals interactions.

-On the Drawability of Flexible Polymers

For non-polar polymers, it has been clearly demonstrated that the correlation between the dissolution conditions and the ultimate extensibility can be very large.[16] For more polar polymers this effect of the entanglement density is less pronounced or may even be absent at low polymer concentrations.[22,44] Modern theories describe entanglements as larger contour length interactions[16,45,46] relative to the concept of localized constraints in the form of interchain junction points. The latter approach explains the limited extensibility of polymer networks. but in this case an intermolecular entanglement is often simply represented as interlocking hairpins.

Obviously, there is a much greater variety in entanglement complexity in polymer systems. We presume that mainly the more complex topological interactions will be strongly affected by a dilution of the arrangement of macromolecules, because they originate from the chain overlap present in a non-dilute solution. In case of more polar polymers a less complex interchain coupling may also cause an appreciable reduction in the contour length between network nodes; these interactions can be very effective in a polar environment. Additional investigations into the effects of the initial polymer concentration on the maximum extensibility revealed that the fibers studied in the present work are prepared at sufficiently low polymer concentrations so that no constraints of the dissolution conditions on the drawability are observed. This particular subject is considered to be outside the scope of this thesis and we will elaborate on the influence of the initial polymer concentration in a forthcoming contribution.[47] In this section the importance of cohesive interactions on the ultimate extensibility will be demonstated for an extensive number of polymers.

Experimental data of a number of flexible polymers, collected from the literature and this work, are listed in Table I. The Arrhenius-type plot given in Figure 5, reveals that for this relatively large data set, a correlation is obtained between the heat of cavity formation (i.e., cohesive energy) and the maximum attainable draw ratio. The two new flexible polymers follow the same relation, corroborating the idea that the extensibility is largely governed by the chemical structure of the polymer. Also two recently investigated polymers are included in this data set, viz. poly-*p*-xylylene[50] and poly-*trans*-(1,4)-butadiene.[52] Both polymers are oriented in a conformationally disordered phase, but Figure 5 shows that the drawing behavior is not fundamentally different from that of the other polymers.

In the case of poly-*p*-xylylene the drawing procedure is very effective in inducing molecular orientation, implying that the conformationally disordered phase is sufficiently tough to provide the required stress transfer between adjacent chains. The molecular alignment in poly-*trans*-(1,4)-butadiene has been introduced via solid-state coextrusion of single crystal mats, because it was impossible to achieve high draw ratios for melt-crystallized films, which is probably due to the low molecular weight of

the sample used.

Table I. *The Experimental Maximum Attainable Draw Ratio of Various Flexible Polymers Correlated with the Heat of Cavity Formation and the Limiting Drawing Temperature.*

polymer	λ_{max}(exp.)	T_{draw} exp.	T_{draw} lim.	limitations in T_{draw}	$E_{coh.}/RT_{draw}$(lim.) [a]
	[-]	[K]	[K]		[-]
polyethylene[48]	150	423	425	CONDIS (hexagonal)→MELT	1.3
polypropylene[49]	47.5	413	480	CRYSTAL→MELT	2.6
poly-*p*-xylylene[50]	43	693	700	CONDIS (β_2)→MELT	4.8
polyacrylo nitril[51]	28	473	590	CRYSTAL→MELT, DEGRADATION	5.0
poly(vinyl alcohol) (this work)	26	520	520	CRYSTAL→MELT	4.4
poly-*t*-(1,4)-butadiene[52]	25[b]	393	410	CONDIS (hexagonal)→MELT	3.9
polyketone (this work)	22	550	550	CRYSTAL→MELT	5.5
poly-*l*-lactic acid[53]	20	477	477	CRYSTAL→MELT	4.7
EVAl-copolymeer (F_E=0.11)[41]	18.5	463	497	CRYSTAL→MELT	4.6 [c]
EVAl-copolymeer (F_E=0.26)[41]	15.5	413	469	CRYSTAL→MELT	5.0 [c]
EVAl-copolymeer (F_E=0.34)[41]	15	403	455	CRYSTAL→MELT	5.2 [c]
polyalcohol (this work)	10	415	415	CRYSTAL→MELT	7.0
poly(ethylene terephthalate)[47]	7	533	545	CRYSTAL→MELT	11.4
polamide-6,6[54]	6	533	535	CRYSTAL→MELT	17.3[d]
polyamide-6[21]	6	473	495	CRYSTAL→MELT	18.7

[a] cohesive energy corrected for drawing temperature $E_{coh}(T) - E_{coh}(298)$-RT

[b] solid-state extrusion draw ratio

[c] cohesive energy of the vinyl alcohol units is used

[d] cohesive energy calculated per peptide linkage.

A number of approaches have been offered in the literature to provide a quantitative description of the extensibility of flexible polymers, viz. chain length ($\lambda_{max} \approx$(molecular weight)$^{1/2}$),[55] entanglement density ($\lambda_{max} \approx$(polymer concentration)$^{-1/2}$),[16,56] and the number of intermolecular entanglements per chain ($\lambda_{max} \approx$ (molecular weight*polymer concentration)$^{-1/2}$).[22,57] The present work clearly demonstrates the additional influence of the effectiveness of entanglement transport in different chemical environments. Although the merits of the observed phenomena are not yet fully understood the interpretation that entanglements act as the predominant barriers for large scale deformation remains the same, at least in non-polar and weakly polar polymers.

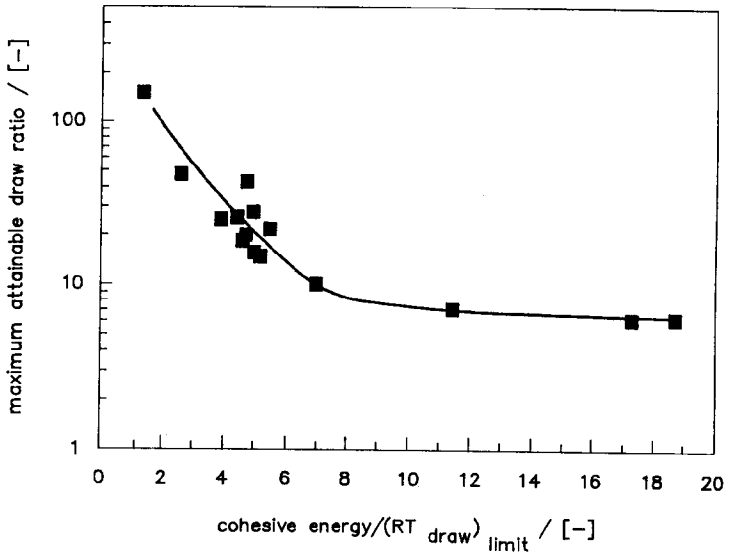

Figure 5. *The maximum attainable draw ratio of a series of flexible chain polymers vs the heat of cavity formation (data points are taken from Table I).*

In highly polar polymers, with a high lattice energy (e.g. nylon 6, nylon 6,6: [right half section of Figure 9]), exceedingly small crystallites are thought to act as very effective crosslinks .

The demonstrated correlation between the cohesive energy and the maximum attainable draw ratio is slightly different from equation (1), initially proposed by Smook et al.[21]. The relation provides a tool for predicting the ultimate degree of orientation, which can be induced in (new) gel-crystallized polymers by solid state deformation close to the melting temperature of unoriented material. We have omitted the use of an additional parameter to obtain a linear description of the experimental results. The non-linearity of the found correlation finds its origin in the difference in deformation behavior of highly polar polymer systems. This subject will be part of a detailed discussion in a forthcoming contribution.[58]

5.5 Conclusions

The drawability of flexible polymers is strongly affected by the lateral interactions between the chains, which is due to the effect of the polar interactions along the effective contour length between entanglements. The cohesive energy appears to provide for a good measure of the grand total of those lateral chain interactions, and may be used to predict the orientability of new, low- or moderately polar, starting materials for fibers. The low melting temperature of the new polyalcohol limits its ultimate extensibility and also the performance in various end-uses. High melting polyketone fibers can be drawn to relatively high draw ratios and mechanical properties similar to those of poly(vinyl alcohol) may be anticipated.

5.6 References and Notes

1. I.M. Ward, *Mechanical Properties of Solid Polymers*, 2nd ed., Wiley, New York, 1983.
2. H.G. Weyland, *Polym. Bull.*, **3**, 331 (1980).
3. S.J. Picken, S. v.d. Zwaag and M.G. Northolt, *Polymer*, **33**, 1998 (1992).
4. M.G. Northolt and D.J. Sikkema, *Adv. Pol. Sci.*, **98**, 115 (1990).
5. A. Ziabicki, *Fundamentals of Fiber Spinning*, Wiley, London, 1976.

6. A. Ziabicki and H. Kawai, *High-speed Fiber Spinning*, Wiley, New York, 1985.
7. A.J. Pennings, M. Roukema and A. v.d. Veen, *Polym. Bull.*, **23**, 353 (1990).
8. B. Kalb and A.J. Pennings, *Polym. Bull.*, **1**, 871 (1979).
9. P. Smith and P.J. Lemstra, *J. Mater. Sci.*, **15**, 505 (1980).
10. J. D. Ferry, *Viscoelastic Properties of Polymers*, 3th ed., Applied Science, London, 1983.
11. H.H. Kausch, *Polymer Fracture*, Springer Verlag, Berlin, 1978.
12. E.J. Kramer, *Adv. Pol. Sci.*, **52/53**, 1 (1983).
13. M.C.M. v.d. Sanden, H.E.H. Meijer and T.A. Tervoort, *Polymer*, **34**, 2961 (1993).
14. P.G. de Gennes, *Scaling Concepts in Polymer Physics*, Cornell University Press, Ithaca, 1979.
15. B. Wunderlich, *Macromolecular Physics*, Vol. II, *Crystal Nucleation, Growth, Annealing*, Academic Press, New York, 1976.
16. P. Smith, P.J. Lemstra and H.C. Booij, *J. Polym. Sci. Phys. Ed.*, **19**, 877 (1981).
17. T. Kanamoto, A. Tsuruta, K. Tanaka, M. Takeda and R.S. Porter, *Polym. J.*, **15**, 327 (1983).
18. A.V. Savitsky, I.A. Gorshkova, I.L. Frolova, G.N. Shmikk and A.F. Ioffe, *Polym. Bull.*, **12**, 195 (1984).
19. H. v.d. Werff and A. J. Pennings, *Coll. Pol. Sci.*, **269**, 747 (1991).
20. M.G. Northolt, *J. Mater. Sci.*, **16**, 2025 (1981).
21. J. Smook, G.J.H. Vos and H.L. Doppert, *J. Appl. Pol. Sci.*, **41**, 105 (1990).
22. C.W.M. Bastiaansen, *Ph.D. Thesis*, University of Eindhoven, The Netherlands (1991).
23. C. Sawatari, Y. Yamamoto, N. Yanagida and M. Matsuo, *Polymer*, **34**, 956 (1993).
24. J.H. Hildebrand, J.M. Prausnitz and R.L. Scott, *Regular and Related Solutions*, Van Nostrand Reinhold, New York, 1970.
25. C. Reichardt, *Solvent and Solvent Effects in Organic Chemistry*, 2nd ed., VCH Verlag, Weinheim, 1988.
26. E. Drent, J.A.M. v. Broekhoven and M.J. Doyle, *J. Organomet. Chem.*, **417**, 235 (1991).
27. A. Peterlin, *J. Mater. Sci.*, **6**, 490 (1971).

28. A. Peterlin, *Coll. Pol. Sci.*, **265**, 357 (1987).
29. A.J. Pennings, J. Smook, J. de Boer, S. Gogolewski and R.F. v. Hutten, *Pure & Appl. Chem.*, **55**, 777 (1983).
30. J. Smook and A.J. Pennings, *J. Appl. Pol. Sci.*, **27**, 2209 (1982).
31. B.J. Lommerts, H. Ter Maat, and R. Huisman, (submitted for publication).
32. B.J. Lommerts, H. Ter Maat, and R. Huisman, (in preparation).
33. Y. Termonia, S.R. Allen and P. Smith, *Macromolecules*, **21**, 3485 (1988).
34. E.J. Kramer and L.L. Berger, *Adv. Pol. Sci.*, **91/92**, 1 (1990).
35. J.P Penning, *Ph.D. Thesis*, University of Groningen, The Netherlands (1994).
36. Y. Termonia and P. Smith, *Macromolecules*, **21**, 2184 (1988).
37. A.S. Argon and J.G. Hannoosh, *Phil. Mag.*, **36**, 1195 (1977).
38. J.A.M. Remmerswaal in: *Deformation, Yield and Fracture of Polymers.*
39. S. v.d. Zwaag, *J. Test. Eval.* **17/5**, 292 (1989).
40. H. Tanaka, M. Suzuki and F. Ueda, *European Patent*, 146,084 (Toray) (1984).
41. R. Schellekens and H. Ketels, *Polym. Comm.*, **31**, 212 (1990).
42. H.H.T.M. Ketels, Ph.D. thesis, University of Eindhoven, The Netherlands (1989).
43. An estimate for the cohesive energy density of polyketone at room temperature has been derived from the Hildebrand solubility parameter, which was determined by measuring the solubility in over 200 low-molecular-weight liquids and solids.
44. B.J. Lommerts, E. Klop, J. Aerts, J. Veurink, and S.J. Picken, Rolduc Polymer Meeting 1992, Kerkrade, The Netherlands.
45. P.G. de Gennes, *J. Chem. Phys.*, **55**, 572 (1971).
46. M. Doi and S.F. Edwards, *J. Chem. Soc. Faraday Trans.*, **74**, 1789 (1978).
47. B.J. Lommerts and A.J. Pennings, in preparation.
48. J.P. Penning, H.E. Pras and A.J. Pennings, *Coll. Pol. Sci.*, submitted.
49. A. Peguy and R. St. John Manley, *Polym. Comm*, **25**, 39 (1984).
50. H. v.d. Werff and A.J. Pennings, *Polym. Bull.*, **19**, 587 (1988).
51. D.Y. Kwon, S. Kavesh and D.C. Prevorsek, *European Patent*, 144,793 (Allied) (1983).
52. N.A.J.M. v. Aerle, P.J. Lemstra, T. Kanamoto and C.W.M. Bastiaansen, *Polymer*, **32**, 34 (1991).
53. J.W. Leenslag and A.J. Pennings, *Polymer*, **28**, 1695 (1987).

54. The maximum attainable draw ratio of 6 for polyamide-6,6 is typical for melt-crystallized material. Just as with polyamide-6 (see ref. 21) solution spinning does not enhance the drawability of this polymer.

55. P. Smith, R.R. Matheson, Jr. and P.A. Irvine, *Polym. Comm.*, **25**, 294 (1984).

56. W.W. Graessley, *Adv. Pol. Sci.*, **16**, 58 (1974).

57. C.W.M. Bastiaansen, *J. Polym. Sci. Polym. Phys. Ed.*, **28**, 1475 (1990).

58. B.J. Lommerts and A.J. Pennings, (in preparation).

Chapter 6.

POLYMORPHISM IN ALTERNATING POLYOLEFIN KETONES

Reproduced in part from:
E.A. Klop, B.J. Lommerts, J. Veurink, J. Aerts, and R.R. van Puijenbroek,
J. Polym. Sci. Polym. Phys. Ed. (accepted for publication).

6.1 Summary

The perfectly alternating ethylene-carbon monoxide copolymer shows a reversible phase transition between 110-130 °C from the dense POK-α (orthorhombic) to the POK-β (orthorhombic) crystal structure with a 10 % change in crystalline density. Although the packing density of the β-structure is significantly smaller, the heat effect associated with the transition is relatively small. The occurrence of the POK-α structure at room temperature is strongly influenced by the amount of chain defects randomly incorporated into the polymer backbone. The effect of the incorporation of propylene-carbon monoxide segments on the α/β-transition is studied on oriented fiber samples. With more than 5 mole-% of defects, polyketone terpolymers are not capable of forming the POK-α structure in oriented fibers prepared from semi-dilute or concentrated solutions. The polymerization conditions have a pronounced effect on the occurrence of the α-structure in as-polymerized samples. The α-phase content in isotropic samples can be enriched by recrystallization from solution, which indicates that a certain (segmental) mobility is required to accomplish the formation of the dense α-modification.

6.2 Introduction

Already since the early '50 's olefins and carbon monoxide were recognized as a potential cheap feedstock for new polymer materials (polyketones).[1] Initially, these polyketones were prepared from ethylene and carbon monoxide via a radically

induced polymerization process. But polymers with a ethylene/CO ratio close to 1 could only be synthesized under extreme conditions.[2] Chatani et al.[3,4] determined the crystal structure of such a polyketone with an ethylene/CO ratio of 1.05. The latter structure is designated here as the POK-β modification.

Sen and coworkers[5-7] at Penn. State university have studied the polymerization of polyolefin ketones using organometallic catalyst systems. Their palladium (Pd(II)) phosphine complexes were capable of forming alternating ethylene-carbon monoxide copolymer. A significant improvement in the rate of polymerization has been established by Drent et al.,[8] who developed the group of *cis*-fixed palladium bidentate catalyst compounds. In contrast to the radically induced copolymerization this special class of catalyst systems enables the manufacturing of high-molecular-weight polymers, whereas no defects, like non-alternating sequences, could be detected. Hence, the mechanism of polymerization seems to prohibit the incorporation of chain defects into the polymer backbone during chain growth.

At the beginning of this decade the field of homogeneous catalysis for the production of polyketones has rapidly emerged and at present a number of groups have become active. Their work is primarily focused on an understanding of the polymerization mechanism,[9-12] and on the application of this class of catalyst systems for the production of novel polymers.[13-16] Within our laboratories, we have focused our efforts on the application of these new polymers in fiber materials.[17,18] The perfectly alternating ethylene-carbon monoxide copolymer (POK-C_2) seems to be the most promising one in this respect as this material shows a high melting temperature (260 °C). The crystal structure of this perfectly alternating material (i.e, the POK-α structure)[17] turned out to be different from the POK-β structure observed in imperfectly alternating ethylene-carbon monoxide copolymers. The chain conformation in both structures is all-*trans* but the crystalline density of the POK-β structure is significantly lower than that of the POK-α structure.

In the present investigations, we study a structural transition in the POK-C_2 copolymer in order to gain insight into the high-temperature performance of polyketone fibers. At

present melt processing of high melting polyketones seems to be impossible. The poor thermal stability of the 1,4-arrangement of carbonyls gives rise to both intra- and intermolecular condensation reactions at high temperatures. For example, the well-known Paal-Knorr cyclization reaction[19] results in the formation of furan structures (see Figure 1) and water is formed as the condensation product. To avoid thermal degradation the melting temperature of POK-C_2 can be lowered via the random incorporation of a certain amount of propylene-carbon monoxide segments into the polymer backbone.[17]

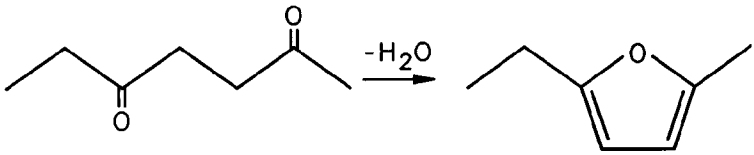

Figure 1. *Paal-Knorr type of cyclization reaction in 1,4-diketones.*

The melting point depression of these so-called POK-C_2/C_3 terpolymers has been described in detail in Chapter 2. In this Chapter the influence of the fraction of chain defects on the room temperature crystal structure together with a structural transition in perfectly alternating ethylene-carbon monoxide copolymers will be reported.

6.3 Experimental

-Materials

POK-C_2 copolymers were prepared from ethylene and carbon monoxide according to the description given in refs. 20 and 21, using the 1,3-*bis*(diphenyl-phosphino) propane palladium bidentate complex as the catalyst system. For the preparation of

low-molecular-weight polymers the so-called methanol slurry polymerization process is applied.[20] The catalyst is dissolved in methanol and during polymerization the polymer precipitates from solution. After drying, a low bulk density powder is obtained. For the preparation of high-molecular-weight polymer the catalyst is coated on a small amount of low-molecular-weight polymer and the reaction is carried out in the polymer/gas interphase.[21] Since methanol causes chain transfer reactions the absence of a large amount of solvent results in appreciably higher molecular weights. For the preparation of the POK-C_2/C_3 terpolymers via the methanol slurry process a small amount of propylene is added to the autoclave prior to pressurizing with a 1:1 mixture of ethylene and carbon monoxide.

The molecular weight of the polymer formed is strongly influenced by the temperature and pressure conditions in the autoclave. We conducted our polymerization experiments typically at a temperature between 40-60 °C and at a pressure between 60-80 bar. The intrinsic viscosity (*m*-cresol, 25 °C) of polymers obtained under these conditions via the methanol slurry process ranges from 0.4-2 dL/g, whereas the gas-phase process yields polymer with an intrinsic viscosity between 3-10 dL/g. For the terpolymers the amount of propylene randomly incoporated was measured using ^{1}H-NMR in d^6-phenol. The same correlation between the melting temperature and the fraction of chain defects was obtained as the one presented in Chapter 2. This correlation was based on the melting point depression of both perfectly alternating polyketone terpolymers and imperfectly alternating copolymers.

-Yarn samples

Polyketone fibers were prepared by solution spinning from phenol/acetone mixtures (9:1 weight ratio). Since melt spinning of high melting polyketones is seriously hampered by polymer degradation, the former spinning technique allows significantly lower processing temperatures, whereby the formation of chain defects via (thermal) degradation is completely avoided. The intrinsic viscosity ($[\eta]$), propylene content (mole %-C_3) and melting temperature (T_m) of the various as-polymerized co- and terpolymers are given in Table I. Also the dissolution and spinning conditions are included (x_{pol} is the polymer concentration). The solutions were spun into a (cold)

acetone bath by application of an air-gap and using a piston-cylinder apparatus. The winding speed was slightly less than the extrusion speed (1 m/min). Hence, some relaxation and shrinkage of the swollen fiber were allowed. The fibers were washed with acetone, dried in air and subsequently drawn continuously at elevated temperatures using hot plates. The difference between the drawing temperature and the melting temperature was comparable in all cases.

Table I. *Spinning and Drawing Conditions Applied for the Preparation of Polyketone Fibers with Different Propylene Content*

Sample	$[\eta]$	%-C_3	T_m	x_{pol}	T_{spin}	T_{bath}	T_{draw}	λ
	[dL/g]	[mole/mole]	[°C]	[wt. %]	[°C]	[°C]	[°C]	[-]
POK-C_2	9.0	0	258	5.1	80	-6	220-257[a]	10-20[a]
POK-C_2/C_3	1.9	3	238	22.0	68	20	210	10.3
POK-C_2/C_3	1.0	5	231	24.2	65	23	200	10.0
POK-C_2/C_3	1.5	12	206	20.0	30	25[b]	179	10.5
POK-C_2/C_3	0.8	15	196	31.0	25	25	171	10.5

a Fibers were drawn according to a multi-stage procedure; $\lambda_1 = 5.6$, $\lambda_2 = 2.3$ and $\lambda=\lambda_1\lambda_2\lambda_3$, where λ is the draw ratio.

b No air-gap was applied.

-Analysis

DSC measurements were carried out using a Perkin Elmer DSC-7 thermal analyzer at a scanning speed of 20 °C/min. X-ray diffraction patterns were recorded using several techniques. A detailed description of the applied x-ray diffraction techniques is given in ref. 22.

6.4 Results and Dissusion

-Solid-Solid Phase Transformation in Oriented POK-C_2 Fibers

Thermal analysis on oriented POK-C_2 fibers revealed a small endothermic effect in the temperature range between 110-130 °C (see Figure 2).

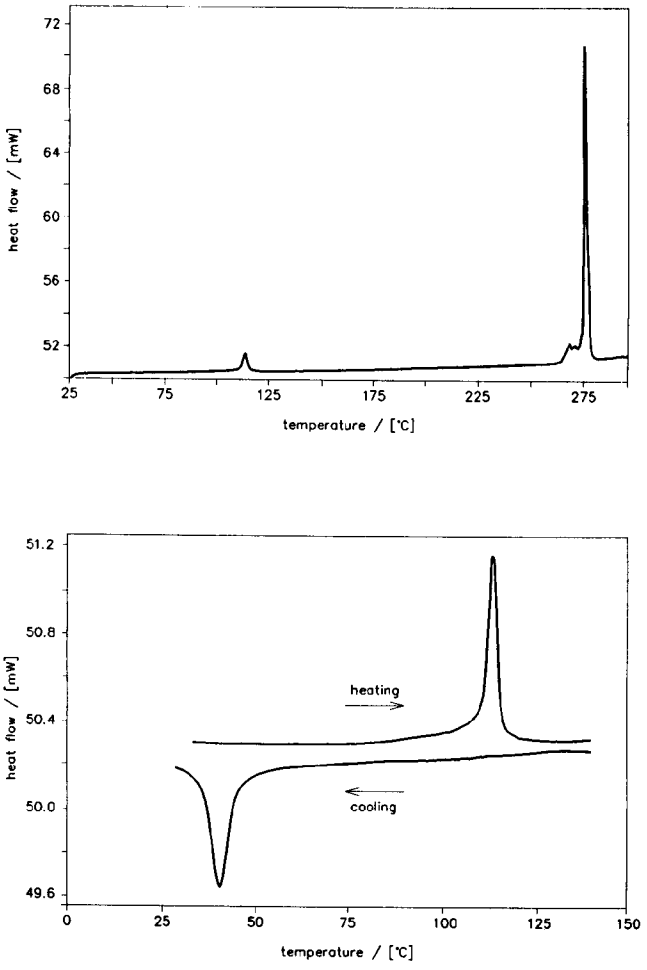

Figure 2. *DSC scans of perfectly alternating POK-C_2 fiber. ((a) heating to 300 °C; (b) heating to 150 °C (top curve) followed by cooling down (bottom curve))*

Upon cooling, an exotherm (with undercooling) is observed with a corresponding heat effect as the endotherm upon heating (see Figure 2[b]; endotherm: 14.4 J/g; exotherm: 13.8 J/g). This result clearly indicates a reversible phase transition in oriented POK-C_2 polymers at about 110 °C. Initially, this was a point of concern to us, because some linear, less polar, flexible polymers with an all-*trans* conformation of the chains in the crystal lattice, like polyethylene (PE),[23] poly tetra(fluoro ethylene) (PTFE),[24] poly-*p*-xylylene (PPX)[25,26] or *trans*-1,4-polybutadiene,[27] exhibit a solid-solid phase transition at elevated temperatures. Such a phase transition results in an increase in conformational disorder, allowing a liquid-like motion in the direction of the *c*-axis of the crystal. Therefore, these so-called condis-crystals are rather pliable and the mechanical properties rapidly deteriorate, when the transition temperature is approached.

In order to investigate the structural transformation in polyketone-C_2 fibers at 110-130 °C various x-ray diffraction techniques were employed. An equatorial Guinier-Lenné photograph of an oriented POK-C_2 fiber is shown in Figure 3. At low temperatures the equatorial diffraction pattern corresponds to the POK-α (orthorhombic) structure. At about 110 °C a structural transition becomes noticeable, which causes a significant change in the equatorial diffraction pattern. Upon cooling, the low-temperature POK-α modification is formed again and almost no remnants of the high-temperature modification are visible. Clearly, the reversible nature of the found structural transformation in oriented POK-C_2 copolymers is in line with the thermal analysis experiments (see Figure 2). The high-temperature modification of oriented POK-C_2 copolymers was studied by recording flat-plate x-ray diffraction photographs (see Figure 4) at 20 °C and slightly above the transition temperature (i.e., at 140 °C). The fiber under investigation was drawn to a ratio of 20 and the low degree of arcing of the reflections points to a high degree of crystalline orientation in this material. The high-temperature modification [right diffraction pattern: Figure 4[b]] matches the crystal structure reported by Chatani et al.[3,4] (i.e., the POK-β (orthorhombic) structure found in oriented imperfectly alternating ethylene-carbon monoxide copolymers). The latter structure can be indexed with an orthorhombic unit cell with dimensions 8.24(2), 4.74(2) and 7.58(2) Å and spacegroup Pnam.

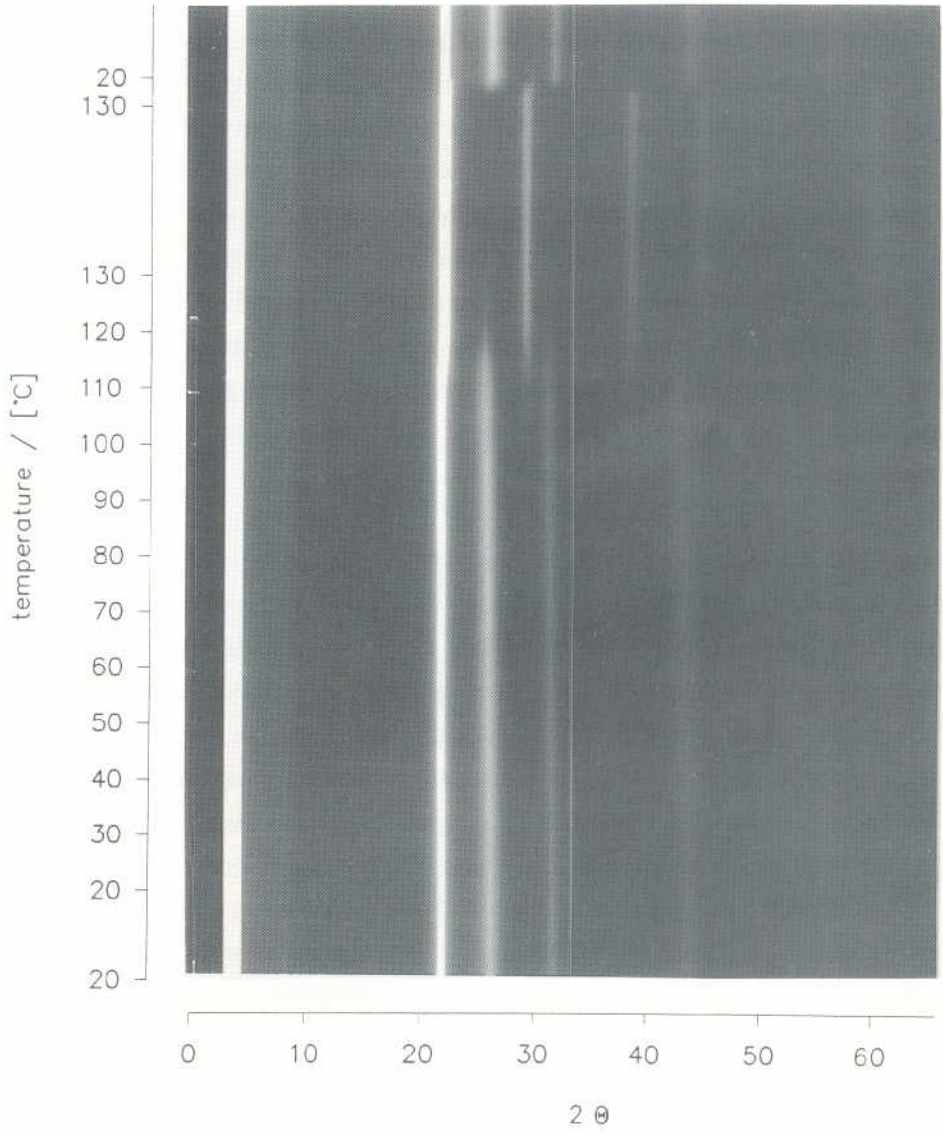

Figure 3. *Guinier-Lenné photograph of perfectly alternating POK-C_2 fiber. Starting at the bottom of the photograph the applied temperature program was as follows: fixed temperature of 20 °C; heating from 20 to 130 °C at a rate of 2 °C/hr; fixed temperature of 130 °C; fast (uncontrolled) cooling from 130 to 20 °C; fixed temperature of 20 °C.*

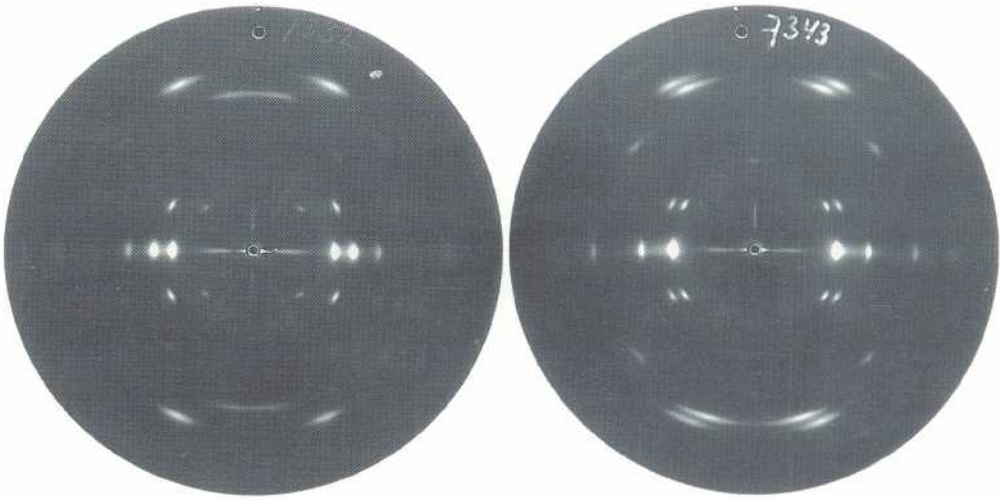

Figure 4. *Flat plate photographs of perfectly alternating POK-C_2 fiber ((a) at room temperature; (b) at 140 °C).*

The crystal unit cell dimensions and crystalline density of the modifications found in polyketones and those of polyethylene are compiled in Table II. Only small differences are observed between the crystal structure in oriented POK-C_2 copolymers at 140 °C and the POK-β structure of Chatani et al. at room temperature, keeping in mind that part of the differences may be due to thermal expansion. In view of the similarities between the two structures, we have designated both structures as the POK-β modification.

Views of both the POK-α and the POK-β structure were presented in Chapter 2. The all-*trans* conformation of the polymer backbone remains unaffected when POK-α is transformed into the POK-β structure. Apart from the change in cell dimensions, the differences between the two structures can be described by an increase in the angles between the *bc*-plane and the planes of the polymer chains from 26 ° to 40 °,

accompanied by a rotation of the center chain over 180 ° or equivalently by a shift ½*c* of the center chain in the direction of the fiber axis. The structural transformation results in a 10 % increase in volume of the crystal unit cell. This is a significant change in crystal packing density, but the heat effect associated with the change in the orientation of the carbonyls is relatively small and amounts to roughly 5-10 % of the heat of fusion (ΔH_f=140-200 J/g for oriented fibers). This result suggests that the longe-range dipolar interactions between adjacent chains are not strongly affected by the structural transformation. The latter is substantiated by the arrangement of the carbonyl dipoles in the POK-β crystal lattice.

Table II. *Unit Cell Dimensions and Crystalline Density of Alternating Polyketone Copolymers and Polyethylene (PE).*[28]

Sample	modification	*a* [Å]	*b* [Å]	*c* [Å]	ρ_c [g/cm^3]
POK-C_2 (20 °C)	α	6.87(2)	5.12(2)	7.60(2)	1.39
POK-C_2 (140 °C)	β	8.24(2)	4.74(2)	7.58(4)	1.26
POK-C_2 (Chatani et al.)	β	7.97	4.76	7.57	1.30
PE	-	7.40	4.93	2.534	1.00

In the dense POK-α structure the carbonyl groups are more directed along the *bc* plane in the crystal unit cell (see Chapter 2), which gives rise to limited dipolar

interactions perpendicular to the *bc* plane. The overall thermal expansion of the POK-α unit cell with temperatures increasing from 22 °C to 100 °C amounts to 1.5 %. The expansion occurs mainly in the direction of the *a*-axis. In the POK-β structure the electrostatic interactions perpendicular to the *bc* plane are probably more effective relative to the POK-α structure due to the different arrangement of the dipolar interactions in the POK-β structure. Based on these results, we presume that the α/β-phase transition is not accompanied by a significant decrease in tensile properties of oriented POK-C_2 fibers. This is in contrast to the less polar polymers, which exhibit a condis-phase transition at elevated temperatures. Since the *c*-axis of the crystalline unit cell is not affected by the solid-solid phase transition the volume change will only have a minor effect on the length of an oriented fiber. In fact the measured shrinkage of an oriented fiber at an applied load of 7 MPa was below 0.1 % at the transition temperature. However, for isotropic crystallized samples, which show the POK-α structure at room temperature, the volume change might be an important aspect. Assuming a crystallinity of 50 % in isotropic material, the net volume change will be 5 %. For various end-uses this may be a point of concern as 110-130 °C is below the maximum end-use temperature for a number of engineering plastic applications. The effect of the α/β-transition on the tensile modulus and tensile strength of polyketone fibers will be described in more detail in the next Chapter.

-Parameters Influencing The α/β-Transition

The α/β-transition temperature and melting point of POK-C_2 fibers, drawn to different ratios, are presented in Figure 5. These particular fibers are drawn at a feeding speed of 1 mm/s between two roller sets over a hot plate (T_{draw}=228 °C). Hence, after the fiber is oriented, it is cooled from 228 °C to room temperature under the drawing tension. The melting temperature of high-molecular-weight POK-C_2 fiber increases with the degree of orientation, which can be attributed to a reduction in surface free energy of the oblong-shaped crystals formed. In contrast to the melting temperature, the α/β-transition temperature decreases slightly with the draw ratio. It should be noted that the drawing of as-spun material is carried out at temperatures exceeding the α/β-transition temperature (i.e., at temperatures where the β modification is the most stable one). Hence, after the drawing procedure is completed the crystal

structure transforms from the β- to the α-structure. The increase in melting temperature indicates that the degree of perfection of the β-crystals formed is significantly improved by the orientation procedure. The drawing stress increases substantially with the draw ratio. The higher tension at higher draw ratios affects the degree of perfection of the α-modification formed upon cooling. This result points to a limited ability to form perfect POK-α crystals under more constraint conditions.

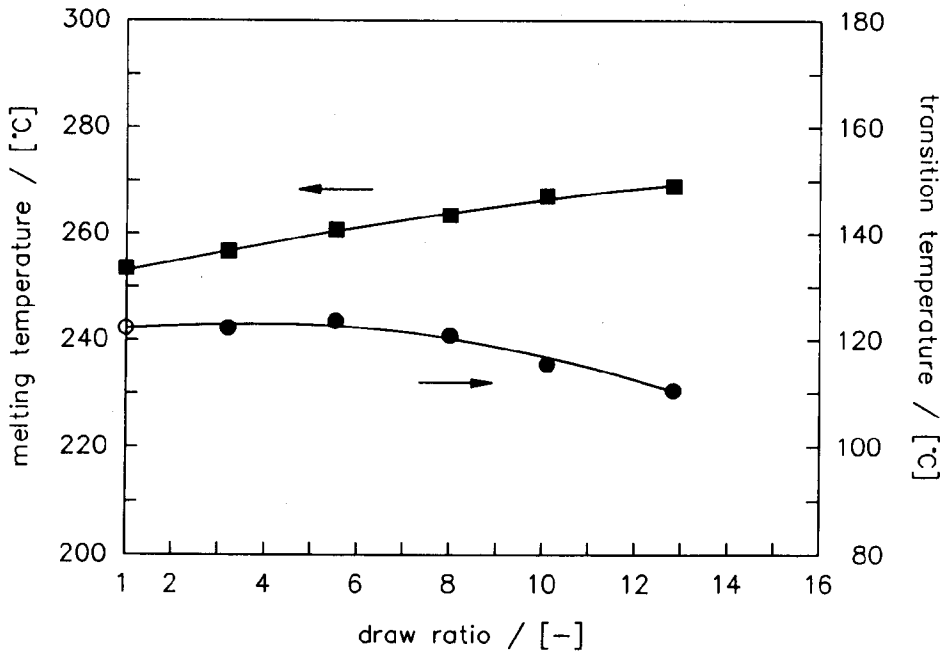

Figure 5. *Melting point and α/β-transition temperature of polyketone-C_2 fibers, drawn to different ratios at 228 °C ((O) : data point taken from Fig. 3).*

To gain further insight into the kinetics of the transition process, we looked into the crystalline modifications in two as-synthesized (virgin) polymers, viz. a low-molecular-weight polymer prepared according to the methanol-slurry process and a high-molecular-weight polymer prepared according to the gas-phase process. Diffraction

patterns of these materials, measured with a reflection diffractometer, are displayed in Figure 6 together with the calculated powder patterns of POK-α and POK-β, respectively. The patterns were calculated from the crystal structure reported in ref. 17, and that of Chatani et al.[3,4] for CuKα radiation and assuming an overall isotropic temperature parameter of 5.0 Å^2. The high-molecular-weight powder crystallizes almost completely in the POK-β modification, as can be concluded from Figure 6.

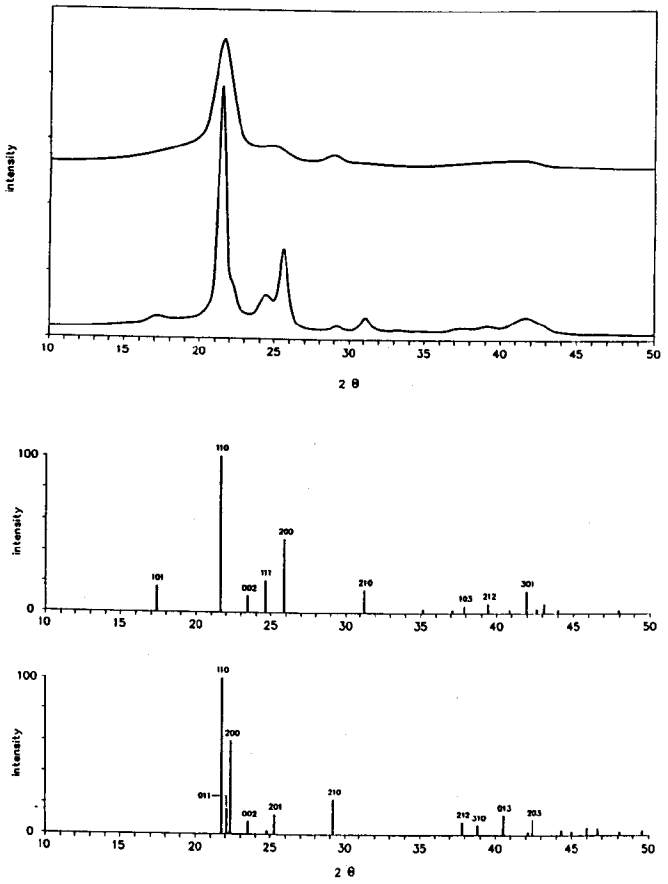

Figure 6. *(a) Diffraction patterns of perfectly alternating POK-C_2 powder, upper curve: high-molecular-weight powder; lower curve: low-molecular-weight powder. (b) Calculated powder diffraction pattern of POK-α. (c) Calculated powder diffraction pattern of POK-β.*

The low-molecular-weight material consists of a mixture of both POK-α and POK-β and its crystalline perfection is considerably larger than for the high-molecular weight polymer, as is indicated by the differences in the width of the intensity peaks. After recrystallization from a poor solvent, viz. propylene carbonate (T_c = 140 °C), the POK-β to POK-α transformation is almost complete, as can be deduced from Figure 7.

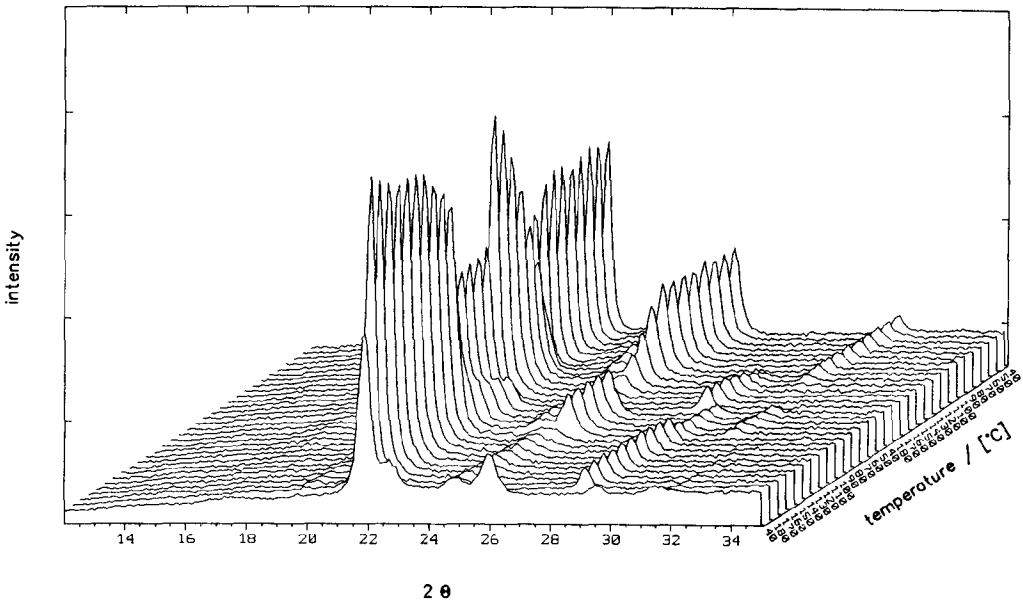

Figure 7. *High-temperature x-ray diffraction scans of low-molecular-weight POK-C_2 recrystallized from propylene carbonate.*

In the x-ray diffraction temperature scan the α/β-transition takes place in a temperature range between 120-140 °C. Upon cooling, the β-structure is not completely transformed into the α-structure, since still remnants of the β-modification are present at room temperature. When the sample is subjected to another

temperature cycle (20 °C→180 °C→20 °C) the β-modification is again partly transformed into the α-modification. Hence, crystallization from solution enables the formation of the dense α-structure in isotropic samples, and when no solvent is present a certain amount of the β-modification remains untransformed.

Recrystallization of high-molecular-weight POK-C_2 from a good solvent system, viz. a phenol/acetone mixture (9:1 weight ratio), results also in an enriched α-content at room temperature. Since after drawing the fiber consists exclusively of POK-α [at room temperature] it can be concluded that the process of dissolution, spinning and drawing leads a transformation of unoriented β-rich material into oriented POK-α structures.

The results may be summarized by concluding that low-molecular-weight as-polymerized (virgin) material crystallizes at least partly in the α-modification, whereas (virgin) high-molecular-weight POK-C_2 crystallizes almost completely in the β-modification with a lower degree of crystalline perfection. These particular differences in crystallization behavior can be attributed to the kinetics of the crystallization process. For as-polymerized sample the latter process is predominantly determined by the polymerization conditions, viz. temperature, solvent, etc., yielding differences in molecular weight and morphology of the polyketone powders formed. Since our primary goal is to establish insight into crystal transition phenomena during fiber spinning and into the high-temperature performance of polyketone fibers, we will not discuss the influence of these parameters extensively. Recrystallization from solution results in an increase in α-content compared with as-polymerized material, indicating that a certain segmental mobility is required to facilitate the formation of the α-structure. During drawing the α/β-transition temperature decreases with the draw ratio, implying that the chain mobility under tension is noticeably reduced relative to unconstraint conditions, and as a result less perfect α-crystals are formed. In unoriented materials the nucleation of the β/α-transition is significantly hampered by the low degree of molecular alignment. In view of the relatively small heat effect associated with the α/β-transition, topological defects incorporated during crystallization can easily prevent the formation of the dense α-structure. The influence of these defects is less noticeable for oriented fibers, since during drawing lamellar

crystals are transformed into fibrillar structures. In the next section, we will describe the influence of other defects, viz. chain defects, in the form of small methylene side-groups on the occurrence of the α/β-transition in oriented polyketones.

-Polyketone Terpolymers

Fiber samples of polyketone (POK-C_2/C_3) terpolymers were prepared in essentially the same way as the POK-C_2 fibers. These polymers differ from the perfectly alternating POK-C_2 polymers by the presence of CH_3-groups randomly located along the polymer backbone.

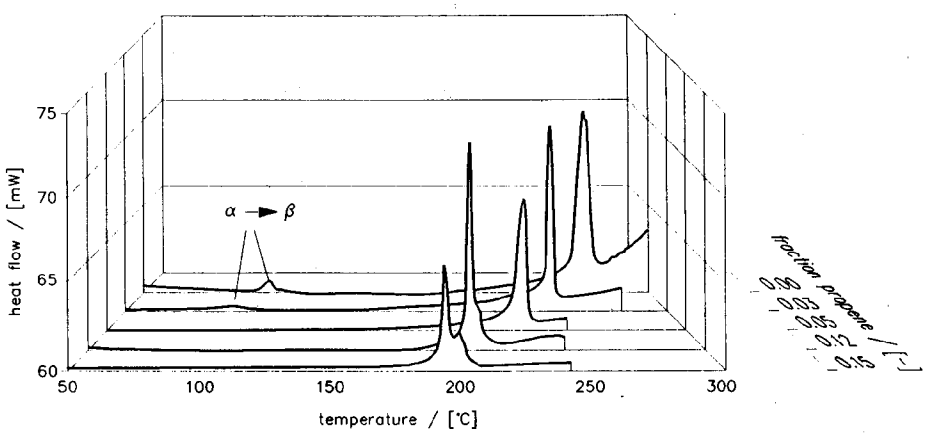

Figure 8. *DSC scans (20 °C/min) of alternating polyketones with varying propylene content.*

In Figure 8. the DSC scans (20 °C/min) of terpolymer fibers, drawn to about the same ratio, are displayed and in Table III the results of the thermal analysis investigations are summarized. For oriented fiber samples with a propylene content above 5-mole % the endothermal peak associated with the α/β-transition is not observed.

Table III. *DSC Data of Perfectly Alternating Polyketones with Varying Propylene Content.*

Sample	%-C_3 [mole/mole]	λ [-]	$T_{\alpha\rightarrow\beta}$ [°C]	$\Delta H_{\alpha\rightarrow\beta}$ [J/g]	T_m [°C]	ΔH_f [J/g]
POK-C_2	0	10.0	112	16	269	157
POK-C_2/C_3	3	10.3	101	9	247	129
POK-C_2/C_3	5	10.0			232	123
POK-C_2/C_3	12	10.5			206	122
POK-C_2/C_3	15	10.5			194/199	98

A precession photograph of POK-C_2/C_3 fiber with 12 mole-% propylene is presented in Figure 9. The diffraction pattern matches the POK-β structure found in imperfectly alternating copolymers and in perfectly alternating POK-C_2 copolymer above 100-130 °C. This result indicates that the POK-β lattice is better suited to accommodate chain defects or thermal effects. It should be noted that we observed no trace of the POK-α structure in the oriented fiber sample with 12 mole-% of propylene. As will be demonstrated in forthcoming contributions[29,30] epitaxially grown crystals of the same sample on a hydroquinone substrate can indeed show the POK-α structure at room temperature. Since the hydroquinone substrate solely nucleates crystallization of the POK-α modification some segregation between defect-rich and defect-poor chain segments might take place prior to crystallization. Although the occurrence of POK-α structure in these epitaxially crystallized terpolymers remains to be investigated further, the nucleation of the β/α-transition in oriented fiber samples prepared from semi-dilute or concentrated solutions is inhibited by the incorporation of chemical defects.

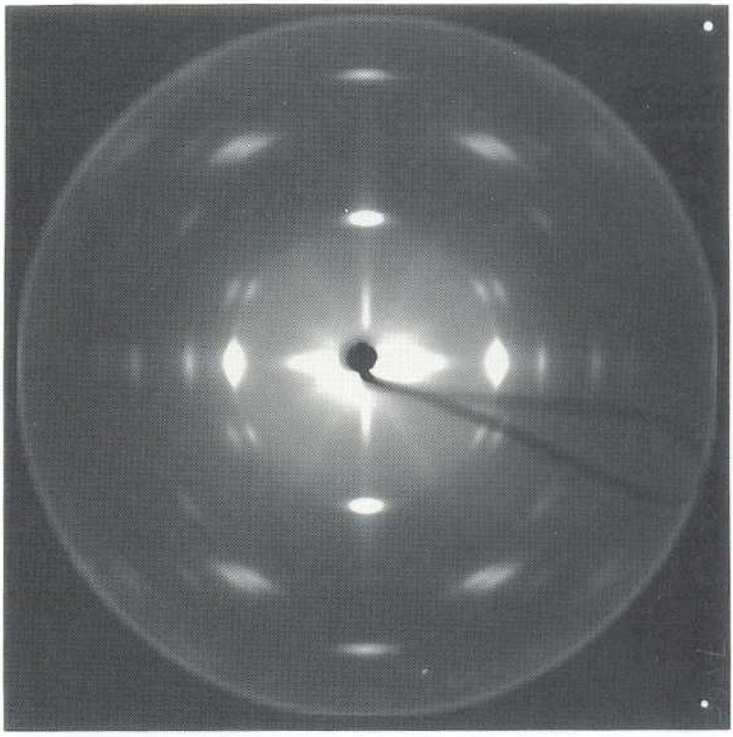

Figure 9. *A precession x-ray diffraction photograph of perfectly alternating POK-C_2/C_3 terpolymer with a fraction of 12 mole-% propylene-carbon monoxide chain defects.*

6.5 Conclusions

Alternating polyolefin ketones exhibit polymorphism, and depending on temperature, composition, applied stress or kinetic factors, the POK-α or the POK-β crystal structure or a mixture of the two are observed. Oriented defect-free polyketones show the POK-α structure at room temperature, which reversibly transforms into the POK-β structure at 110-130 °C. This solid-solid phase transition is accompanied by a

decrease in crystalline density of 10 %, whereas the heat effect associated with the transition is small (5-10 % of the heat of fusion). The formation of the POK-α structure in crystallized samples prepared from semi-dilute or concentrated solutions is inhibited by the random incorporation of more than 5 mole-% of chain defects. This result explains the occurrence of the POK-β structure, as observed in previous investigations for oriented imperfectly alternating copolymers. The larger volume of the POK-β unit cell makes that this structure is better suited to accommodate temperature effects or chemical defects. In as-polymerized POK-C_2 samples both structures are observed, depending on the conditions during polymerization, which yield differences in molecular weight and morphology of the powders formed.

6.6 References and Notes

1. M.M. Brubaker, D.D. Coffman and H.H. Hoehn, *J. Am. Chem. Soc.*, **74,** 1509 (1952).
2. P. Colombo, L.E. Kukacka, J. Fontana, R.N. Chapman, and M. Steinberg, *J. Polym. Sci. Part A-1,* **4,** 29 (1966).
3. Y. Chatani, T. Takizawa, S. Murahashi, Y. Sakata, and Y. Nishmura, *J. Polym. Sci.*, **55,** 811 (1961).
4. Y. Chatani, T. Takizawa and S. Murahashi, *J. Polym. Sci.*, **62,** S27 (1962).
5. T-W. Lai and A. Sen, *Organometallics,* **3,** 866 (1984).
6. A. Sen, *Chemtech* **1986,** 48.
7. A. Sen, *Acc. Chem. Res.*, **26,** 303 (1993).
8. E. Drent, J.A.M. v. Broekhoven and M.J. Doyle, *J. Organomet. Chem.*, **417,** 235 (1991).
9. M. Barsacchi, A. Batistini, G. Consiglio, and U.W. Suter, *Macromolecules,* **25,** 3604 (1992).
10. P.W. Wong, J.A. van Doorn, E. Drent, O. Sudmeijer, and H.A. Stil, *Ind. Eng. Chem. Res.*, **32,** 986 (1993).
11. A. Batistini and G. Consiglio, *Organometallics,* **11,** 1766 (1992).

12. M. Brookhart, F.C. Rix, and J.M. DiSimone, *J. Am. Chem. Soc.*, **114,** 5894 (1992).
13. A.X. Zhao and J.C.W. Chien, *J. Polym. Sci., Part A,* **30,** 2735 (1992).
14. M.A. Del Nobile, G. Mensitieri, L. Nicolais, A. Sommazzi, and F. Garbassi, *J. Appl. Polym. Sci.*, **50,** 1261 (1993).
15. F.Y. Xu and J.C.W. Chien, *Macromolecules,* **26,** 3485 (1993).
16. Z. Jiang and A. Sen, *Macromolecules,* **25,** 880 (1992).
17. B.J. Lommerts, E.A. Klop, and J. Aerts, *J. Polym. Sci. Polym. Phys. Ed.*, **31,** 1319 (1993).
18. B.J. Lommerts, J. Smook, B. Krins, A. Piotrowski and E. Band, European Patent 456,306 (Akzo Nobel), (1989).
19. A.R. Katritzky, *Handbook of Heterocyclic Chemistry,* Pergamon Press, Oxford, 1985.
20. J.A.M. Broekhoven and R.L. Wife, European Patent 257,663 (Shell), (1987).
21. M.J. Doyle, J.C. Van Ravenswaay-Claasen, G.G. Rosenbrand and R.L. Wife, European Patent 248,483 (Shell), (1987).
22. E.A. Klop, B.J. Lommerts, J Veurink, J. Aerts, and R.R. van Puijenbroek, *J. Polym. Sci. Polym. Phys. Ed.*, (accepted for publication).
23. D.C. Bassett, S. Block, and G. Piermarini, *J. Appl. Phys.*, **45,** 4146 (1974).
24. A.J. Pennings and A. Zwijnenburg, *J. Polym. Sci. Polym. Phys. Ed.*, **17,** 1011 (1979).
25. S-F Lau, H. Suzuki, and B. Wunderlich, *J. Polym. Sci. Polym. Phys. Ed.*, **22,** 379 (1984).
26. D.E. Kirkpatrick and B. Wunderlich, *Makromol. Chem.*, **186,** 2595 (1985).
27. G. Natta and P. Corradini, *J. Polym. Sci.*, **39,** 29 (1959).
28. C.W. Bunn, *Trans. Faraday Soc.*, **35,** 492 (1939).
29. V. Grayer, B.J. Lommerts, P. Smith, B. Lotz, and J-C Wittmann, *Polym. Comm.*, (submitted).
30. J-C. Wittmann and coworkers, (in preparation).

Chapter 7.

HIGH-TEMPERATURE STRENGTH AND DIMENSIONAL STABILITY OF POLYKETONE FIBERS

Reproduced from:
B.J. Lommerts, A.J. de Vries, and H. Jansen,
J. Polym. Sci. Polym. Phys. Ed. (submitted for publication).

7.1 Summary

The shrinkage of oriented polyketone fibers in hot air of 160 °C increases with an increasing fraction of chain defects (i.e., propylene-carbon monoxide segments), due to a reduction in crystallinity. Apart from the poor dimensional stability, the initial tensile modulus of these low-melting polyketone fibers is also relatively low. Perfectly alternating ethylene-carbon monoxide copolymers are more appropriate to be used as starting materials for fibers. These high-melting polyketone fibers retain at 140 °C in a nitrogen atmosphere 75-80 % of the tensile strength at -50 °C and 85-90 % of the tensile strength at 20 °C. The retention of the tensile strength is independent of the degree of molecular orientation in the fiber. The creep resistance at room temperature is excellent in comparison with polyethylene fibers. The α/β-transition found in oriented perfectly alternating ethylene-carbon monoxide copolymers at 110-130 °C does not strongly affect the mechanical performance. The tensile modulus increases even slightly upon transition. This remarkable phenomenon is attributed to a higher average shear modulus, due to the different arrangement of the dipoles in the β-structure.

7.2 Introduction

For a number of industrial fiber applications (e.g., tyres and other mechanical rubber goods) a good mechanical performance up to temperatures of 180 °C is required.[1,2] At elevated temperatures, usually above the glass transition temperature, shrinkage of highly oriented fibers can occur, due to the semi-crystalline nature of flexible chain

polymers.[3] This is accompanied by some loss of molecular orientation and, concomitantly, by a decrease in the initial tensile modulus. The retention of the tensile modulus and the fiber length at elevated temperatures is here referred to as the dimensional stability of the material.

The aim of the present investigations is to determine the dimensional stability and the high-temperature strength of polyketone fibers. High-melting polyketones suffer from thermal degradation during melt processing. Melt processing can be achieved by lowering the melting temperature via the incorporation of chain defects into the polymer backbone.[4] It is well known that the incorporation of defects can affect the crystallinity[5] and therefore also the dimensional stability of oriented semi-crystalline polymers. To investigate the influence of the defect concentration on the dimensional stability of polyketone fibers, perfectly alternating ethylene-carbon monoxide (POK-C_2) copolymers and ethylene-carbon monoxide/propylene-carbon monoxide (POK-C_2/C_3) terpolymers with varying propylene content were spun from phenolic solutions.

Furthermore, oriented POK-C_2 polymers exhibit a solid-solid phase transition at 110-130 °C,[6] which is below the end-use temperature of many industrial fiber applications. In this temperature range the POK-α crystal structure transforms into the POK-β structure, which is accompanied by a 10 % increase in the volume of the crystal unit cell. Initially this was a point of concern, as such a significant change in packing density might result in a deterioration of the tensile properties.[7] In order to gain insight into the effect of the structural transition on the mechanical performance of POK-C_2, tensile tests were performed on as-spun and oriented fibers at temperatures between -50 and 140 °C. Moreover, long-term loading experiments were conducted to determine the creep resistance of POK-C_2 fibers.

7.3 Experimental

-Materials

Three different polyketones with varying molecular weight and propylene content were

spun from solution in phenol/acetone mixtures (9:1 weight ratio) into an acetone coagulation bath according to the dry-jet-wet spinning technique described in Chapters 3 and 6. Some polymer properties and preparation conditions, viz. melting temperature (T_m), heat of fusion (ΔH_f), intrinsic viscosity ([η] : *m*-cresol, 25 °C), polymer concentration (x_{pol} in wt/wt), dissolution temperatures (T_{dis}), dissolution times (t_{dis}), and drawing temperatures (T_{draw}) are listed in Table I.

Table I. *Spinning and Drawing Conditions Applied for the Preparation of Polyketone Fibers with Varying Propylene Content.*

mole-% propylene	T_m [°C]	ΔH_f [J/g]	[η] [dL/g]	x_{pol} [-]	T_{dis} [°C]	t_{dis} [hr]	T_{draw}[a] [°C]
15	196	67	0.78	0.31	90	5	165/183
3	238	112	1.9	0.22	120	4	210/237
0	258	112	6.1	0.06	80	30	227/255

[a] Two-stage drawing with $\lambda=\lambda_1 \cdot \lambda_2$ ($\lambda=\lambda_1$ for $\lambda<10$ and $\lambda_1=9.5$ for $\lambda>10$), where λ is the draw ratio

The fibers were washed with acetone; dried at room temperature; and subsequently drawn in two stages to various ratios over hot plates at a feeding speed of 1-2 mm/s.

-Mechanical Properties

The mechanical properties of the monofilaments produced with different draw ratios were measured at room temperature (21 °C) and 65 % relative humidity. An Instron Tensile Tester was used, operating at a cross-head speed of 10 mm/min for a sample gauge length of 100 mm. A pre-tension of 7 MPa was applied and prior to analysis the fibers were conditioned for at least 24 hours. The grips of the clamps were

covered with an Arnitel™ film to avoid sample slippage. The linear density of the filaments was determined with a vibroscope at a test length of 20 mm. In order to obtain values for the tensile modulus and tensile strength in GPa units the linear density was converted using density values, which amount to 1.19, 1.26 and 1.32 g/cm^3, for the various polyketones, with a propylene content of 15, 3 and 0 mole-%, respectively. The modulus-strain curve was determined by taking the first derivative of the stress-strain curve from which the initial modulus (Young's modulus) can be derived. Tensile tests at different temperatures; -50, -20, 20, 60, 100 and 140 °C, were performed on a Zwick 1474 Tensile Tester, equipped with a Brabender furnace.

-Dynamic Mechanical (Thermal) Analysis

DM(T)A measurements were performed in the temperature range of -100 to 250 °C at a scanning speed of 1 K/min in a nitrogen atmosphere. An Eplexor (GABO-Qualimeter), equipped with a 25 N load-cell and heat resistant flat clamps was used. The initial sample length, measured at an applied load of 7 MPa, was 40 mm. The static load was regulated at a certain stress level, whereas the dynamic load, corresponding with 0.05 % strain, was applied at a frequency of 10 Hz.

-Hot-Air-Shrinkage

The hot-air-shrinkage at 160 °C was determined in triplicate by measuring the initial length of the filament at an applied load of 7 MPa (L_1). The filament is placed tensionless in an oven at 160 °C for 15 min after which the filament was left to condition at 21 °C and 65 % relative humidity for 1 h. When measuring again the length of the filament at an applied load of 7 MPa (L_2), the shrinkage can be calculated from

$$HAS(160\ °C,\ 15\text{min.}) = \frac{L_1 - L_2}{L_1} \qquad (1)$$

-Thermal and Microscopic Analysis

Thermograms were recorded, using the Perkin Elmer DSC 7 thermal analyzer, at a scanning speed of 20 °C/min. The morphology of the polyketone fibers was studied using a Carl-Zeiss-Jena polarization microscope.

7.4 Results and Discussion

-Hot-Air Shrinkage

The melting temperature of polyketone terpolymers depends on the amount of propylene-carbon monoxide segments randomly incorporated into the polymer chain.[7] In the present study, we studied terpolymers with a propylene content of 3 and 15 mole-% having a melting temperature of 238 °C and 196 °C, respectively.

Polyketone terpolymers with a propylene content above 5 mole-% show the POK-β crystal structure at room temperature.[6] The crystalline fraction of oriented fiber samples with about 3 mole-% of propylene consists of a mixture of the two crystal modifications (i.e., the POK-α and the POK-β structure) found in polyketones.

The difference between the heat of fusion of fibers prepared from these materials (see Figure 1) indicates that the crystallinity is significantly reduced by the incorporation of a large amount of chain defects. For poly(ethylene terephthalate) fibers it has been well-established that the shrinkage of a fiber depends on the volume fraction of non-crystalline domains and the degree of molecular orientation within these domains.[3] As presented in Figure 2 the reduction in crystallinity due to the incorporation of a larger amount of chain defects is reflected in a higher shrinkage level in hot air of 160 °C.

The improved molecular alignment up to a draw ratio of 17 results in an increase of the crystallinity, and correspondingly, in a decrease of the hot-air-shrinkage. However, at even higher draw ratios the shrinkage increases with the draw ratio.

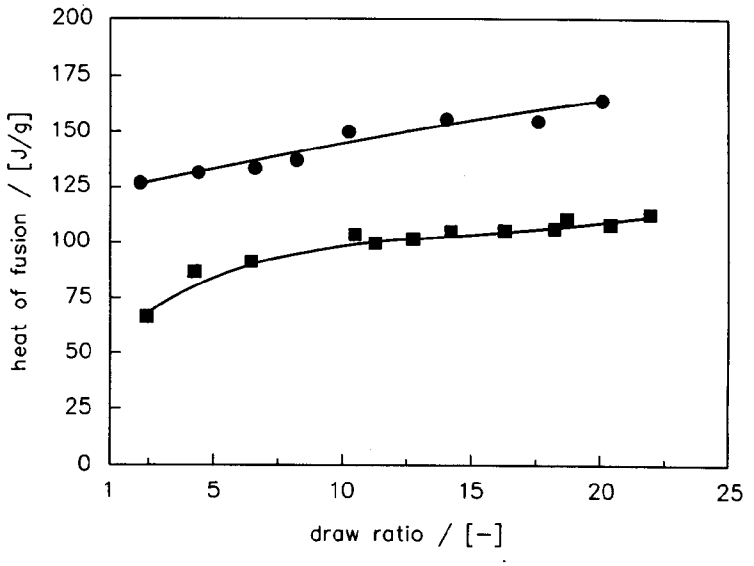

Figure 1. *Heat of fusion of polyketone fibers with 3 mole-% (●) and 15 mole-% (■) propylene drawn to different ratios.*

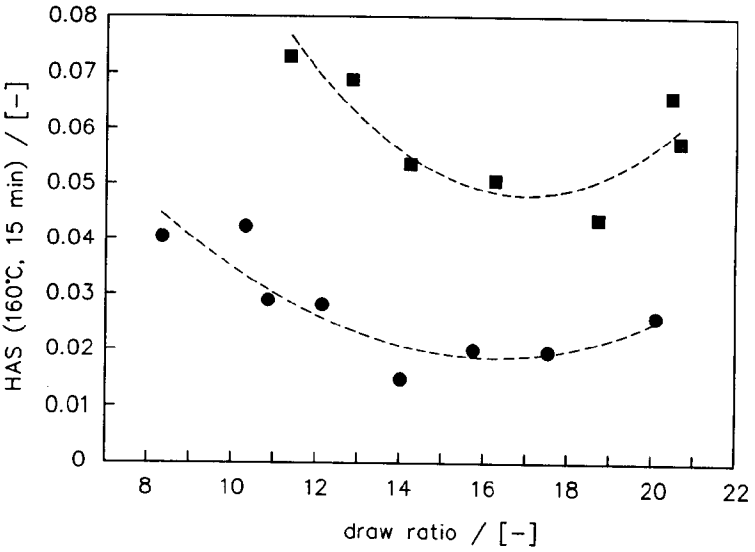

Figure 2. *Hot-air-shrinkage of polyketone fibers with 3 mole-% (●) and 15 mole-% (■) propylene vs the draw ratio.*

Similar to what has been observed for POK-C_2 fibers (see Chapter 3), the two polyketone terpolymers under investigation show "overdrawing" characteristics at draw ratios exceeding the value of 17, as can be deduced from the optical micrographs presented in Figure 3. A draw ratio of 17 seems to be the limiting value for a continuous drawing operation, as an appreciable amount of (macro) voids and cracks become visible in multi-filament polyketone fibers at higher draw ratios.

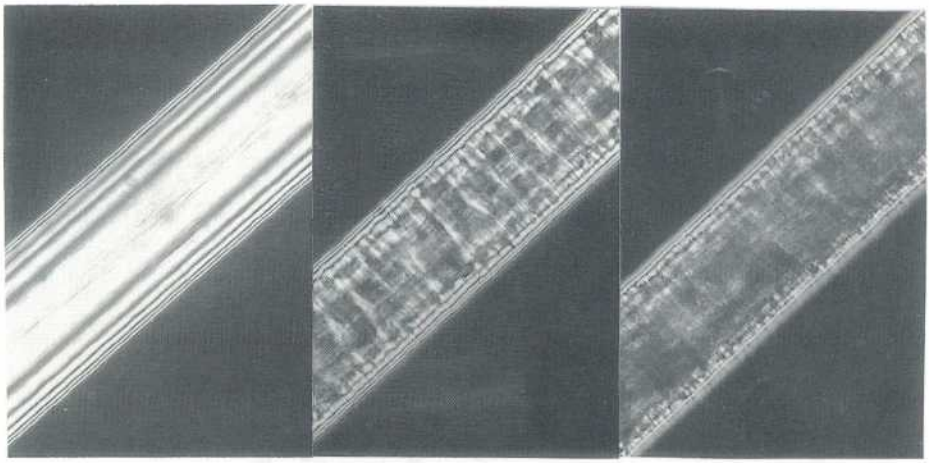

Figure 3. *Optical micrographs of polyketone fibers with 15 mole-% propylene drawn at 183 °C to a ratio of 12, 18 and 20, respectively.*

The formation of these morphological defects strongly affects the shrinkage level, probably due to the increased porosity in the material. The formation of voids is accompanied by a lateral isolation of the fibrils, which creates the mobility to allow the non-crystalline domains to disorder and thereby to gain conformational entropy.

The initial tensile modulus of oriented polyketone terpolymer fibers is presented in Figure 4.

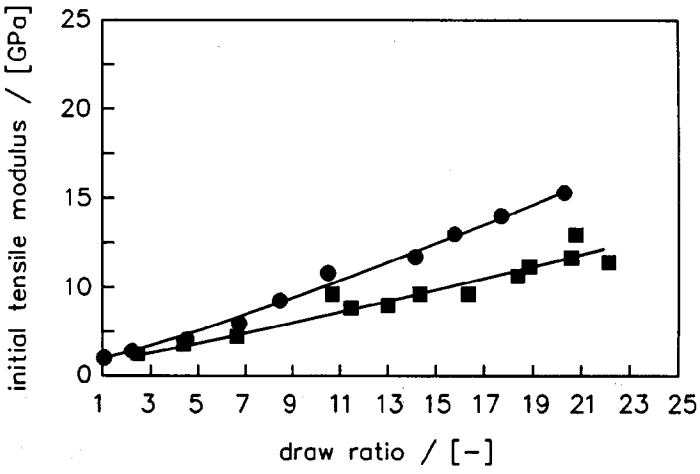

Figure 4. *Initial tensile modulus of polyketone fibers with 3 mole-% (●) and 15 mole-% (■) propylene vs the draw ratio.*

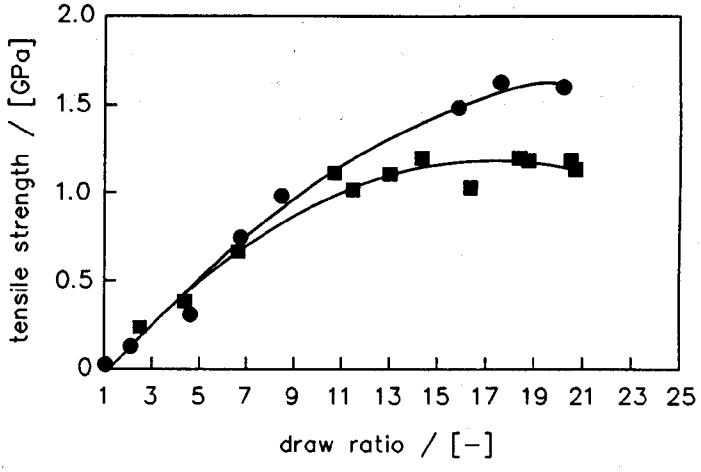

Figure 5. *Tensile strength of polyketone fibers with 3 mole-% (●) and 15 mole-% (■) propylene vs the draw ratio (for λ>17 only the maximum observed values are displayed).*

In addition to the increase in shrinkage at elevated temperatures, the incorporation of a larger amount of chain defects also causes a pronounced deterioration of the tensile modulus.

In Figure 5 the tensile strength of the polyketone terpolymer fibers is displayed. Similar to POK-C_2 fibers a large scatter in tensile strength data for overdrawn terpolymer fibers is observed and in this draw ratio range only the maximum values are displayed. The variation in molecular weight of the samples used does not allow the drawing of any conclusions with respect to the effect of the number of chain defects on the tensile strength.

The properties of low-melting polyketone terpolymers described above demonstrate the pronounced deterioration of the mechanical performance and dimensional stability due to the incorporation of a large amount of chemical defects. In a sequel to this work, we have restricted ourselves to perfectly alternating ethylene-carbon monoxide copolymers, in view of the expected superior properties of high-melting POK-C_2 fibers.

-The POK-α to POK-β Transition in POK-C_2 Fibers

Some linear, less polar, flexible polymers, with an all-*trans* or close to all-*trans* conformation of the chains in the crystal lattice exhibit a solid-solid phase transition at elevated temperatures.[7] Such a phase transition results in an increase in conformational disorder, which causes a significant reduction in the average shear modulus between adjacent chains. Thermal and x-ray diffraction analysis experiments revealed a solid-solid phase transition at 110 °C in POK-C_2 fibers (i.e., the POK-α (orthorhombic) to the POK-β (orthorhombic) crystal structure). Although the POK-C_2 copolymer does not show a conformationally disordered solid phase at elevated temperatures, our initial concern about a sudden decline in dimensional stability and shear modulus remained. In this section, we report on the investigations into the effect of the α/β-transition on the high-temperature strength and dimensional stability of POK-C_2 fibers.

The tensile strength at different temperatures between -50 and 140 °C [relative to the values at 20 °C] of three POK-C_2 fibers, drawn to different ratios, is presented in Figure 6. Over the whole temperature range the fibers break by brittle failure and scanning electron microscopy revealed a highly fibrillar fracture surface. The relative decline in tensile strength of the three POK-C_2 fibers presented in Figure 6 is comparable. These results indicate a similar fracture mechanism over the whole temperature range, which is independent of the drawing induced molecular orientation. At a temperature of 140 °C the retention of the tensile strength is about 85-90 % of the tensile strength at room temperature and 75-80 % of the tensile strength at -50 °C. This is a small change in tensile strength compared with less polar flexible polymers like, for example, polyethylene.[9] This important feature of highly crystalline POK-C_2 fibers can be attributed to the dense crystal packing,[8] resulting in a high packing energy, which inhibits the slip of chains out of the crystal lattice at relatively high temperatures.

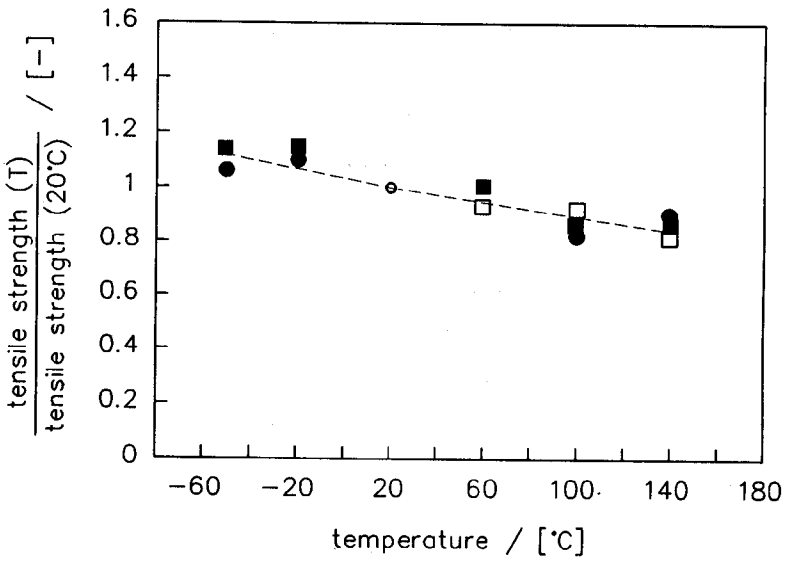

Figure 6. *Retention of the tensile strength of three different polyketone (POK-C_2) fibers at various temperatures (tensile strength at room temperature (●) : 1.4 GPa; (■) : 1.7 GPa; and (□) : 2.4 GPa).*

At 110 °C the POK-α crystal structure transforms into the POK-β structure, but above the transition temperature the same relative decline in tensile strength is observed. This implies that the POK-β modification is sufficiently tough to provide the lateral stress transfer between the polymer chains to accommodate the applied load. We were not able to perform tensile test at temperatures exceeding 140 °C as the time to condition in the heating chamber became too long to obtain reproducable results. Discoloration of the fibers occurred mainly due to thermal and/or oxidative degradation.

Representative stress-strain curves at 100 and 140 °C of two POK-C_2 fibers, with a tensile strength of 1.4 and 1.7 GPa at room temperature are presented in Figure 7.

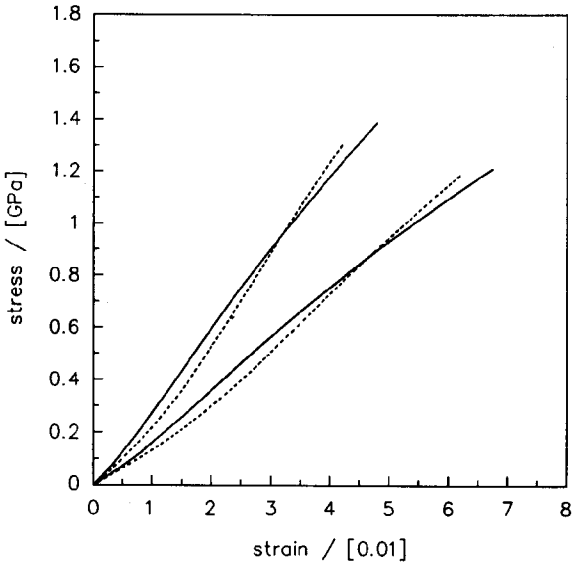

Figure 7. *Stress-strain curves of two polyketone (POK-C_2) fibers (tensile strength at 20 °C : 1.4 and 1.7 GPa) at 100 °C (dashed line) and 140 °C (solid line).*

The derivative of the stress-strain curves at different temperatures between -50 and 140 °C is displayed in Figure 8. Remarkably, the initial tensile modulus at 140 °C is

slightly higher than the initial tensile modulus at 100 °C. Between -50 and 100 °C the expected, though limited, decline in initial tensile modulus is observed, but above the α/β-transition temperature the modulus increases. In order to demonstrate that the increase of the tensile modulus was not due to an artefact of the tensile test procedure we investigated a similar fiber by means of dynamic mechanical (thermal) analysis; the DM(T)A traces at different static loads are shown in Figure 9.

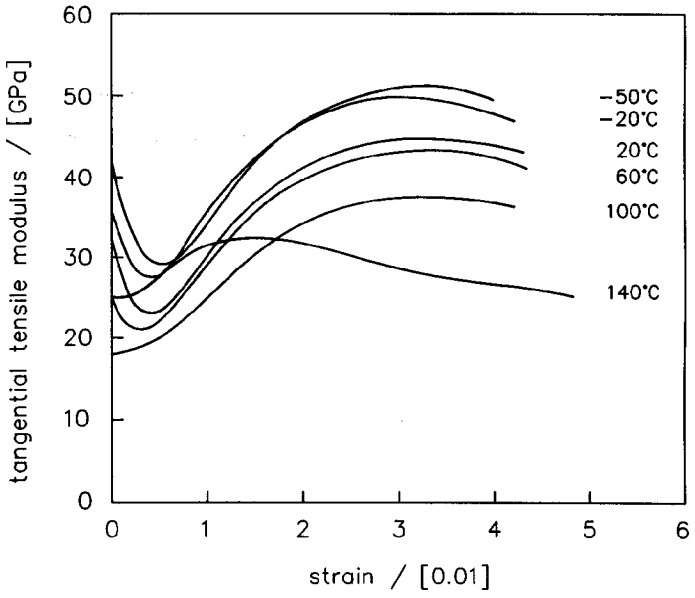

Figure 8. *Derivative of the stress-strain curves of a polyketone (POK-C_2) fiber (tensile strength at 20 °C : 1.7 GPa) at different temperatures.*

At low static loads the increase in modulus at the α/β-transition temperature is also observed, but at higher loads the change in modulus is less noticeable. This observation is in line with the tensile tests, as at higher strains the derivative of the stress-strain curve (i.e., the tangential modulus) at 140 °C is below the one at 100 °C.

Also tensile tests were performed on as-spun fibers (i.e., unoriented polymer). In

Figure 10 the yield stress (i.e., the stress at which the material starts to deform in a dissipative mode) is given as a function of the temperature.

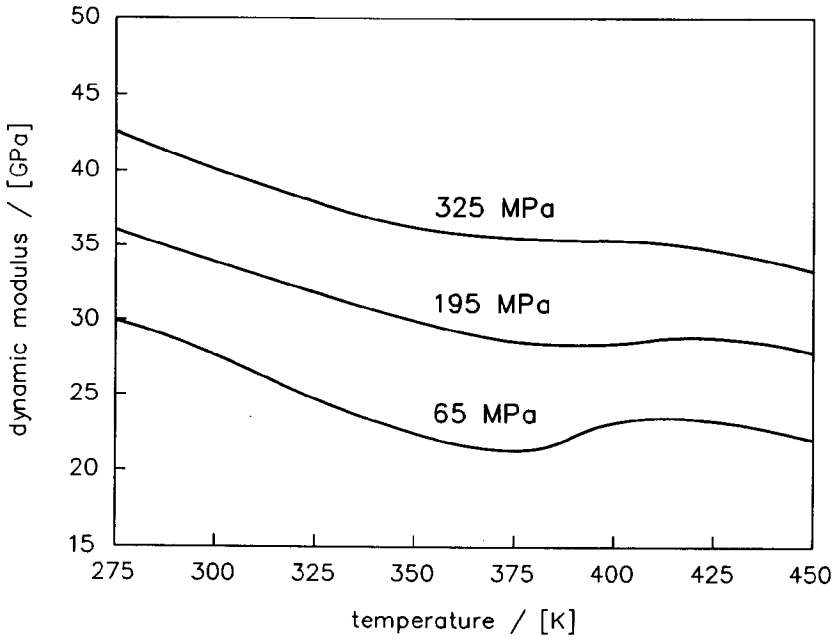

Figure 9. *DM(T)A traces at different static loads of a polyketone (POK-C_2) fiber with a tensile strength of 2.4 GPa at room temperature.*

The increase in the yield stress at the α/β-transition temperature indicates that the change in initial tensile modulus is not due to the high degree of molecular alignment in POK-C_2 fibers. Accordingly, the increase in the modulus must be attributed to the toughness of the crystalline phase. In semi-crystalline polymers the modulus can rise due a certain improvement of the crystallinity. Thermal analysis experiments revealed that this does not occur when the material is annealed above 130 °C. It should be noted that the POK-C_2 fibers are drawn at temperatures above the α/β-transition temperature and after the drawing is completed the crystal structure transforms from POK-β to the POK-α structure. Furthermore, the drawing procedure is carried out at

temperatures above 250 °C, and it is unlikely that additional crystallization occurs when the drawn fiber is reheated to 140 °C after the drawing is completed.

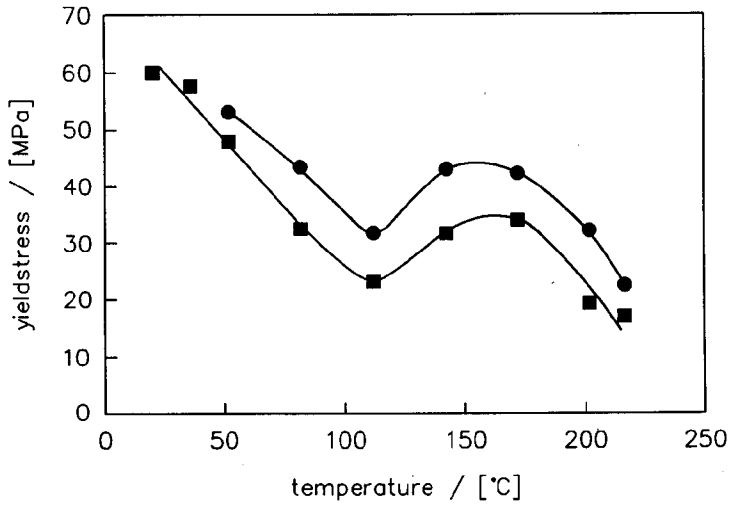

Figure 10. *Yield-stress of a solution spun unoriented polyketone-C_2 fiber at different temperatures (deformation rate : 100 %/min. (■) and 1000 %/min. (●)).*

In view of the 10 % larger volume of the POK-β crystal unit cell relative to the POK-α unit cell, the theoretical modulus along the *c*-axis of the POK-β structure is probably even lower than that of the POK-α structure. However, at the attained degrees of molecular orientation the elastic extension of covalent bonds is still small compared with the extension due to shear deformation.[10] Accordingly, the increase in initial tensile modulus might be attributed to a higher shear modulus of the POK-β structure.

Although the observed phenomena are still obscure, a possible explanation has been presented in the previous Chapter. In the POK-α crystal lattice the dipoles are predominantly arranged parallel to the *bc*-plane in the crystal unit cell. Consequently, the crystal shear compliances in the *bc*-plane and *ac*-plane (s_{44} and s_{55} according to the engineering notation (see Ward[11])) are widely different.

Para-aramid (P*p*PTA) fibers spun from concentrated solutions in sulfuric acids also show a large difference between the moduli for the shear between two adjacent chains.[12] The crystal structure of *para*-aramid fibers has been reported by Northolt and Van Aartsen.[13,14] The strong lateral interactions (hydrogen bonds) in this aromatic polyamide are directed along the *b*-axis of the monoclinic unit cell. These strong interactions in the other direction with respect to the chain axis are absent. A shear modulus between adjacent chains in the hydrogen bonded *bc*-plane (s_{44}^{-1}) of 4.1 GPa has been calculated.[15] For PpPTA fibers an average shear modulus of 2 GPa[12] and a filament torsional modulus of 1.8 GPa[16] have been determined experimentally. Hence, the lower experimental value for the shear modulus can be attributed to the absence of strong interactions in one of the unit cell directions transverse to the chain axis.

Based on computational chemistry results, Klop et al.[6] stated that the electrostatic interactions in the POK-β structure are higher than those in the POK-α structure. In the POK-β structure the lateral interactions perpendicular to the *bc*-plane are even more effective due to the different orientations of the carbonyl dipoles. Presumably, the difference between the values for s_{44} and s_{55} are (much) smaller in the POK-β structure than in the POK-α structure, which in case of fiber geometry results in a larger value for the average shear modulus. To our knowledge the increase in modulus at the α/β-transition temperature, even though the volume of the crystal unit cell increases, has never been observed before for other polymer materials. Clearly, more work has to be done to provide a better understanding of the change in modulus of POK-C_2 fibers at the α/β-transition temperature.

Based on the above described results, we conclude that the solid-solid phase transition at 110 °C does not cause a significant deterioration of the mechanical performance of POK-C_2 fibers. Due to the high crystallinity of high-melting POK-C_2 fibers, a much better dimensional stability has been observed than for low-melting polyketone terpolymers. The limited decline in initial tensile modulus of 20 % at 140 °C relative to the value at 20 °C and the good retention of the tensile strength demonstrate the superior high-temperature performance of POK-C_2 fibers compared with oriented less polar polymers. Obviously, the α/β-transition contributes to the

good high-temperature performance.

-Creep Resistance of POK-C_2 Fibers

The polar nature of the highly crystalline perfectly alternating ethylene-carbon monoxide copolymer is also reflected in a good resistance to creep (see Figure 11). As is obvious from the slope (i.e., the creep rate) of the curve in Figure 11, high-melting polyketone fibers are less susceptible to creep compared with the other two flexible chain polymers (i.e., a polyethylene fiber (Spectra™ 1000 (Allied Signal)) and a poly(ethylene terephthalate) fiber (Diolen™ 1125 (Akzo Nobel))). However, the high modulus/high strength *para*-aramid fiber (Twaron 1000 (Akzo Nobel)) performs significantly better during long term loading compared with the semi-crystalline POK-C_2 fiber.

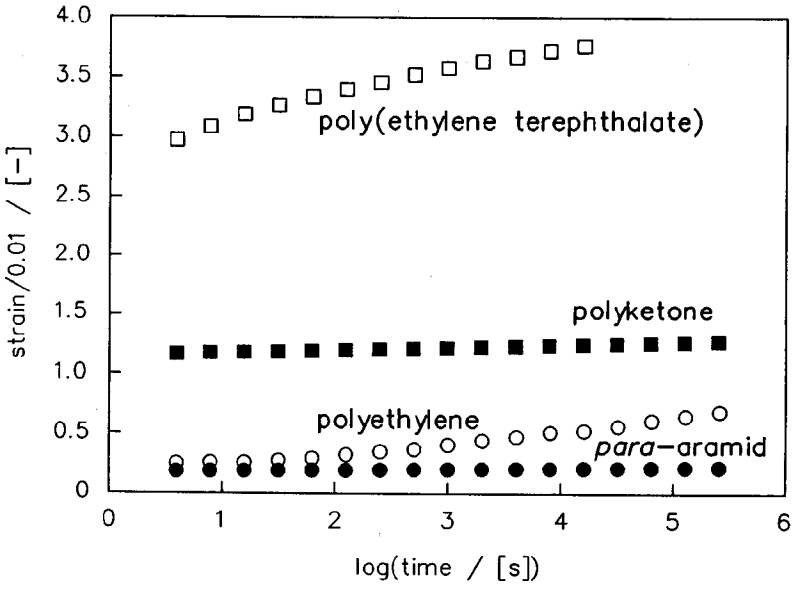

Figure 11. *Creep resistance of four polymer fibers at 20 °C and at a load of 0.22 GPa.*

7.5 Conclusions

The results presented in this Chapter demonstrate the potential of the perfectly alternating ethylene-carbon monoxide copolymer for industrial or technical fiber applications. The excellent high-temperature strength, creep resistance and dimensional stability of these materials are of paramount importance for various advanced industrial fiber end-uses. The dimensional stability and the development of the tensile modulus of low-melting polyketone terpolymers are significantly lower than for POK-C_2 fibers. This is due to the incorporation of chain defects, resulting in a pronounced reduction of the crystallinity.

The remarkable, though slight, increase in modulus and yield stress of POK-C_2 at the α/β-transition temperature is attributed to a higher average shear modulus of the β-structure, due to the different arrangement of the dipoles in this structure.

7.6 References and Notes

1. G. Ruitenberg, *Enka Presentation to the Tyre Industry 1982,* Product Group Industrial Fibers, Enka Information, Arnhem, The Netherlands, 1982.
2. F.W. Bridié, L. Daan, C.C.J. de Jong, G. Ruitenberg, and W.H. Hupjé, *Enka Industrial Fibers MRG Symposium 1985,* Industrial Fibers, Enka Information, Arnhem, The Netherlands, 1985.
3. R. Huisman and H.M. Heuvel, *J. Appl. Polym. Sci.*, **37,** 595 (1989).
4. J.M. Beyen, E. Klei, H.S. Brown, and P.A. Westbrook, European Patent 310,171 (Shell), (1988).
5. B. Wunderlich, *Macromolecular Physics,* Volume III, *Crystal Melting,* Academic Press, New York, 1980.
6. E.A. Klop, B.J. Lommerts, J. Aerts, J. Veurink, and R.R. van Puijenbroek, *J. Polym. Sci. Polym. Phys. Ed.*, (accepted for publication).
7. B. Wunderlich and J. Grebowics, *Adv. Polym. Sci.*, **60/61,** 1 (1984).

8. B.J. Lommerts, E.A. Klop, and J. Aerts, *J. Polym. Sci. Polym. Phys. Ed.*, **31,** 1319 (1993).
9. D.J. Dijkstra, J.C.M. Torfs, and A.J. Pennings, *Coll. Polym. Sci.*, **286,** 866 (1989).
10. M.G. Northolt and R. v.d. Hout, *Polymer,* **26,** 310 (1985).
11. I.M. Ward, *Mechanical Properties of Solid Polymers,* 2nd ed., Wiley, New York, 1983.
12. M.G. Northolt and D.J. Sikkema, *Adv. Polym. Sci.*, **98,** 115 (1990).
13. M.G. Northolt and J.J. van Aartsen, *J. Polym. Sci. Polym. Lett. Ed.*, **11,** 333 (1973).
14. M.G. Northolt, *Eur. Polym. J.*, **10,** 799 (1974).
15. H. Kooijman, L.M.J. Kroon-Batenburg, M.G. Northolt, (to be published).
16. W.F. Knoff, *J. Mater. Sci.*, **6,** 1392 (1987).

SUMMARY

This thesis is devoted to the structure development in two oriented flexible chain polymers, viz. the perfectly alternating ethylene-carbon monoxide copolymer (polyketone; POK-C_2) and a new polyalcohol (PAl), produced by reduction of the polyketone. Both polymers exhibit a 1,4-arrangement of the polar functionality. However, the polyketone shows a much denser crystal packing than the polyalcohol. The (orthorhombic) crystal structure observed in oriented POK-C_2 fibers at room temperature (POK-α) differs from the (orthorhombic) crystal structure previously found in imperfectly alternating polyketones (POK-β). The unit cell dimensions and the crystalline density of the two structures are compared in Table I.

Table I. *Melting Temperature (T_m), Unit Cell Dimensions (a,b,c) and Crystalline Density (ρ_c) of Various Flexible Chain Polymers with an All-Carbon Backbone.*

	T_m [K]	*a* [Å]	*b* [Å]	*c* [Å]	ρ_c [g/cm^3]	structure
POK-α	- [a]	6.91	5.12	7.60[b]	1.38	orthorhombic
POK-β	550	7.97	4.76	7.57[b]	1.30	orthorhombic
PAl	410	8.78	5.47	7.47[b]	1.08	-
PE	414	7.40	4.93	2.54[b]	1.00	orthorhombic
PVAl	540	7.81	2.52[b]	5.51	1.35	monoclinic (β=91.7 °)

[a] prior to melting POK-α transforms into the POK-β structure at 110-130 °C

[b] direction of the fiber axis

The cross sectional area of the POK-α unit cell perpendicular to the chain axis (35.2 $Å^2$) is even smaller than that of the polyethylene unit cell (36.2 $Å^2$), and the packing fraction of the atoms in this structure (78 %) is amongst the highest ever observed for organic polymers. Both features are favorable for achieving good mechanical properties in oriented fibers

Even though the polyalcohol is basically an atactic material, oriented ordered samples could be prepared by solid-state drawing of solution cast films. The reflections in the x-ray diffraction pattern of oriented film samples were indexed on the basis of an orthorhombic lattice and the unit cell dimensions derived are presented in Table I. A packing of the chains is observed, which is significantly less than found for poly(vinyl alcohol), which has a 1,3-arrangement of the hydroxyl substituents. The low melting temperature of the polyalcohol (137 °C) is attributed to the low packing density, which results from the different orientation of the hydroxyl substituents in a 1,4-arrangement.

POK-C_2 fibers show a reversible phase transition between 110-130 °C. In this temperature range the POK-α structure transforms into the POK-β structure (i.e., the crystal structure previously found in imperfectly alternating copolymers) with a 10 % change in volume of the crystal unit cell. Although the increase in volume is rather high, the heat effect associated with the transition is relatively low (5-10 % of the heat of fusion). A certain (segmental) mobility is required to transform the POK-β structure into the dense POK-α structure. In (virgin) as-polymerized samples both structures are observed. The α-content [at room temperature] depends on the polymerization conditions, which also yield differences in molecular weight and morphology of the polyketone powders formed. The α-content can be enriched by recrystallization from solution. Solution spun oriented high-molecular-weight fibers crystallize exclusively in the dense α-modification. However, the degree of perfection of the α-crystals formed, depends on the applied stress during transition. Since virgin high-molecular-weight POK-C_2 consists largely of the β-modification, spinning and drawing leads to a transformation of the β-structure to the α-structure. Oriented ethylene-carbon monoxide/propylene-carbon monoxide terpolymers with a propylene

content above 5 mole-% show the POK-β structure at room temperature. This result explains the POK-β structure previously found in imperfectly alternating ethylene-carbon monoxide copolymers, as the β-modification is better suited to accommodate chain defects or temperature effects. Some incorporation of chemical defects occurs in the POK-β lattice. As a consequence, Flory's lattice theory is not applicable for describing the melting point depression of these terpolymers. To establish, a first, estimate for the heat of fusion of perfectly crystalline material, a modification of the Flory-Vrij equation is used to describe the chain length dependency of the melting point of low- molecular-weight (symmetrical) polyketone homologs. Based on these results it was concluded that the high melting temperature of the POK-C_2 copolymer (260-280 °C) can be ascribed to a high packing energy in the crystal lattice and not to the previously presumed limited rotational mobility due to the presence of the carbonyl functionality. Based on an estimate for the heat of fusion for crystals of infinite chain length (215-330 J/g) a crystallinity of 60-80 % was derived for highly oriented POK-C_2 fibers.

The maximum attainable draw ratio of polyalcohol films is about 10, whereas polyketone fibers could be drawn to a ratio of 26. Beyond a draw ratio of 17, however, the formation of local stress concentrations (i.e., voids and cracks) in POK-C_2 multi-filament yarns seems to be inevitable. In addition to molecular weight and entanglement density effects, the maximum degree of extension of moderately polar and apolar polymer systems is largely governed by chemical structure, mainly polarity, and temperature. A good measure for the polarity is the cohesive energy (E_{coh}), which reflects the difficulty to transport topological defects along and through the oriented structures formed. Moreover, the maximum temperature for effective drawing is at the melting temperature of the polymer. The onset of melting is accompanied by a decline in the lateral stress-transfer mechanism. Under these conditions stress-transfer by means of topological interchain couplings (i.e., entanglements) becomes increasingly important. Since an appreciable amount of network imperfections is present in the samples used, slippage of chain ends through entanglements is caused above the onset temperature of melting. The found correlation between the melting temperature and the drawability of a number of poly-hydroxy-polymers (i.e., polymers

with a comparable polarity) corroborates the presumed limitations in drawability due to the decline in the lateral stress-transfer mechanism. For highly polar polymers, with a high lattice energy (e.g., nylon-6, nylon-6,6), exceedingly small crystallites are thought to act as very effective crosslinks. In this cohesive energy range the drawability of flexible polymer systems hardly depends on the polarity of the polymer.

Highly oriented POK-C2 fibers, drawn to a ratio of 26, show a tensile strength of 3.8-3.9 GPa, an initial tensile modulus of 50-55 GPa, and an elongation at break of 4-5 %. The semi-crystalline nature of the POK-C_2 copolymer becomes very noticeable when orientation relaxation within non-crystalline domains is allowed. The loss of orientation (i.e., relaxation) is more pronounced at higher drawing temperatures and lower drawing stresses. As a result of relaxation the elongation at break can be increased to 7-8 % at the expense of a lower modulus (40-45 GPa). To a first approximation the drawing induced orientation development in unrelaxed POK-C_2 fibers can be described, using the affine deformation concept of Kuhn and Grűn in combination with a value for the birefringence of perfectly axially oriented fiber of $710 \cdot 10^{-4}$.

The crystallinity in polyketone terpolymers is reduced due to the incorporation of propylene defects. As a result, the shrinkage of oriented terpolymers in hot air of 160 °C increases with increasing propylene content. Furthermore, the development of the initial tensile modulus with the draw ratio decreases significantly with increasing propylene content. In view of these particular properties low melting polyketone terpolymers seem to be unattractive starting materials for the preparation of dimensionally stable fibers. The α/β transition in oriented POK-C_2 fibers at 110-130 °C is not accompanied by a marked deterioration of the mechanical properties. The average shear modulus of the POK-β structure is even (slightly) higher than that of the POK-α structure due to the different (more polar) arrangement of the dipolar interactions in the POK-β lattice. This unique feature of POK-C_2 fibers, in combination with a superior high-temperature performance, and a good creep resistance [relative to less polar polymers, like polyethylene], demonstrates the potential of these materials for advanced industrial applications.

SAMENVATTING

Deze dissertatie beschrijft de structuurontwikkeling in vezels die gemaakt zijn van twee nieuwe flexibele polymeren, te weten het perfect alternerende etheen-koolmonoxide copolymeer (polyketon; POK-C_2) en een polyalcohol (PAl) gemaakt door reductie van het polyketon. Beide polymeren zijn opgebouwd uit een 1,4-rangschikking van de polaire functionaliteit. De pakkingsdichtheid van de polyketon ketens in het kristalrooster is echter veel hoger dan die van het polyalcohol. De (orthorhombische) kristalstructuur, die gevonden is in POK-C2 vezels bij kamertemperatuur (POK-α), verschilt van de structuur zoals eerder gevonden is in niet perfect alternerende copolymeren (POK-β). In Tabel I is een overzicht gegeven van de dimensies van de eenheidscel en de kristallijne dichtheid van de twee structuren.

Tabel I. *Smelttemperatuur (T_m), Dimensies van de Eenheidscel (a,b,c) en Kristallijne Dichtheid (ρ_c) van Verschillende Flexibele Polymeren met een Koolstof Hoofdketen.*

	T_m [K]	*a* [Å]	*b* [Å]	*c* [Å]	ρ_c [g/cm^3]	structuur
POK-α	- [a]	6.91	5.12	7.60[b]	1.38	orthorhombisch
POK-β	550	7.97	4.76	7.57[b]	1.30	orthorhombisch
PAl	410	8.78	5.47	7.47[b]	1.08	-
PE	414	7.40	4.93	2.54[b]	1.00	orthorhombisch
PVAl	540	7.81	2.52[b]	5.51	1.35	monoclien (β=91.7 °)

[a] De POK-α structuur gaat over in de POK-β structuur bij 110-130 °C.

[b] richting van de vezelas.

De doorsnede van de POK-α eenheidscel loodrecht op de ketenas (35.2 $Å^2$) is zelfs kleiner dan die van polyetheen (36.2 $Å^2$), terwijl de pakkingsdichtheid van de atomen in dit rooster een van de hoogste is die ooit werd waargenomen voor flexibele organische polymeren. Deze specifieke eigenschappen zijn van groot belang voor het vervaardigen van hoog-modulus vezels.

Het polyketon werd gereduceerd met behulp van natrium boorhydride tot een polyalcohol. Ondanks het feit dat het gevormde polyalcohol een atactisch material is kunnen georiënteerde geordende structuren gemaakt worden door het heet verstrekken van uit oplossing vervaardigde films. De reflecties in het röntgen-diffractiepatroon van georiënteerde films werden geïndiceerd op basis van een orthorhombisch kristalrooster. De hieruit afgeleide eenheidsceldimensies staan vermeld in Tabel I. De pakkingsdichtheid van het polyalcohol is aanmerkelijk lager dan die van poly(vinyl alcohol), welke een 1,3-rangschikking heeft van de hydroxyl substituenten. Het lage smeltpunt van polyalcohol (137 °C) is het gevolg van de lage pakkingsdichtheid, dat zijn oorzaak vindt in het verschil in oriëntatie van de hydroxyl substituenten ten op zichte van de ketenas in een 1,4-rangschikking.

POK-C_2 vezels vertonen bij 110-130 °C een reversibele vaste-stof overgang, waarbij de POK-α structuur overgaat in de POK-β structuur. Deze structuur is eerder gevonden in niet perfect alternerende copolymeren. De overgang gaat gepaard met een toename van 10 % in het volume van de eenheidscel. Het warmte-effect van de overgang is echter slechts 5-10 % van de smeltwarmte. Een zekere ketenmobiliteit is noodzakelijk om de POK-β structuur over te laten gaan in de dichte α-structuur. In het polymerisatieprodukt zijn beide structuren aanwezig. De fractie aan α-structuur [bij kamertemperatuur] is afhankelijk van de polymerisatiecondities, die tevens resulteren in verschillen in molgewicht en morfologie van de gevormde polyketon poeders. De fractie aan α-structuur kan worden verhoogd door middel van rekristallisatie vanuit oplossing. Hoog-moleculaire vezels gesponnen uit oplossing vertonen na verstrekken uitsluitend de α-structuur. De perfectie van de gevormde α-kristallen hangt sterk af van de spanning die op de vezel uitgeoefend wordt wanneer de β-structuur overgaat in de α-structuur. Daar hoog-moleculair polyketon polymerisatieprodukt hoofdzakelijk

bestaat uit de β-modificatie kan geconcludeerd worden dat spinnen gevolgd door het heet naverstrekken een omzetting van de β-structuur in de α-structuur als resultaat heeft.

Georiënteerde etheen-koolmonoxide/propeen-koolmonoxide terpolymeren die meer dan 5 mol-% propeen bevatten vertonen uitsluitend de β-structuur bij kamertemperatuur. Dit resultaat verklaart de eerder waargenomen β-structuur in niet perfect alternerende copolymeren, omdat deze minder dichte structuur beter geëigend is om zowel temperatuur-effecten als ook ketendefecten te herbergen. Aangezien ketendefecten gedeeltelijk ingebouwd kunnen worden in het POK-β rooster kan Flory's roostertheorie niet toepast kan worden om de smeltpuntsdepressie van deze terpolymeren te beschrijven. Om een eerste afschatting te krijgen van de smeltwarmte van perfect kristallijn materiaal werd de Flory-Vrij vergelijking toegepast voor het beschrijven van de ketenlengteafhankelijkheid van het smeltpunt van een reeks laag-moleculaire (symmetrische) polyketon homologen. Deze resultaten geven aan dat het hoge smeltpunt van POK-C_2 (260-280 °C) is toe te schrijven aan een hoge pakkingsenergie in het kristalrooster en niet, zoals eerder is verondersteld, aan een beperkte rotatie-mobiliteit door de aanwezigheid van de keton functionaliteit. Op basis van de afschatting van de smeltwarmte van perfect kristallijn materiaal (215-330 J/g) kan een kristalliniteit van 60-80 % in goed georiënteerde POK-C_2 vezels worden afgeleid.

De maximaal haalbare strekverhouding van polyalcohol films is ongeveer 10, terwijl polyketon vezels verstrekt kunnen worden tot een faktor 26. Boven een strekverhouding van 17 schijnt de vorming van lokale spanningsconcentraties in de vorm van voids en cracks in POK-C_2 multifilament garens onvermijdelijk te zijn. Behalve door de invloeden van het moleculairgewicht en de entanglement dichtheid is de maximaal haalbare strekverhouding van beperkt polaire en apolaire polymeer systemen ook bepaald door de chemische structuur (polariteit) en de temperatuur. Een goede maat voor de polariteit is de cohesieve energie (E_{coh}). Deze maat geeft de polariteits-barriere aan die het transport van topologische defecten in de richting van de deformatie tegenwerkt. De maximale temperatuur voor een optimale verstrekking

ligt dichtbij de smelttemperatuur van het polymeer. Het begin van het smeltproces gaat gepaard met een afname in de capaciteit om lateraal spanning over te dragen tussen de ketens. De overdracht van spanningen vindt onder deze condities hoofdzakelijk plaats door topologische keteninteracties in de vorm van entanglements. Door de merkbare hoeveelheid ketenuiteinden in de gebruikte polymeermonsters wordt slip van ketenuiteinden door entanglements mogelijk aan het begin van het smeltproces. De gevonden correlatie tussen de smelttemperatuur en de verstrekbaarheid van een aantal poly-hydroxy-polymeren (polymeren met een vergelijkbare polariteit) bevestigt de beperkingen in verstrekbaarheid ten gevolge van de vermindering van de laterale spanningsoverdracht boven de smelttemperatuur. In zeer polaire polymeren met een hoge roosterenergie, zoals polyamide-6 en polyamide-6,6, fungeren (kleine) kristallieten als zeer effectieve crosslinks, die slechts zeer moeilijk of geheel niet verbroken kunnen worden tijdens het verstrekproces. De verstrekbaarheid van polymeren met een hoge cohesieve energie is daarom niet sterk afhankelijk van de polariteit van het polymeer.

Hoog georiënteerde POK-C_2 vezels, verstrekt tot een faktor 26, vertonen een treksterkte van 3.8-3.9 GPa, een initiële trekmodulus van 50-55 GPa en een rek bij breuk van 4-5 %. Het semi-kristallijne karakter van het POK-C_2 polymeer wordt duidelijk merkbaar wanneer oriëntatierelaxatie in niet-kristallijne domeinen kan plaatsvinden. Het verlies aan oriëntatie is in toenemende mate merkbaar bij hogere strektemperaturen en lagere strekspanningen. Als gevolg van de oriëntatierelaxatie kan de breukrek worden verhoogd tot 7-8 %, waarbij een verlaging van de initiële trekmodulus optreedt (40-45 GPa). Als eerste benadering kan de ontwikkeling van de door verstrekking geïnduceerde dubbele breking beschreven worden met behulp van het affiene deformatie concept van Kuhn and Grűn, in combinatie met een waarde voor de dubbele breking voor perfect georiënteerd materiaal van $710 \cdot 10^{-4}$.

De kristalliniteit in polyketon terpolymeren wordt verlaagd ten gevolge van de inbouw van propeendefecten in de polymeerketen. Hierdoor neemt de krimp in hete lucht van 160 °C toe met een toenemende gehalte aan propeen. Tevens is de ontwikkeling van de initiële trekmodulus met de strekverhouding (oriëntatiegraad) minder bij hogere

propeengehaltes. Deze waarnemingen geven aan dat laag-smeltende polyketon terpolymeren minder geschikt zijn om te gebruiken als uitgangsmaterialen voor vezels.

De α/β-overgang bij 110-130 °C in georiënteerde POK-C_2 vezels gaat niet gepaard met een duidelijke vermindering van de mechanische eigenschappen. De gemiddelde afschuifmodulus van de POK-β structuur is waarschijnlijk zelfs iets hoger dan die van de POK-α structuur ten gevolge van de meer polaire rangschikking van de keton-functionaliteit in het POK-β rooster. Deze unieke eigenschap van POK-C_2 vezels, in combinatie met de superieure hoge-temperatuureigenschappen en kruip-bestendigheid [in vergelijking met minder polaire polymeren, zoals polyetheen], geven de goede potentie aan van deze materialen voor geavanceerde industriële garen-toepassingen.